Universität Dortmund

Fachbereich Chemietechnik

Lehrstuhl für Werkstoffkunde

Prof. Dr. J. Petermann

Diplomarbeit

Haftung und Aufnahme von Druckfarben auf gestrichenen Papieroberflächen

Bearbeiter: Sven Keiter

Angefertigt unter der Aufsicht von Dr.-Ing. Philippe Letzteler in MoDo Iggesund, Schweden

Februar 1998

Index

1. Introduction

Paper and board is commonly used as a carrier of information. The information, text or images are printed on the paper/board surfaces using different printing techniques. The most commonly used printing technique is offset printing, where a fluid, oil containing ink is transferred from the printing press to the paper/board surface.

Most papers/boards intended for offset printing are coated. During this process, a coating color, consisting of mineral pigments and binders, is applied to the paper/board surface, forming an absorbent porous structure on the dry finished paper.

When printing ink is applied to the paper surface, some liquid components of the ink, mainly oil, is absorbed into the paper surface. The viscosity, and the tack of the ink layer remaining on the paper surface, will thus increase with time.

This process is a normal part of the drying process of offset inks applied to a paper surface. However, if this increase in viscosity (and thereby ink-tack) is too fast, problems might occur in the print press as the paper surface is subjected to ever increasing forces in the printing nips. These forces are considered to be the cause of problems like delamination and picking (tear out of particles from the paper/board surface).

A too slow drying, on the other hand, can cause “set off” problems, where ink is smeared from the top side to the back side of the next printed sheet.

Few laboratory methods do exist, that are able to predict the interaction between coated paper surfaces and offset inks.

The objective of this thesis was to investigate the interaction between coated paper surfaces and offset inks, using a new type of dynamic ink-tack measurement equipment, the ISIT [31]

2. Main objectives

The main objectives of this work were:

- To establish a new test method to predict the setting and the tack-force development of offset inks on coated paper substrates.
- To find out weaknesses and limitations of the new instrument
- To investigate which main ink and paper surface parameters do influence on the setting and ink tack development
- To correlate the results to problems in print presses

3. Test methods of properties of paper/board:

Paper and board is described by using a number of parameters. Some of the most important ones are:

Gloss*:* The gloss of the paper/board surface is expressed in % units. The surface is illuminated at an angle and the reflection from the surface is recorded by a photo – electric cell. A surface having a measured value below 40% is regarded as matt. A medium gloss paper/board is in the range of 40 % to 70 %. A high gloss board has a value of greater than 70 %.

Surface roughness: Surface roughness or smoothness is commonly measured using the Parker Print Surf (PPS) Roughness Tester at 980 kPa using a soft backing. Air is evacuated in a chamber applied to the surface. Due to the gaps in the rough surface air passes into the chamber. The resulting pressure difference correlates to the air amount transferred, which correlates to the existing surface roughness expressed in µm. Lower results indicate smoother surfaces.

Density: The print density is measured with a densitometer. Density is the amount of light reflected compared to the light emitted. The colors are separately measured using filters. The density value rises with increasing amount of ink applied.

The print density is calculated with following equation:

$$D = \log k\left(\frac{R_\infty}{R_t}\right) \qquad \text{(eq. 3.1)}$$

With

D The print density

R_∞ The reflection factor of an ideal white surface (calibrated within the instrument)

k Apparatus constant

R_t The reflection factor of the measured sample

Color	Density
black	1,9
cyan	1,4
magenta	1,3
yellow	1,25

Table 3.1: Typically recommended target values for print densities at full scale offset printing [10]

Surface strength: Plastic adhesion (surface strength) is a dimensionless property defining the relation between adhesive and cohesive strength in the paper/board surface. One usual method involves pulling off the surface of the coated paper/board by means of an adhesive tape and determining the degree of failure in the interlayer.

Ink tack: Ink tack is defined as the resisting force against separation from a wet ink covered substrate. In the German DIN 16515 ink tack is determined by touching with an object or a finger.

4. The Offset printing process

4.1 General description

The most common printing process is offset printing.
Ink is transferred from the inking system via a series of distribution rollers to the printing plate and finally to the substrate. The distribution rollers are of varying diameters in order to create sufficient shear to achieve a thin and even distribution of the ink film to the form roller in contact with the plate. For each successive rotation of the distribution rollers, the ink is compressed and decompressed. The ink viscosity is lowered by this procedure. From the dampening system a fountain solution is applied to the plate cylinder. Due to high speed, the ink rapidly emulsifies with the fountain solution on the plate cylinder, which is a low viscous solution of water and alcohols. The ink emulsion can contain up to 40% water. The printing image is usually a thin flexible metal plate which is wrapped around a cylinder known as the plate cylinder. The image area of this plate accepts ink and repels water. The non image areas attract water and repel ink. The plate is first dampened with an aqueous solution which keeps the non-image area free of ink. The image areas are than inked. The plate cylinder then transfers the inked design to a rubber covered blanket cylinder. The blanket cylinder transfers the design to the paper surface in the printing “nip” where pressure is maintained between the blanket and impression cylinders. The linear load in the nip is of the order of magnitude of 5-30 kN/m. Nip width ranges from approximately 5 to 20 mm, which means that nip pressure ranges from 0,1 to 10 MPa. The offset process is also called lithography (from greek lithos = stone, grafein = carve, write). In a four-color printing unit four of the below sketched printing systems are employed one for each color. The usual printing sequence is: 1) black, 2) cyan 3) magenta 4) yellow

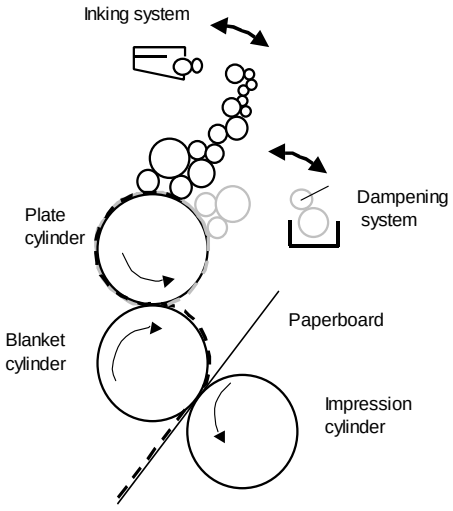

Figure 4.1: Offset printing method

4.2 Most frequent used offset printing methods

Sheet–fed lithographic offset: One sheet after the other is subject to the printing process. Over 10000 sheets per hour can be printed.

Web-offset: A continuously running web with paper is printed at higher speed. Usually magazines, catalogues and brochures are printed in this manner.

4.3 Methods to achieve drying in printing:

The inks applied in the print process must be dried. The drying methods usually employed in the print industry are:

Heat set: The substrate is dried with hot air after the printing units due to evaporation.

Cold-set: This process is usually applied to newspaper and books. The ink is absorbed by the uncoated paper.

Quickset mechanism: The quickset mechanism is the dominant drying mechanism. It is employed for all forms of paper and board. Quick-setting involves a physical absorption process followed by a longer period of time with chemical drying (oxidation and polymerization).

The type of ink has to be adapted to the offset process. In this thesis, substrates and inks mainly for sheet-fed or web-fed offset and inks that use the quickset mechanism are focussed on.

5. Paper and board:

Paper is made of cellulose fibers, which are produced from chipped wood. A number of processes and materials are used to refine the end product. In contrast to paper, paperboard is built up in several layers of base board and coating.

5.5.1 Papermaking process

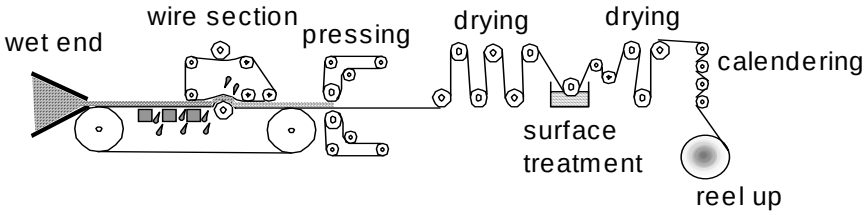

Fig. 5.1: The paper machine

Forming on the wire section

A low concentration of 0,3 % cellulose fibres and 99,7 % water is supplied via the wet end of the paper machine. A low concentration is essential in order to obtain a uniform distribution of fibers in the paper. First the paper is formed on a metal wire. Water drains downwards and is removed upwards by suction. In the wet state, layers of fiber consolidate easily.

Pressing

When the paper reaches the press section, water content has dropped to 80-85 %.

The press section is important for achieving a uniform fiber consolidation. Sandwiched between two felts, the paper web is pressed between hard rolls. The water is effectively removed so that moisture content in the paper at the end of the press-section, is 60 – 65 %.

Drying

In order to dry the paper web, it passes over steam–heated, polished cylinders, which gradually reduce moisture. A sophisticated system controlling the temperature of the cylinders ensures that drying takes place without sudden stresses on the web.

Surface Sizing

A starch solution is applied to both sides of the paper surface mainly to increase strength and stiffness. Surface sizing binds the fibers to the surface.

Calendering and Burnishing

The final gloss of the surface is achieved by calendering in a gloss calendar or brush polisher. In the gloss calendar the paper web passes between a heated hard steel roller and a soft polymerroller.

In the brush polisher the paper is polished by a number of rotating brushes. These processes give a uniform smooth surface, which is essential for good printing and varnishing.

The paper can be nipped between steel rollers (super calendering) to further increase surface strength and smoothness. During this process the density of the paper increases.

Surface Coating

A liquid, white, pigmented coating consisting of pigments (clay, $CaCO_3$,), binders (latex, starch,...) and additives is applied and distributed over the surface. Application methods include a blade, an air knife, which is a thin ray of air, or cast coating, which is a slowly rotating large chrome-drum.

1 -3 layers of coating, depending on the paper type, are applied to the surface. Each layer is independently dried by hot air and infra-red dryers. Coating composition and amount will strongly influence the ink receptivity at the surface.

5.2 The main components of paper and board

There are many different products of paper and board on the market, depending on the raw materials for fibers, composition of coatings, the kind of printing process to which the product is subjected and, the end use of the product.

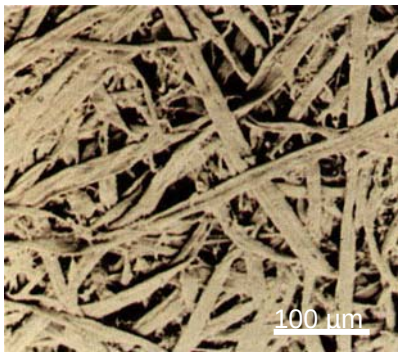

Fig. 5.2.a: Chemical pulp [7]

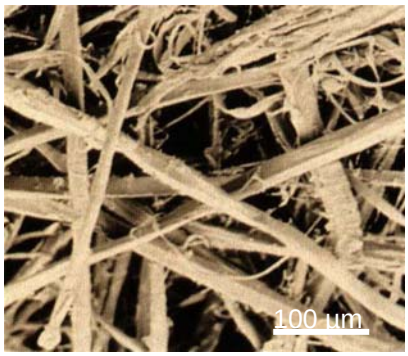

Fig. 5.2.b: Mechanical pulp [7]

The main raw material in the paper production is wood fibers. The fibrous material of the wood can be separated either mechanically (i.e. mechanical pulp), or chemically (i.e. chemical pulp)

5.3 The composition of paper coating:

Pigments:

The coating colors used in paper coating usually consists of 80-95 weight % of pigments like clay and $CaCO_3$, 10-20 weight % binders like starch or latex and additives.

Clay pigments consist of aluminumsilicate $Al_2O_3(SiO_2)_2(H_2O)_2$. This material is also called kaolin. Clay pigment particle sizes range from 0,5 µm to 10 µm with an usual particle size distribution of 90 % by weight below 2 µm. A small particle size distribution usually improves gloss as well as opacity of the coating layers. Clay particles have a flat polyeder shape. The shape can be characterized by the aspect ratio:

$$f = \frac{D}{T} \tag{5.1}$$

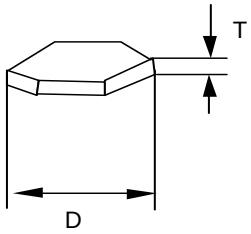

Fig 5.3 Aspect ratio of a pigment particle

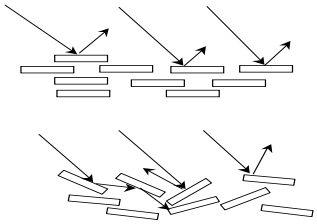

Fig. 5.4 Influence of orientation of pigment particles on gloss

The gloss of the coating layer usually improves with higher aspect ratios, but also the orientation of the pigments has an impact on the final gloss. Fig. 5.4 shows that tortuosity increases with greater orientation and higher aspect ratios. These factors should influence the ink drying behavior. Earlier experiments show, that coatings with pigments of higher aspect ratios due to delamination of clay staples contribute to a slower ink drying [31], [11].

$CaCO_3$ pigments are whiter and cheaper than clay particles. Calcium carbonate pigments have a more irregular spherical block-like shape. In nature, $CaCO_3$ can be found in the shape of chalk or marble. Aspect ratio lies between 1 and 1,5.

Both particle size and orientation have an impact on the packing structure of the dried coating layer. The diameter of the pores in the dried coating structure will diminish with both smaller particle size distribution and increased particle orientation.

Other commonly used mineral pigments in the paper coating industry are $Al(OH)_3$, titaniumdioxide and talc (magnesiumsilicate).

As a polymer pigment, polystyrene is used as an additive.

Binders:

Binders have the function to bind the pigments both together and to the basepaper. Depending on the type of paper and board and the print technique, different addition levels of binders are used. The binder, should have the properties of being uniformly distributed and to form a porous structure together with the pigments, to ensure an even and good absorption of ink-components. For offset paper 10-20 parts binder to 100 parts pigments are normally used. A higher binder content usually leads to a less porous structure, which has a negative effect on the ink drying during printing [11].

There are two main groups of binders:

- Water soluble binders (starch, CMC)
- Polymerdispersions (latex).

The water soluble binders can further be divided into:

- Natural binders, like starch, proteins and kasein and carboxymethylcellulose (CMC)
- Synthetic binders, like polyvinylalcohol (PVOH).

Polymerdispersions (latices):

Latex binders are very strong binders. Latex is a crosslinked polymer that is disperged in water. Latex particles are usually kationic particles surrounded by OH^- - anions. Thus a stabile latex dispersion idepends on the pH-value. With higher pH-value the latex particles can agglomerate.

The solubility of the latex polymer is known depending on the physical state of the polymer (linear vs. crosslinked) as well as on the chemical structure (surface energy/polarity level). When increasing the surface energy/polarity of the latexpolymer the difference between the solubility parameter of the polymer and of the ink increases. As a result the interactivity with the ink is less and this leads to a lower ink-tack rate build up [12].

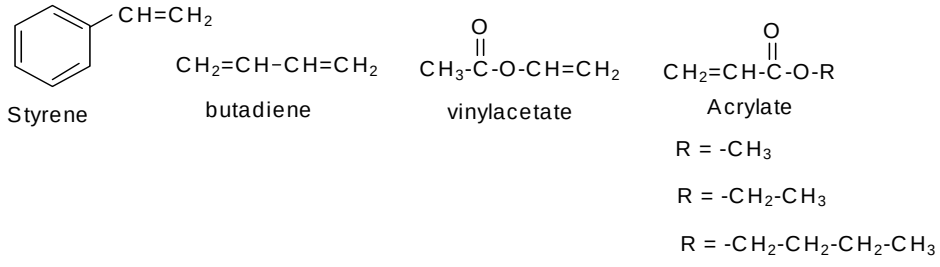

Fig. 5.5: Monomers for latex binders

Usual monomers for latices are styrene, butadiene, acrylates and vinylacetate. The size of an individual latex particle is in the range of 0,1-0,2 µm. Latex particles are usually

carboxyled after reacting with a vinylacid. With carboxylating the latex's binding abilities and the latex dispersion's mechanical and electrolytic stability is improved.

An important property is the glass transition temperature T_g. This is the temperature where a polymer changes from a hard glass-like state to a soft rubber-like state. Earlier experiments show, that an increasing particle size of the latex and a decreasing crosslinking state leads to a faster rise of ink tack [11], [12]. There are 3 main types of latices:

- styrene-butadiene:
- acrylates
- polyvinylacetate

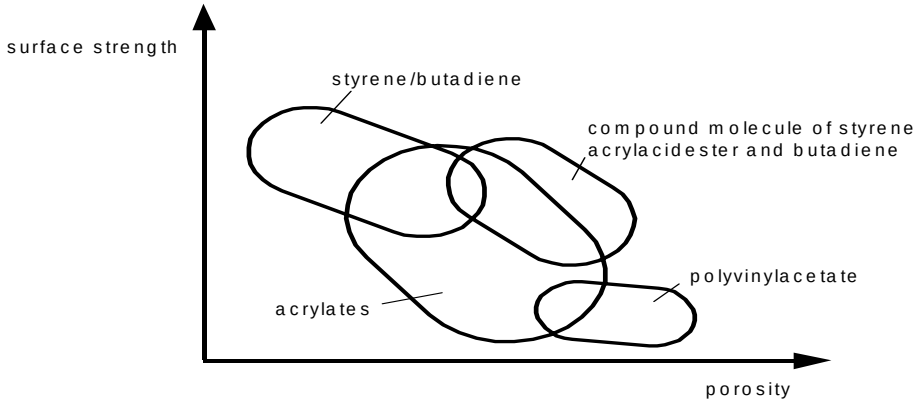

Fig. 5.6: Influence of latex on coating layer properties.

In the above picture it is illustrated, that latex contributes to different properties which are important for the printing method applied. Depending on the printing technique used, different properties of the dried coating layer are required. For gravure printing a compressible coating is suitable. Thus a latex with a low Tg, giving binding strength, is recommended. For sheet fed and web fed offset a strong coating is required, which is possible with a latex with higher Tg.

Polyvinylacetate contributes to a higher porosity, while a styrene/butadiene latex contributes to a high surface strength.

Styrene-butadiene:

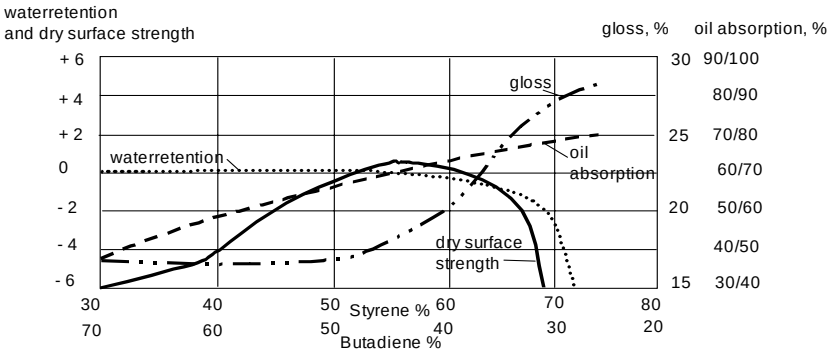

Fig. 5.7: Change of properties of coating due to polymer amount

A typical styrene butadiene latex contains 60 parts styrene and 40 parts butadiene. Due to it's bulkier molecule shape the glass transition temperature of the latex is higher with increasing styrene content. The coating will be harder, more brittle, more glossy and more porous. The ability to swell is enhanced with a lower Tg. So with a higher butadiene content the ability to absorb oil increases due to swelling of the latex [11]. This means that not only the porosity of the coating layer contributes to ink setting, but also the latex itself actively participates in the absorption process. This can be seen from Fig. [5.7].
The higher the oil absorption value is, the longer it takes for the oil to be absorbed by the coated surface.

Acrylates:

These are compound polymers between styrene and akrylacidester. In this group of latices types with extremely low Tg (-15°C) can be found. Coatings with acrylates have a low tendency to get yellow with time.

Polyvinylacetates:

It can be seen from the Fig. 5.6 that this group of latices contributes to a weaker coating surface, but to a higher porosity of the coating. Often these latices are combined with other ones in order to increase the coating porosity.

Additives:

The function of additives can be described as:

- coating hardener and plasticiser
- enhancing the brightness and whiteness
- additives to prevent the coating colors tendency to foam and to prevent bacterial attack.

6 Composition of inks:

Each printing process has a demand for inks with certain specifications. In gravure and flexo printing, liquid inks are used. In offset and letterpress, oil based inks are used and in flexo printing, water based inks are used.

A general formulation for any offset ink is as follows:

- Pigments
- Resin/vehicles
- Solvent/dilutes = carrier phase
- Additives

Pigments: Pigments are insoluble fine particles that are dispersed in a continuous phase. This phase is called vehicle, and consists of carrier phase and binder. Pigments have the function to absorb light of a certain wavelength to give a desired color. Very often are pigments like other color materials, aromatic systems with delocalized Π–electron systems [14]. The color appearance is influenced by the side groups that contribute to a positive or negative mesomeric effect to the aromatic base molecule. The pigment content in any ink is in general 10-30 %. Black pigments consist of carbon black. These are very small spherical agglomerates of 50-1000 Å [13]. For Cyan colored phtalocyanes pigments, for magenta colored pigments azo pigments and salts, for yellow azo pigments are used.

Pigments have different sizes, and the size determines the rheological properties of an ink. Ink is a dispersion of small solid particles (pigments) in a high viscous fluid. Pigment size determines the setting behavior of an ink since a formed filter cake of small pigment particles is not as easily penetrated by the oil phase, as a filter cake of bigger particles.

Pigment shape is also an important property, it influences many ink effects. Flat, platy pigments are valuable in reducing the transmission properties of the ink film. Fibrous pigments tend to increase thixotropy. Sharp, needlelike pigments are valuable in strengthening the ink's cohesiveness. Most colored pigments fall into the range between 0,1 and 5 µm. The size curve of a pigment shows a normal-distribution.

With increasing pigment volume concentration the gloss of the film decreases [15]. Small pigment particles increase the surface, and thus more binder matrix is needed. The size of pigment particles can be determined by sedimentation analysis [16].

Binder: The percentage of binder in an offset color lies between 10 and 30 percent. The binder has the function to adhere the pigment to the paper and to give gloss. The binder has to be compatible with the carrier phase. Solubility of the binder in the carrier phase and the substrate surface determines the speed of ink setting [12], [40]. The choice of binder influences the amount of ink tack [19]. Binders are amorphous polymeric materials, called resins. Phenolic resins and alkyds are often used in offset inks. For sheet fed offset inks drying oils are applied, and for UV inks (ultra-violet drying) acrylates are utilized.

Carrier phase (solvents): The amount of carrier phase ranges from 0-70 %. The carrier phase has the function to provide the color with the necessary fluidity. Mineral and vegetable oils are used for offset printing.
Depending on the offset printing process, solvents of different boiling range are used:
240-260 °C for heat-set inks,
260-290°C for slow heat-set or ultra fast quickset inks and
280-320°C for quickset inks.

Additives: A large quantity of additives are used in inks:
Filler pigments and white mineral pigments are used to reduce the color strength of the ink and to give the ink a higher consistency.
Wetting, emulsion and dispersion agents are used to wet and improve dispersability and stability of pigments and emulsion type binders in inks.
Gelling agents are aluminum compounds, that are used to increase the consistency of the ink by forming a network after ink transfer to the paper, in order to reduce smearing and spreading of the ink. These agents are specially used in oil based inks.
Waxes of polyethylenes, polytetrafluoroethylenes and paraffin are used in heat-set and sheet fed offset inks to reduce surface energy. Through this, the adhesion of wet ink films to other surfaces should be prevented and ink tack should be reduced.
Plasticisers are esters with high molecular weights. They improve the flexibility of printed ink layers by having a dissolving effect on binders. These agents are used in special high quality inks.
Drying agents are organic compounds, containing Co and Mn, used in offset inks, drying by oxidation and polymerization. They have the function to initiate and speed-up chemical drying by acting as a catalyst for the polymerization process.
Drying inhibitors are reactive compounds used in order to prevent drying in the container.

7 Setting and drying of an offset ink:

After transfer to the paper, the ink should solidify as quickly as possible. Drying of ink on the paper is described to take place in two more or less separated stages:

- Setting and
- Drying

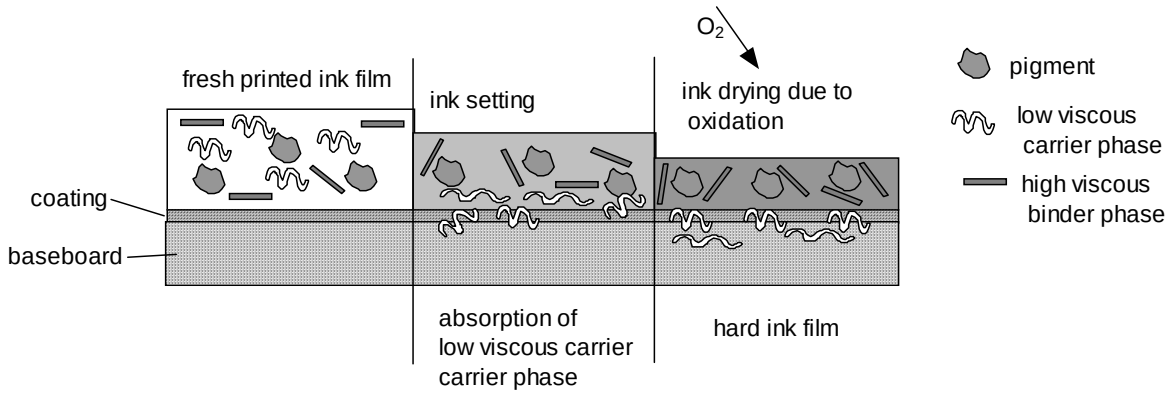

Fig. 7.1: Mechanism for ink setting and drying of an offset ink (quickset mechanism)

The absorption of lighter components in the carrier phase takes place immediately after printing. As a consequence the viscosity rises, the concentration of binders in the ink increases and ink tack increases. This phase is called the setting phase.
An ink layer is considered to be set, when it is touch-proof. This is measured by laboratory tests in which another unprinted surface is pressed against a printed substrate.
The mineral oils are absorbed into the stock or evaporate into the air. Heavy oils like vegetable oils, penetrate into the paper very slowly. Vegetable oils dry by oxidation, which is sometimes assisted by the use of metallic dryers (catalysts) like cobalt or manganese [36]. An ink layer is considered to be dry when it can be sheared without ink debonding from the surface. The test is called rub-off test.
The oxidation of vegetable oils is believed to be an auto-oxidative polymerization which proceeds by several stages [3]:

1) Peroxide/ hydro-peroxide formation
2) Decomposition to form free radicals, which initiate
3) Polymerization
4) Termination

In the peroxide/hydro-peroxide formation the atmospheric oxygen attacks at activated sites on the fatty acid chains of the drying oil. One such site is the methylene group next to one of

the carbon – carbon double bonds present in all drying molecules [3]. With linseed oil as an example of a typical drying oil, the following reaction has been proposed [3]:

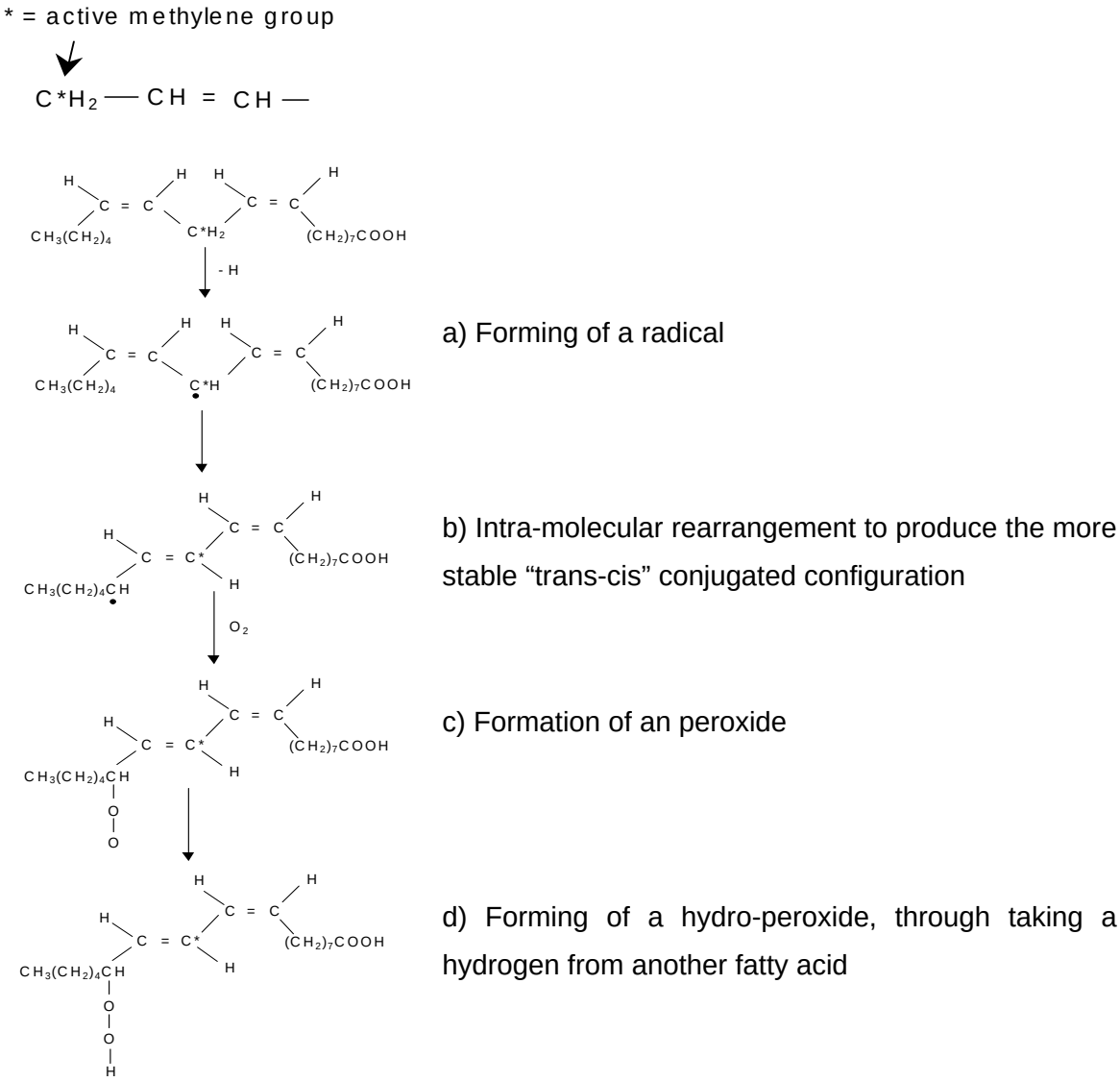

(step a). The CH_2 group marked with an asterisks$^{(*)}$ is more reactive than the others, because it is adjacent to two double bonds and is therefore the major reaction site.

When conjugated structures are present, as in tung-oil (wood oil), direct oxygen addition to the conjugated system is possible in order to form a 1,4 –cyclic peroxide [3]:

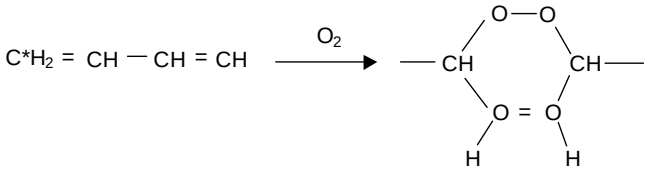

Any further oxidation of the hydroperoxides in d) will also give a 1,4-cyclic peroxide.

Decomposition of free radicals:

Once hydroperoxides or cyclic peroxides have been formed, they can decompose into free radicals as follows [3]:

The following reactions are then possible:

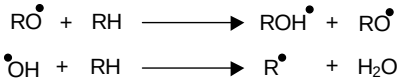

The radicals formed in the last step can react with atmospheric oxygen to form peroxides and hydroperoxides thus propagating the chain reaction.

Polymerization:

The radicals formed in the above reaction can add on to another molecule of the drying oil, and these addition reactions can continue increasing the molecular weight until termination occurs. There is also more than one site for the growing radicals to attack and this produces cross linked molecules. The increasing molecular weight and the cross-linking reactions cause the ink vehicle to become a solid material, encapsulating the pigment [3]. The degree of cross-linking and the kind of polymerization depends on the kind of oil or binder used in the ink.

Termination:

The radicals formed in the above reactions can also react with each other leading to the termination reaction:

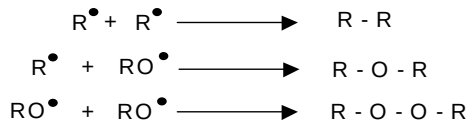

Nowadays, oxidation as the sole drying mechanism, is normally encountered in inks for printing impervious substrates such as foils and plastics. With the introduction of techniques like radiation curing, the overall hardening through polymerization has become possible.

When looking on the overall reaction it appears as if the addition of peroxides, the pH value, air humidity, temperature and the addition of catalysts influence the polymerization. It has been found that inks do not dry on low pH paper (lower than 5) [3], [7].

8. Rheology of ink:

In the following chapter, described changes in ink viscosity due to shear rates are called thixotropy

Mechanical model for a viscoelastic-plastic body

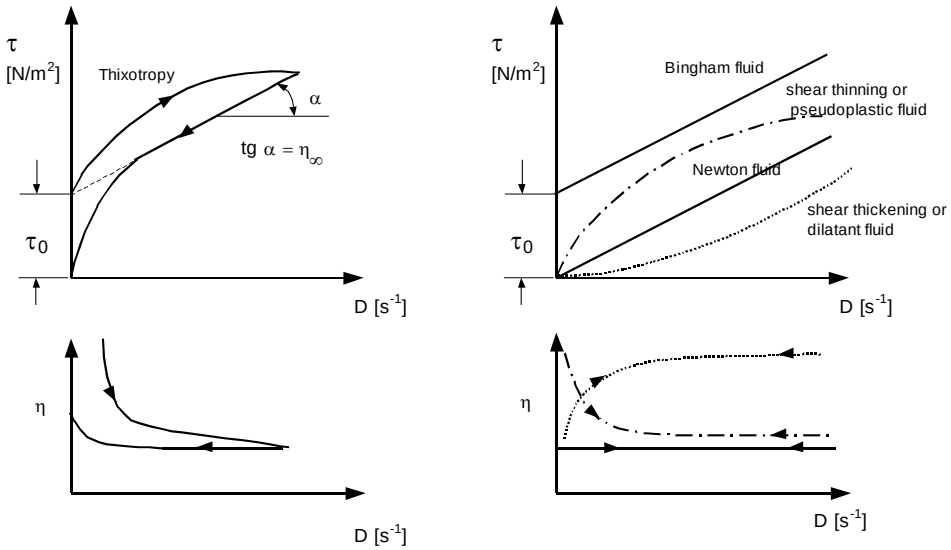

Fig. 8.1: Viscosity diagrams for a sheared ink (thixotropic) and other fluids [17], [26], [27]

With

D: shear gradient

τ: shear tension

η: momentarily viscosity

τ_0: flow limit

η_∞: plastic viscosity

From figure 8.1 it can be seen, that the viscosity of inks depends on the shear forces they are subjected to, as well as on the shearing history. One common behavior is the shear thinning behavior, where the viscosity decreases with increasing shear force. A practical example are paints: Paint needs to be stirred to be more fluent to be applied easily with a brush to the substrate, where it stays without flowing down.

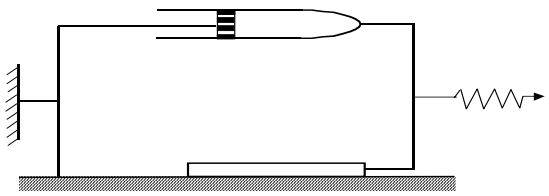

Fig. 8.2: Mechanical model for a visco-elastic-plastic model (Maxwell body), [17]

The rheological curve from Fig.8.1 can be also expressed by a mechanical model (see Fig.8.2). Following stresses are illustrated:

1) The *spring* represents reversible elastic deformation stress
2) The *block on the ground* and the *damping system* represent the irreversible deformation stress.
The *damping system* describes the flow of the body. It refers to the *plastic viscosity* of the fluid.
The *block on the ground* characterizes the *flow limit*.
For high shear rates that appear in the printing press, the stress is predominantly an elastic deformation. At slow shear rates the flow deformation predominates.
The Maxwell equation combines flow and elastic deformation:

$$\eta \frac{du}{dz} = \tau - \tau_0 + \frac{\eta_\infty}{G} . \frac{d\tau}{dt} \qquad (8.1)$$

where

G is the elastic modulus and

$\frac{\eta_\infty}{G} = T$ is the relaxation time

τ_0 is the hypothetical flow limit

The elastic properties of the ink can be supported by the fact, that ink splits in strings, that tear and pull back. The strings appear through cavitation [17]. As stated before inks are dispersions of solid particles in a high viscous fluid. Internal structures are typically a result of van der Waals type attractive interactions. Building of these structures is resisted by the viscous resistance of the carrier medium. So structures are more likely to be built up in liquids with low viscosity. At lower shear rates these internal structures break down. With higher shear rates, shear thinning takes place due to orientation of the particles and the molecules. The shear rate is then more and more controlled by the polymeric properties of the binder, like chain length and configuration. With further rising shear rates, the viscoelastic behavior of the binder-polymer molecules has an increasing impact on resulting stress. Polymers have not the time to respond by viscous flow and behave more and more like an elastic body. Some properties can be foreseen by thixotropic behavior:
An easy oil separation is enhanced with lower viscous oils. Thus the risk of set off decreases [18]. For ink tack an interesting investigation was made: With NMR spectroscopy (nuclear magnetic resonance) measurements, it has been demonstrated, that a lower ability for the binder polymer to move increases the tack values. (NMR spectroscopy determines the magnetic resonance of the nuclei of molecules, through determining the resonance

frequency of an applied high frequency magnetic field perpendicular to a static field of a few Tesla.) The tack did not increase with a higher pigment content that increased the viscosity. The authors speculate, that no shear and viscosity properties of the inks govern film splitting, but the ease with which polymer molecules can orientate under extensional shear [19]. This was confirmed in another article where the “tackiness” of an offset ink was experimentally determined not to be dependent on viscosity alone. Tack was determined mainly by the amount and structure of the binder molecule [28]. The gelling agents like the aluminum compounds, present in inks, do contribute to the thixotropic behavior of inks [20].

Viscosity is highly dependent on temperature. With lower temperature a higher viscosity is obtained.

9. Interaction between solid and liquid systems:

In this part some physical processes, that contribute to the phenomenon ink, tack are simulated. A general valid theoretical explanation for the obtained experimental tack-force curves is strove for.

9.1 Flow profile between two separating plates:

The following calculation deals with the force needed to separate two cylindrical plates connected with a Newtonian fluid. The lower plate is fixed, while the upper plate is pulled with a force. One assumes isothermal conditions.

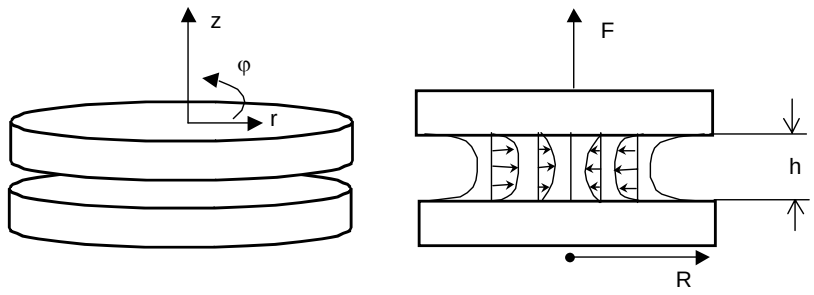

Fig. 9.1: Flow profile between two separating plates.

If Newtonian fluid behavior and isothermal conditions are assumed, the flow between two separating plates can be calculated with the Navier-Stokes equations [22].

$$\rho\cdot\left(\frac{\partial v_r}{\partial t}+v_r\frac{\partial v_r}{\partial r}+\frac{v_\varphi}{r}\frac{\partial v_r}{\partial \varphi}+v_z\frac{\partial v_z}{\partial z}-\frac{v_\varphi^{\,2}}{r}\right)$$
$$=-\frac{\partial p}{\partial r}+\mu\left(\frac{\partial^2 v_r}{\partial r^2}+\frac{1}{r^2}\frac{\partial^2 v_r}{\partial \varphi^2}+\frac{\partial^2 v_r}{\partial z^2}+\frac{1}{r}\frac{\partial v_r}{\partial r}-\frac{2}{r^2}\frac{\partial v_\varphi}{\partial \varphi}-\frac{v_r}{r^2}\right) \quad (9.1)$$

$$\rho\cdot\left(\frac{\partial v_z}{\partial t}+v_r\frac{\partial v_z}{\partial r}+\frac{v_\varphi}{r}\frac{\partial v_z}{\partial \varphi}+v_z\frac{\partial v_z}{\partial z}\right)$$
$$=-\frac{\partial p}{\partial z}+\mu\left(\frac{\partial^2 v_z}{\partial r^2}+\frac{1}{r^2}\frac{\partial^2 v_z}{\partial \varphi^2}+\frac{\partial^2 v_z}{\partial z^2}+\frac{1}{r}\frac{\partial v_z}{\partial r}\right) \quad (9.2)$$

It is assumed that $v_\varphi = 0$ and v_r and v_z are functions depending on r and z only. With this assumption the above equations simplify to:

$$\frac{\partial p}{\partial r}=\mu\left(\frac{\partial^2 v_r}{\partial z^2}\right) \quad (9.3)$$

and

$$\frac{\partial p}{\partial z}=0 \quad (9.4)$$

The pressure is independent of the z-direction, so dp/dr is also independent of the z-direction.

The continuity equation in cylindrical coordinates is:

$$\nabla \underset{\sim}{v} = \frac{\partial v_r}{\partial r} + \frac{1}{r}\frac{\partial v_\varphi}{\partial \varphi} + \frac{\partial v_z}{\partial z} + \frac{v_r}{r} = 0 \tag{9.5}$$

With the flow speed distribution independent of φ, the equation of continuity simplifies to

$$\frac{1}{r}\frac{\partial (r v_r)}{\partial r} + \frac{\partial v_z}{\partial z} = 0 \tag{9.6}$$

Integrating the equation (9.3) on the z-component leads to:

$$\eta \frac{\partial v_r}{\partial z} = \frac{\partial p}{\partial r} z + C_1 \tag{9.7}$$

$$\eta\, v_r = \frac{1}{2} z^2 \frac{\partial p}{\partial r} z + C_1 z + C_2 \tag{9.8}$$

With the boundary conditions v_r (z = 0) = 0 and v_r (z = h) = 0 one gets the form:

$$v_r = \frac{1}{2\eta} z (z - h) \frac{\partial p}{\partial r} \tag{9.9}$$

Integrating the equation (9.6) on the z-direction with the boundary conditions v_z (z = 0) = 0 and v_z (z = h) = u (the speed of the lifted plate) and the above expression for v_r one gets:

$$-v_z = \int_0^z \frac{1}{r}\frac{\partial}{\partial r}(r v_r)\, dz \tag{9.10}$$

$$\Leftrightarrow \qquad v_z = -\frac{1}{r}\frac{\partial}{\partial r}\left(\frac{r}{2\eta}\frac{\partial p}{\partial r}\right)\left(\frac{z^3}{3} - \frac{z^2}{2} h\right) \tag{9.11}$$

With the boundary condition v_z (r, z = h) = u the above equation becomes:

$$u = -\frac{1}{r}\frac{\partial}{\partial r}\left(\frac{r}{2\eta}\frac{\partial p}{\partial r}\right)\left(-\frac{1}{6} h^3\right) \tag{9.12}$$

$$\Leftrightarrow \qquad \frac{\partial}{\partial r}\left(r \frac{\partial p}{\partial r}\right) = \frac{12 \eta r u}{h^3}$$

Integration on the r-component gives:

$$\frac{\partial p}{\partial r} = \frac{12 u \eta}{h^3}\frac{r}{2} + \frac{A}{r} \tag{9.13}$$

Further integration gives the expression:

$$p_{(r)} = \frac{12 u \eta}{h^3}\frac{r^2}{2} + A \ln r + B \tag{9.14}$$

The pressure at r = 0 must be finite, so the constant A must be 0. The boundary condition p (r = R) = p_0, gives the expression:

$$B = p_0 - \frac{12u\eta}{h^3}\left(r^2 - R^2\right) \tag{9.15}$$

This gives the expression for the pressure $p_{(r)}$ and dp/dr:

$$p_{(r)} = p_0 + \frac{3u\eta}{h^3}\left(r^2 - R^2\right) \tag{9.16}$$

$$\frac{\partial p}{\partial r} = \frac{6u\eta}{h^3} r \tag{9.19}$$

Putting this result into the above equation for v_z one gets:

$$v_z = -\frac{6u}{h^3} r\left(\frac{z^3}{3} - \frac{z^2}{2}h\right) \tag{9.20}$$

This expression is larger than 0 for the z-component smaller than h.

Finally the expression for v_r becomes:

$$v_r = \frac{3u}{h^3} r\, z\left(z - h\right) \tag{9.21}$$

$$F_{(r)} = \int p_{(r)}\, dA \tag{9.22}$$

$$= \int_0^{2\pi} \int_0^{R} p_{(r)}\; r\, \partial r\, \partial \varphi$$

$$F_{(r=R)} = \pi R^2 p_0 - \frac{3\pi\eta u R^4}{2h^3} \tag{9.23}$$

Where $F_{(r=R)}$ is the force needed to separate the plates.

The first part comes from the extensional pressure p_0 . The second part is the maximum force needed to lift the plate.

The force is directly proportional to the viscosity. It is also proportional to u, and depends on R^4 and $1/h^3$.

9.2 Force balance if only surface energy is apparent:

The following chapter deals with the case, that two plates are separated with a non flowing fluid in between. The only forces that contribute to the separation force are pressure and the surface tension of the fluid.

A change in the surface of a body can be expressed by the thermodynamic equation:

$$dA = -S\Delta T - p\,dV + \gamma\, d\sigma_a \tag{9.24}$$

Where:

A: the Helmholz- energy

S: the entropy

T: the temperature

p: the pressure

V: the Volume

γ: the surface energy

σ_a: the change of the surface area.

For a spherical body with a variable surface one gets the following equilibrium of forces:

$$4\pi r^2 p_i = 4\pi r^2 p_a + dW \tag{9.25}$$

The surface energy is $4\,\pi\, r^2\, \gamma$

p_i = pressure within the body

p_a = pressure outside the body

The change of energy is equal to the work:

$$\frac{\partial}{\partial r}\left(4\pi r^2 \gamma\right) = 8\pi r \gamma = dW \tag{9.27}$$

By putting this expression into the force balance one gets the expression:

$$\Delta p = p_i - p_a = \frac{2\gamma}{r} = \frac{2\sigma\cos\alpha}{r} \tag{9.28}$$

Where

α: is the contact angle between liquid and surface

σ: is the surface tension

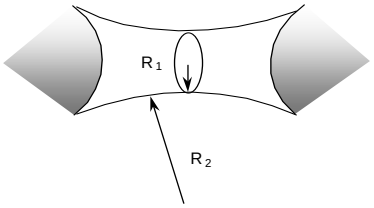

Fig. 9.2: Fluid bridge between two solid bodies.

The change of pressure due to pulling apart two bodies can be estimated with the Laplace equation as:

$$\Delta p = \sigma\left(\frac{1}{R_1} - \frac{1}{R_2}\right) \tag{9.29}$$

Where

σ: the surface tension [N/m]

For a separation of two plates with a liquid between the plates, which is not flowing, the problem can be expressed as followed: The only forces that contribute to the separation force are the surface tension and the pressure:

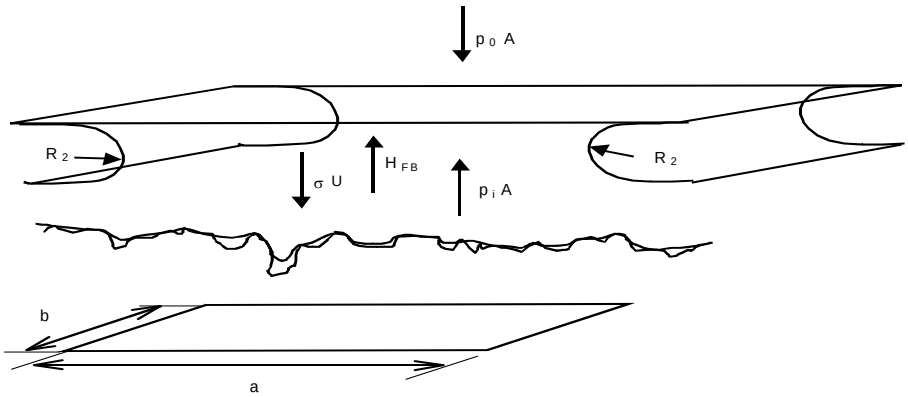

Fig. 9.3: Separating plates with non flowing liquid in between

With

σ : surface tension of the ink on the substrate

U: surrounding line of the surface (=2a + 2b)

A: area of relevant surface

$$\begin{aligned} H_{FB} &= \sigma \cdot U - p_i + p_0 \cdot A \\ &= \sigma \cdot U + \Delta p \cdot A \end{aligned} \tag{9.30}$$

By substituting the pressure difference with the Laplace-equation one gets:

$$\Delta p = p_0 - p_i = \sigma\left(\frac{1}{R_1} + \frac{1}{R_2}\right) \tag{9.31}$$

According to the above definition the radius R_1 is ∞ while R_2 is finite. R_2 is smallest for the critical breaking state this model is applied to. So the surface adhesion force is getting:

$$F_{\text{Ahesion to surface}} = H_{FB} = \sigma \cdot (2 \cdot a + 2 \cdot b) + \frac{\sigma}{R_2} \cdot a \cdot b \tag{9.32}$$

This would be the total separation force.

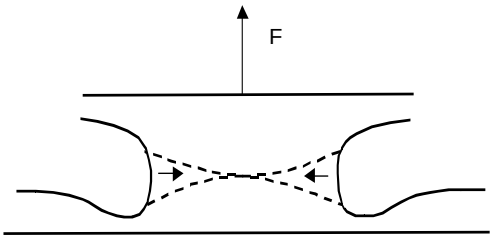

Fig.9.4: Separation of plates with cohesive failure

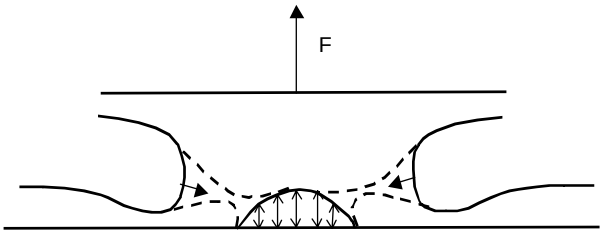

Fig.9.5: Separation of plates with adhesion failure to the substrate

If the splitting occurs to a part between the substrate and the liquid, a new force component has to be added to equation (9.32):

$$F_{\text{Adhesion to surface}} = H_{FB} = \sigma \cdot (2 \cdot a + 2 \cdot b) + \frac{\sigma}{R_2} \cdot a \cdot b - F_{\text{ink}-\text{surface}} \tag{9.33}$$

The total separation force would be then:

$$F_{\text{total}} = F_{\text{Adhesion to surface}} + F_{\text{ink -surface}} \tag{9.33.1}$$

However the radius R_2 is a rough approximation only to what happens in reality. The radius R_2 is determined by the surface tension of the liquid and by the contact angle between the fluid and the above plate and the fluid and the lower substrate.
One can draw following conclusions:

The separation force increases with:

- a greater covered area
- an increased surface tension of the fluid
- with a smaller radius R_2 due to a smaller gap between plate and substrate or a higher surface tension of the substrate surface

In the special case with adhesion failure, the separation force increases with a better connection between ink and surface due to better wetting. This confirms the findings of [31]

9.3 Absorption of solvents through capillary pressure forces:

The following chapter deals with absorption, which effects the rise of ink tack.

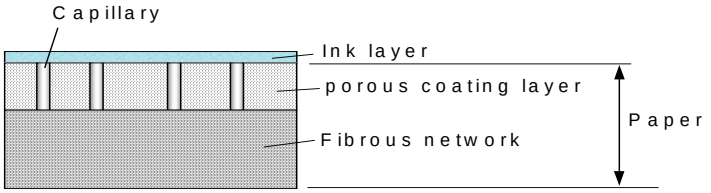

Fig. 9.6.a: Sketch of a capillary absorption of offset ink through a coated board surface

The predominant absorption mechanism of fluid into a porous substrate, like a coating layer , is the capillary absorption. This capillary absorption is however slowed down by the resistance to flow generated by the deposition of ink pigments at the ink-coating layer interface.

The amount of fluid that is passing through a thin capillary can be expressed by the Hagen-Poisseuille-law for laminar flow [22]:

$$\frac{\partial V}{\partial t} = \frac{r_k^{\,4}\,\pi}{8\eta} \cdot \frac{\Delta p_k}{l_k} \tag{9.34}$$

where

dV/dt is the volume-flow [m^3/s]

r_k is the radius of the capillary [µm]

Δp_k pressure gradient [Pa]

l_k length of the capillary [µm]

η viscosity of the fluid [Pa s]

When looking at the Hagen-Poisseuille-law the expression:

$$R = \frac{8\eta l_k}{r^2} \tag{9.35}$$

Is considered as the resistance connected to the flow. Further increase of the resistance due to increasing amount of particles that cover the pores during absorption of ink is considered linear with the length of the capillary. So the increasing resistance is [30]:

$$\Delta R = k \cdot l_k \tag{9.36}$$

$$\Delta p = (R + \Delta R)\,\frac{\partial V}{\partial t} \tag{9.37}$$

when putting the expression for the pressure gradient and the increasing resistance into the above expression one gets the equation with (9.28):

$$\Delta p = \frac{2\sigma\cos\alpha}{r_k}$$

$$\frac{\partial V}{\partial t} = \frac{\pi r_k^{\,3}\,\sigma 2\cos\alpha}{8\eta l_k + k l_k r^2} \tag{9.38}$$

This expression shows the connection between volume flow and surface tension of a liquid. Assuming a cylindrical shape of the capillary one gets following absorbed volume for the penetration of the capillary:

$$V = \pi r_k^{\,2} l_k \tag{9.39}$$

Putting this into the above expression one gets:

$$\frac{\partial V}{\partial t}\pi r_k^{\,2} l_k = \frac{2\,\pi^2\, r_k^{\,5}\,\sigma\cos\alpha}{8\eta + k r^2} \tag{9.40}$$

$$V\,dV = \frac{2\,\pi^2\, r_k^{\,5}\,\sigma\cos\alpha}{8\eta + k r^2}dt \tag{9.41}$$

$$V^2 = \frac{4\,\pi^2\, r_k^{\,5}\,\sigma\cos\alpha}{8\eta + k r^2}t \qquad \text{(since } V^2 = 0 \text{ is the initial condition)} \tag{9.42}$$

$$V = \pi r^2\sqrt{\frac{4\, r_k\,\sigma\cos\alpha\, t}{8\eta + k r^2}} \tag{9.43}$$

$$\frac{\partial V}{\partial t} = \frac{\pi r^2}{2}\sqrt{\frac{r\sigma\cos\alpha}{8\eta + k r^2}}\cdot\frac{1}{\sqrt{t}} \tag{9.44}$$

So the following conclusions can be drawn:

- The absorption of fluid increases with decreasing fluid viscosity
- The amount of absorbed fluid decreases with the reciprocal of the root of the time. So the absorbed amount is highest in the beginning.
- The radius of the capillary has the highest impact on fluid absorption.
- The surface tension is of smaller influence. With higher surface tension (lower contact angle) the amount of absorbed fluid increases.
- The absorbed amount of ink linearly increases with rising number of capillaries.

To compare the impact of the capillary radius, the above equation (9.43) is resolved with respect to the length:

$$l_k = \sqrt{\frac{4\, r_k\,\sigma\cos\alpha\, t}{8\eta + k r^2}} \tag{9.45}$$

By simulating the absorption with $\gamma =$ 30 m N/m, $\theta = 0°, \eta =$ 2000 mPa s, and a resistance-factor of 0, 10^6, 10^8 mPas/r^2 the following graphs are obtained:

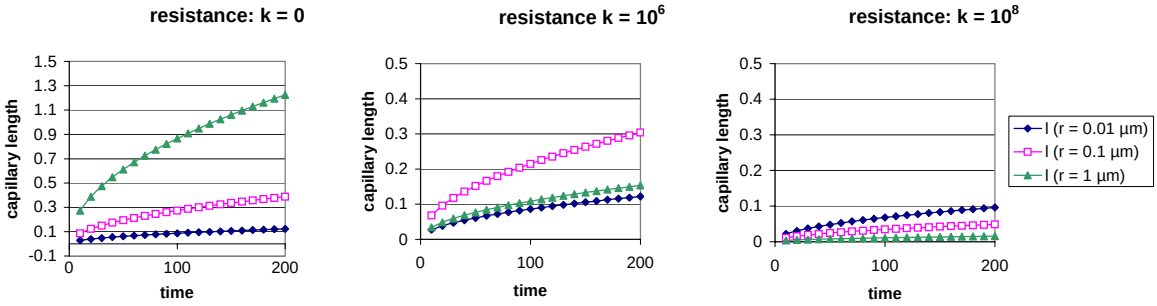

Fig. 9.6: Simulation of absorption with different capillary radii and different resistance factors

The above curves show, that for a process with greater factors of resistance the rate of absorption increases with smaller pores. As to be seen, the absorption rate does not increase linearly. The separation of the carrier phase from a high viscous pigment dispersion, like offset ink, would be such a case.

9.4 Contact of two cylinders:

The following chapter tries to explain what could be responsible for print problems in a real printing process. This chapter deals mainly with the contact area of a blanket cylinder with paper to be printed and the impression cylinder. The results are important for chapter 9.6.

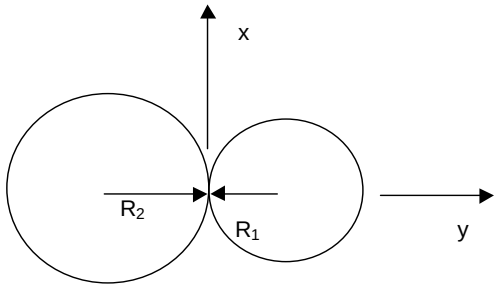

Fig. 9.7: Touching of two cylinders

If two cylinders are pressed together, the contact area that they have in common forms a stripe with the length 2 a. The length of the cylinders is approximated to be infinite.

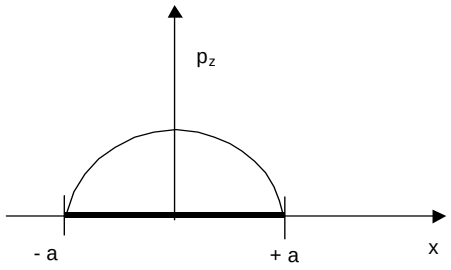

Fig.9.8: Pressure distribution on a strip with the length 2 a

The pressure distribution on the strip is:

$$p_z(x) = \frac{2F}{\pi a}\sqrt{1-\frac{x^2}{a^2}} \tag{9.46}$$

So the pressure is for:

$$p_{z(x=\pm a)} = 0$$
$$p_z = \frac{2F}{\pi a} \text{ for } x = 0 \tag{9.47}$$

F is the load that is acting on the cylinder in [N].

$$\frac{1}{R_1}+\frac{1}{R_2}=\frac{16DF}{3\pi a^2} \tag{9.48}$$

With

$$D=\frac{3}{4}\left(\frac{1-\nu_1^2}{E_1}+\frac{1-\nu_2^2}{E_2}\right) \tag{9.49}$$

Where:

ν : are the cross contraction constants for both cylinders

E: is the E- modulus of the cylinder material

Putting D in the above equation the length of the strip becomes:

$$a=\sqrt{\frac{16DF}{3\pi}\frac{R_1R_2}{R_1+R_2}} \tag{9.50}$$

If the two cylinders represent the printing cylinder and the impression cylinder of a print press and the substrate sticks to the inked printing cylinder due to adhesion between substrate and ink, one can draw following conclusions:

With increasing compressibility of a substrate, the expression D increases. The thicker the substrate is, the greater the radius will be. Thus the length a in eq.(9.50) will rise with thicker and more compressible substrates.

9.5 Flow of a liquid film between two rotating cylinders:

The flow of a liquid film between two rotating cylinders always occurs in the printing process. This chapter is important for the chapters 10.3.2 and 10.3.3.

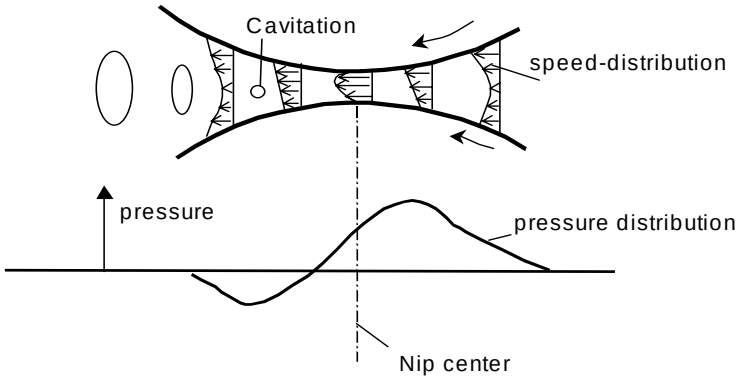

Fig. 9.9: Pressure and speed distribution of a liquid between two rotating cylinders

The fluid passes through the nip undergoing first a high pressure, followed by a region of low pressure or tension. If the surface velocity and fluid viscosity are low enough, the cohesion of the fluid is big enough to withstand the tension developed, and the fluid splits smoothly along a single air liquid surface. At higher speeds and viscosities, the fluid cannot flow rapidly enough to relieve the tension formed as the cylinders separate. Cavities are formed within the film. The growth of these cavities leads to a film split with nearly equal quantities of fluid on each surface.

9.6 Balance of moments and forces in the printing process:

This chapter deals with the mechanical forces occurring in a real printing process. This chapter should help to understand how delamination takes part.

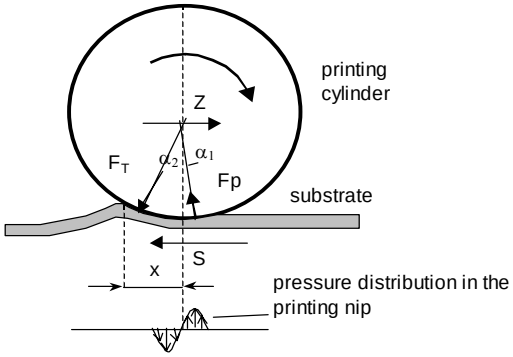

Fig. 9.10: Balance of forces and moments in the sheet fed offset process [17]

Z: bearing force of the printing cylinder

F_T: tack-force at the end of the nip.

F_P: pressure force in the beginning of the nip

S: shear force in the ink film

$\alpha_{1:}$ angle between the resulting pressure force and middle line of the cylinder

$\alpha_{2:}$ angle between the resulting dragging force and the middle of the cylinder

The sum of the forces gives:

$$Z = S + F_p \sin\alpha_1 + F_t \sin\alpha_2 \tag{9.51}$$

The sum of moments gives:

$$S\,r + F_t\,r \sin\alpha_2 + F_p\,r\,\sin\alpha_1 + M = 0 \tag{9.52}$$

Where M is the driving momentum

From the balances it can be seen:

With increasing pressure the shear energy and the forces F_t and F_p will rise as well. In the case of a compressible substrate the angles α_1 and α_2 will increase. Thus the resulting moments increase. By enhancing the driving moment in form of higher print speed, the reacting forces F_p and F_t will increase as well. With increasing coating weight the z-direction strength of a paper/board seems to decrease [41].

Thus the following conclusions can be drawn:

- **Ink tack increases with increasing print speed and increasing printing pressure.**
- **Thus the danger for delamination of the board increases.**

10. Experimental:

The test procedure and the function of the apparatus is described in the following chapter. The influence of the most important settings of the machine, the influence of inks and substrates are investigated

10.1 Description of the apparatus:

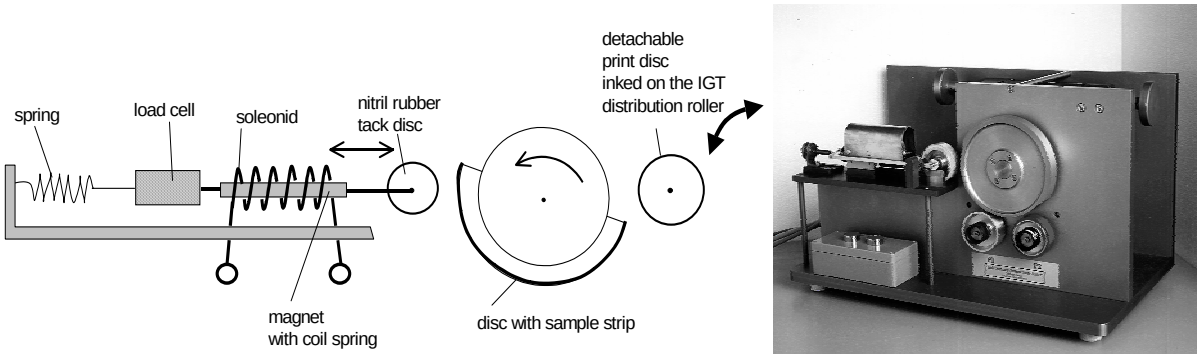

Fig. 10.1: principal function and photograph of the ink tack measuring apparatus

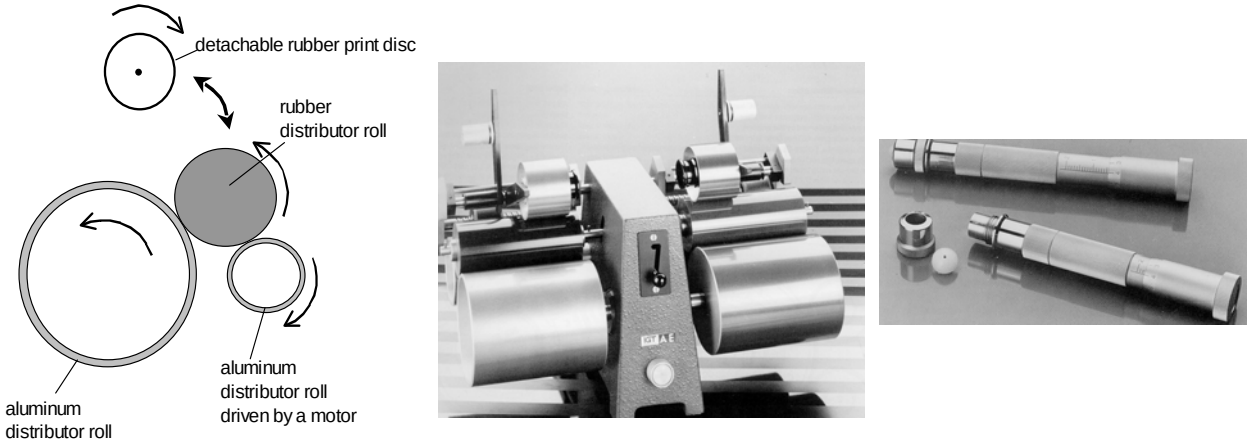

Fig. 10.2.a: Design and photograph of an IGT ink distributor and a photograph of an IGT Ink pipette

A sample is fastened with a double adhesive tape to the sample plate.
With an IGT- ink pipette a defined amount of ink (a standard amount is 0,3 cm^3) is distributed to the IGT-ink distributor. The ink is sheared and distributed over the entire roller surfaces (the standard time for this procedure is 1 minute). The IGT ink distributor consists of a number of rotating cylinders of varying diameters in order to create sufficient shear to achieve a thin and even distribution of the ink film to the detachable rubber printing disc, similar as the duct of cylinders in a full scale offset press.
Then the print disc is added to the distributor. This disk is inked for an additional minute. In the next step the inked printing disc is placed on the ink tack tester. With a PC signal the

sample platen rotates and the sample is printed. The contact pressure between the sample plate and the inking roll can be adjusted from 0 to 600 N.

The tack disc is pushed with an electromagnetic force into contact with the surface of the sample. The duration of the contact can be adjusted from 0,5 to 10 s. The tack disc surface consists of nitrile-rubber, which is the same material used for rubber-blankets in print presses. The electric signal in the solenoid breaks off, the load cell is activated and the spring pulls the construction back with a defined force. The pulling force between tack disc and inked sample is transformed into an electrical signal in the load cell. Thus the splitting process is registered. The actual film split is registered by a light sensor. The highest signal during this splitting process is plotted into the diagram. The sample plate rotates to a new position and the process repeats 12 times. As a result one gets a force to time curve with 13 values that show the highest measured value. The time between the values can be changed. The sample is fastened as a control beside the diagram.

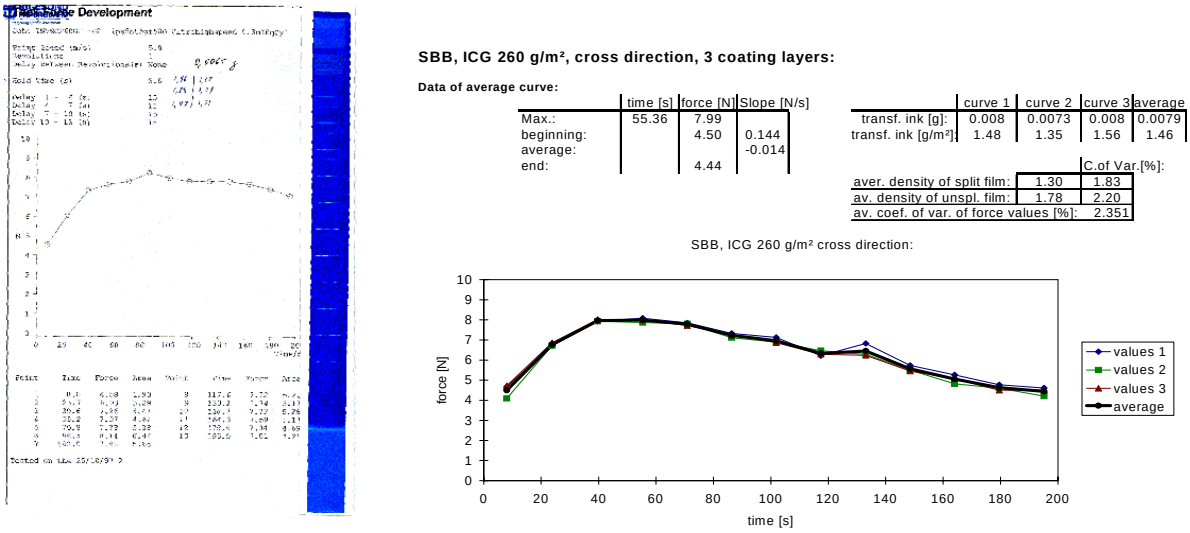

Fig. 10.3: Example of a splitting force/time-diagram and the diagrams already exported

The data of the curves are then exported on a Excel spread sheet. Each curve can be described by considering three segments [31]:

1. **The rise time**: This is predominantly related to the speed of absorption by the coating/paper surface on initial contact with the ink. Typically, the force splitting marks are, compared to the surrounding unsplit area, a lighter area with a very light line in the middle (see Fig. 10.5 for examples). The following tack marks get lighter and more defined marks until the maximum is reached. This time is determined by the available amount and diameter of the pores of the oil absorbing coating layer.
2. **The maximum separation force**: This is a combined measure of the adhesion of the immobilized ink layer in contact with the coating surface and the cohesion within the ink layer.

3. **Surface tack decay**: With time the tack marks turn to darker areas with a very light line in the center. Finally only the light lines can be detected. These lines turn thinner and thinner until they finally vanish. This stage is determined by the overall available pore volume in the coating. The amount of interfacial bondings within the ink-film and to the pigmented surface increase until the film is solid. The ink film has set.

According to the supplier of the equipment the same paper/ ink should be tested 3 times together with a control sample. For detailed comparison the inking should be confined to one sample. This means that after every test print, the ink distributor should be cleaned.

Each pull-off mark is preceded by an area, that shows the film split of the rolling tack disc.
The density of the area before the first tack mark is measured with an densitometer at three different points.
Density can be used as a variable that, is connected with the transferred ink amount.

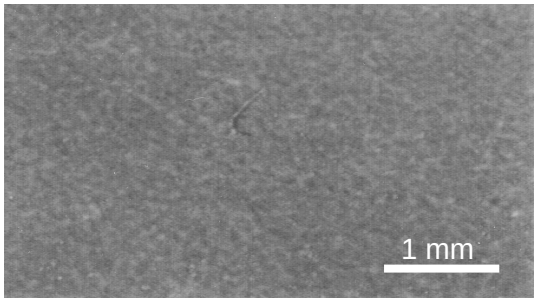

Fig. 10.4: Photograph of a printed board surface

At the unsplit area the density measurement is performed 3 times at different points. In the diagrams (example: see Fig. 10.3), the coefficient of variation of the force values and the density values are calculated:
This is done by using the formulas: [32], [33]

$$S_i^2 = \frac{1}{n} \sum_{i=1}^{n} \left(x_i - \bar{x}\right)^2 \tag{10.1}$$

$$\bar{x} = \frac{\sum_{i=1}^{n} n_i x_i}{\sum_{i=1}^{n} n_1} \tag{10.2}$$

$$\sqrt{\bar{S}^2} = \sqrt{\frac{S_1^2 + S_2^2 + S_3^2 + S_n^2}{n}} \tag{10.3}$$

$$S_{\bar{x}} = \frac{\sqrt{\bar{S}^2}}{\bar{x}} \tag{10.4}$$

In order to mathematically describe a curve of 13 data points, the following data are recorded and calculated:

- tack-force maximum,
- the time until the tack-force-maximum,
- the first measured force value,
- the last measured force value,
- the slope between the first and the second data point (beginning slope),
- the slope of the second and the last data point (average slope)

It has to be mentioned, that the determination of the weight of the transferred ink is not very exact due to evaporating of the cleaning liquid in the inner parts of the rubber inking disc. After every experiment all parts have to be cleaned with a mild solvent.

10.2 Analysis of the tack marks:

Almost always the same pattern in ink tack marks on a coated paper/board surface can be observed:

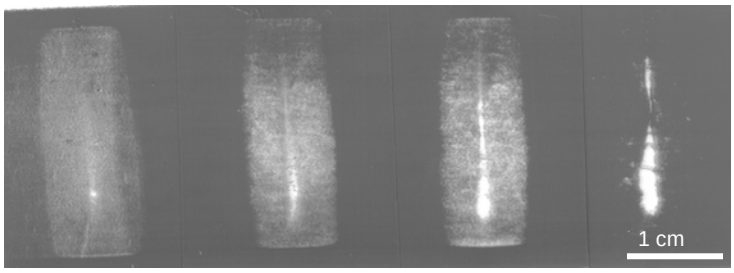

Fig. 10.5: Photographs of ink tack mark development (from left to right) on a coated surface.

These marks present a continuous overlapping of the processes sketched in Figs. 9.4 and 9.5. A more detailed development of those markings can be seen when performing the test on a surface treated mylar film:

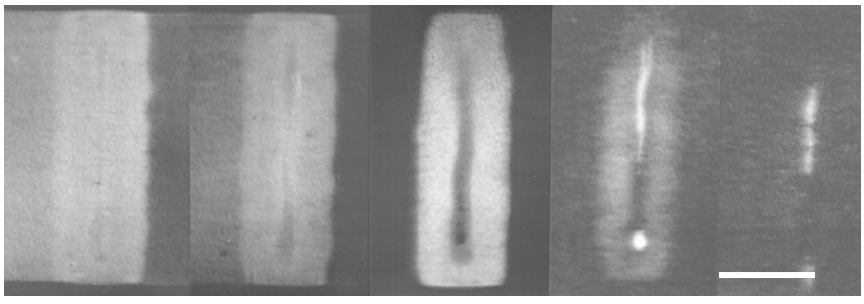

Fig. 10.6: Photographs of ink tack mark development on a surface treated mylar film

By determining the forces, that were measured when the tack marks on the samples appeared, one can draw conclusions for the different effects that contribute to ink tack.

A single light line is seen when only the surface adhesion between ink and substrate is important.

The lighter area around the light line is determined by flow phenomena (see third mark in Fig. 10.5, compare with Fig. 9.5. These marks are always present, when the largest forces are measured.

In the development of tack marks, the force value of the last visually detectable white line, and the force value of the last detectable white line with a lighter surface, that obviously distinguishes from the surrounding unsplit ink film, are determined.

10.3 Machine parameters:

The first part of the thesis deals with the investigation of the parameters that are related to the machine. A factor trial has been performed to rank the influencing parameters. One objective of the thesis is to find a reliable machine setting that gives a low standard deviation or a low coefficient of variance.

For the factor design the following material was used:

- Invercote G 260 g/m^2, printed in the cross direction
- Equinox Cyan Ink supplied by the supplier of the Ink-tack apparatus.

10.3.1 Influence of the applied ink amount on the tack-force/ time-curves:

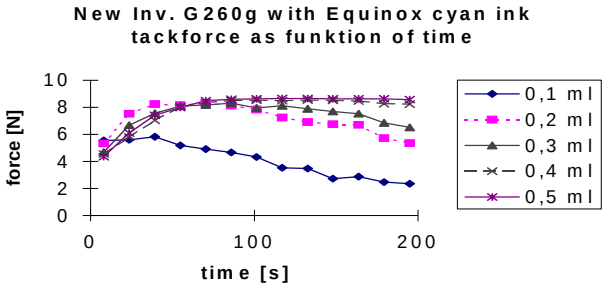

Fig. 10.7: Effect of increase of ink amount on coated board

When decreasing the applied amount of ink to the IGT distributor, the following results are obtained:

Less ink is transferred to the sample, so the solvents can be easier absorbed. Thus the rise of tack is higher. The maximum force level is reached after a shorter time and the decay of the tack-force-curve is more pronounced.

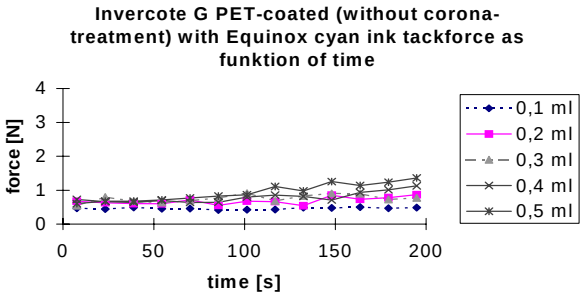

Fig. 10.8: Increase of ink amount on a non-absorbent rough PET foil.

The situation is similar for a non absorbent rough PET-film:
With increasing amount of ink, the measured tack force increases, probably due to a larger area of the tack-roll, which is covered by ink as sketched in Fig. 10.8.1.

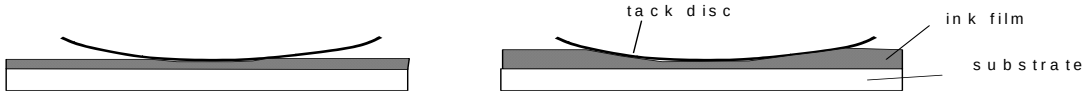

Fig. 10.8.1: Increase of ink tack due to a larger covered area of the inked tack disc

The force values rise with time because some solvent of the ink is evaporating and due to a beginning polymerization of the ink film.

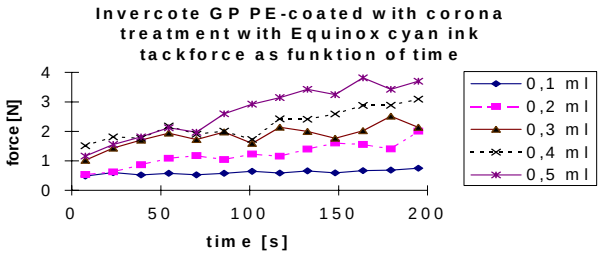

Fig. 10.9: Increase of ink amount on rough corona treated PE-foils

A corona treated film shows the same development. The measured forces increases with higher amount of ink. The overall values are higher due to the higher surface tension. An explanation for this behavior can be found in the balance of forces (9.33).

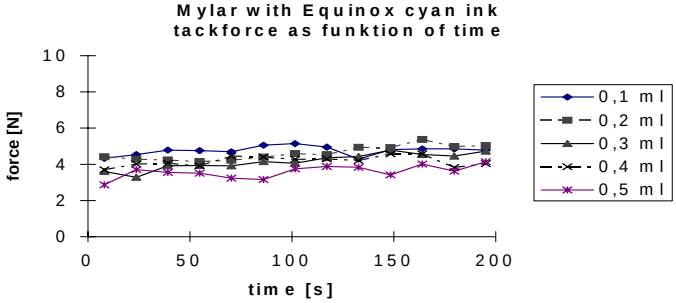

Fig. 10.10: Increase of ink amount on very glossy surface treated mylar films

For a very glossy mylar-film the situation is different:

With increasing ink amount decreasing force values are measured. The reason for this is to be found in the surface roughness. The roughness index was 9,1 µm for PET, 7,7 µm for corona treated rough PE and only 0,75 µm for glossy mylar films (lower values [µm] mean lower roughness).

The roughness has in the case of mylar films the greatest impact, as can be seen in (9.23), where film thickness has a $1/h^3$ – effect on the measured tack force.

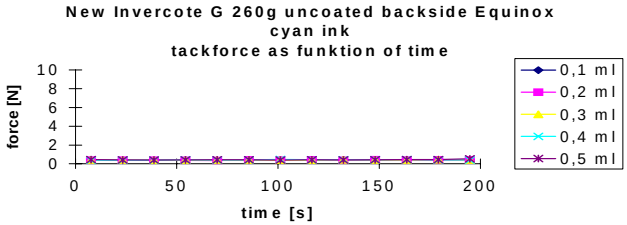

Fig. 10.11: Increase of ink amount on very absorbent uncoated baseboard.

By performing the experiment on the absorbent uncoated backside of a board (Invercote G 260 g/m^2), It can be seen that no tack-force can be measured. 0,3 N is a constant value that appears to suppress electronic disturbing signals from outside. The tested sample is a very rough substrate that had an approximate roughness value of 7 µm. It is very probable that the binder phase migrates together with the oils into the fibrous surface.

Thus ink tack is both

- **A flow phenomenon explainable with the Navier-Stokes equation and**
- **A surface tension problem phenomenon**

Both processes overlap each other.

10.3.2 Increase of print speed:

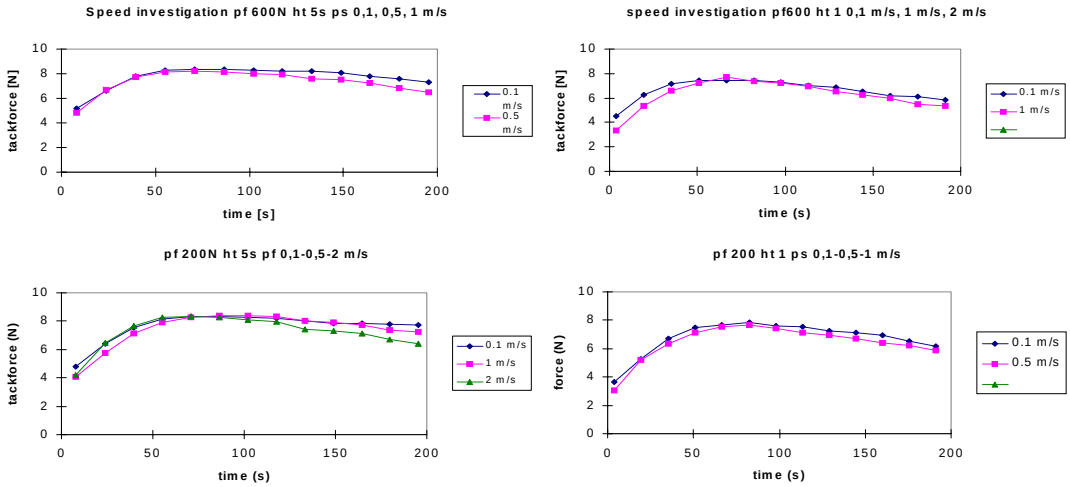

Fig. 10.12: Example curves of tack-force/time for different speeds

When increasing the print speed, the transferred amount of ink slightly decreases. This is confirmed by comparing the color densities of the unsplit films:

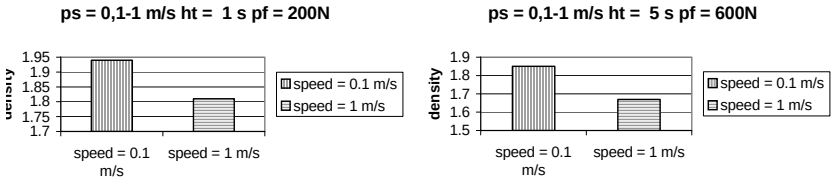

Fig.10.13: Example curves of reduced densities due to less transferred ink at higher speeds.

The fact that the ink needs time to wet the surface and to flow inside the pores, before the film split behind the rubber roll occurs, can explain why, with higher print speeds, the transferred ink decreases. Usually the film split occurs half way through the nip.

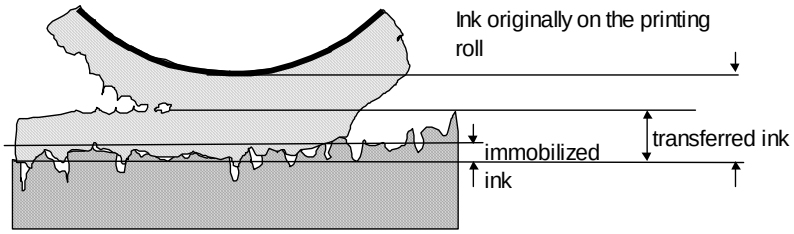

Fig. 10.14: Transferred ink from the print roll to the substrate

A simple linear relation called the `Walker-Fetzko´ equation (1) describes the above situation:

$$y = b + f\,(x - b) \qquad (10.5)$$

y: amount of ink transferred per unit area of a print

x: ink film thickness originally on plate

b: immobilization or acceptance capacity of substrate surface for ink

f: constant fraction of the remaining ink transferred to the stock, usually 50 %

On the other hand, a higher speed induces a higher shear to the ink film. With the sample disc accelerating the inked color disc, a Couette-flow (shear flow) situation is achieved. The ink is sheared to a greater extent near the sample plate.

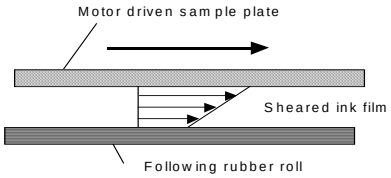

Fig. 10.15: Even Couette flow between two plates

One roll (the sample plate) is accelerated by the motor. The inked color disc is accelerated and the ink between the two cylinders is sheared. The resulting flow profile should be a high speed region near the sample roll, that slightly decreases towards the color roll.

Both processes, a Couette flow, and a time dependent wetting of the surface, contribute to a decreasing amount of transferred ink. With smaller amount of transferred ink, it should be expected, that the absorption would take part quicker and the first measured values would already be higher. This is not the case, as seen from the experiments.
The fact that the first measured force value is lower, although less ink is transferred, might be explained by the thixotropic behavior of the ink. With higher shear rates, the viscosity of ink decreases due to breakdown of internal structures.
A low viscosity of a fluid will give the measuring tack roll lower resistance to the film split.

According to the article of J. H. Taylor and A. C. Zettlemoyer "Hypothesis on the mechanics of ink splitting during printing" [43], cavity growth and ultimate film split proceeds most rapidly in the direction of reduced viscosity towards the substrate.
The above results have been confirmed with a factor trial and an additional test with the highest possible machine speed.
At some pressure and speed combinations the inking roller is accelerated to the outside, so that the inking roll jumps over the first part of the sample strip. The diagram below shows the critical settings, i.e. the maximum speeds and lowest pressure forces to use:

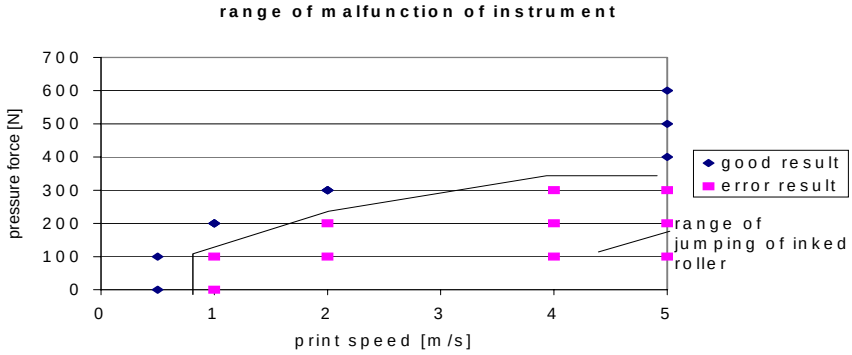

Fig. 10.16: Range of malfunction of the instrument due to jumping

10.3.3 Increasing the pressure force:

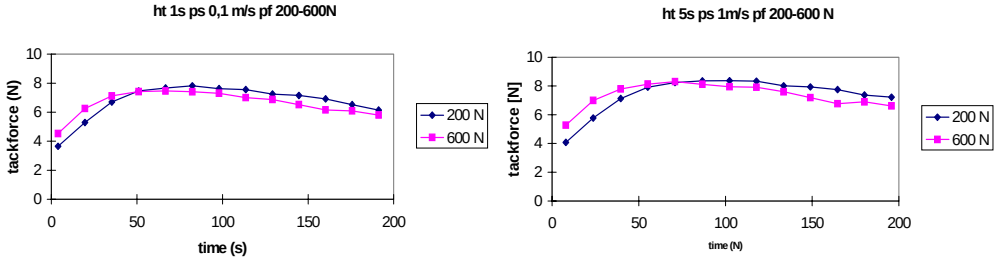

Fig. 10.17: Example curves of reduced transferred ink due to higher pressure

By increasing the pressure force between the inked disc and the sample, the ink is sheared more extensively. The distance between the ink roller and the sample decreases. Due to enhanced pressing of the ink into the pores and the “valleys” in the topography of the rough substrate, the contact is increased. Thus the surface is better wetted by the fluid. According to literature [37], a higher ink transfer to the substrate would be expected. This is not the case, as the curves and the measured densities of the samples show.

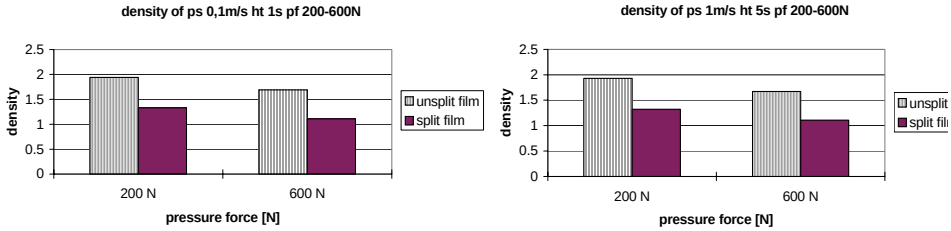

Fig. 10.19: Example values of reduced density due to higher pressure

By evaluating the factor trial it can be observed, that increasing the pressure force has a significant effect (above 95% probability) to a decrease in color density of the ink film. An explanation for this can be, that the material used (i.e. 330 µm board + adhesive tape) was very compressible. This would explain, why some wide macro-pores can be pressed flat. The amount of possibly immobilized ink decreases.

Very often it can be read in literature [37], that due to a higher pressure the ink is already separated from some solvent and some fluid is pressed into the substrate. This would have the consequence, that pigments would accumulate at the porous surface (i.e. formation of a filter cake). A sketch of this possible process is to be seen below.

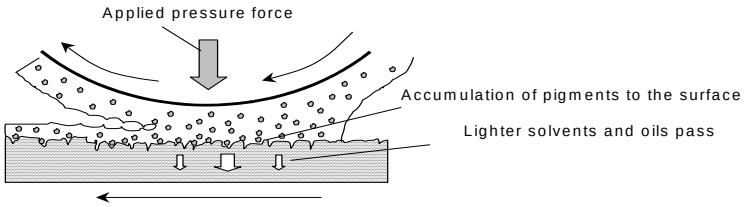

Fig. 10.20: Supposed filtration process during printing under extensive pressure

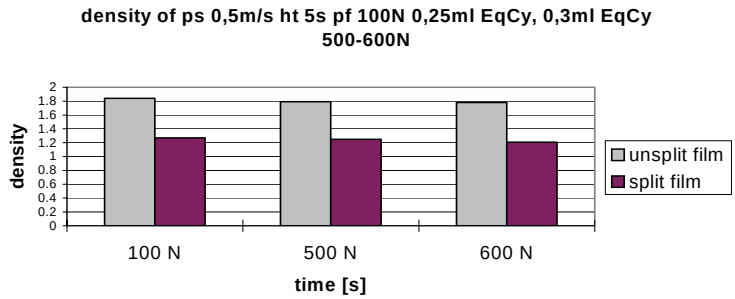

Fig. 10.21: Experimental investigation if densities of split films would change due to higher pressure

When looking at the density of a split film, the conclusion has to be drawn, that a filtration process probably does not take place.

An experiment, in which less ink than usually was used (0,25 ml on the ink distributor), in order to achieve the same densities of the unsplit film printed with higher pressure, showed, that the split film after 8 seconds of setting does not have a lower density than the film split at a higher pressure. Thus at least for these experiments it can be excluded, that higher pressures introduce a filtration process of the ink. Fig. 10.20 therefore does not present what has been observed in the experiments.

The applied pressure ranges from 0 N to 800 N. According to the supplier the spring has a maximum force of 600 N [36]. So it is not recommended to choose higher pressures than 600 N. However according to the results of the factor trial a higher coefficient of variation is obtained with higher pressures.

10.3.4 Increasing the hold time between the measuring tack-roller and the ink covered sample:

Increasing the hold time between the ink-covered sample has a high impact on the resulting curve.

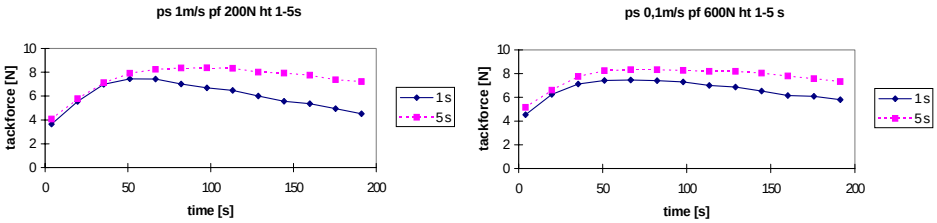

Fig. 10.22: Example tack-force/time curves with increased hold time

An increase in hold time has of course no influence on the transferred ink amount and on the density, nor on the coefficient of variance of density.

Since the first force value is measured after the extra holding time, some part of the ink-solvent absorption has taken place. So a later part of the actual force curve is measured.

Due to convenience, the same time scale for the x-axis is chosen, when exporting the files to Excel. This is necessary to calculate average forces and standard deviations etc.. But even if 4 seconds are added to the time scale, higher values with higher hold times can be observed. This might be due to the thixotropic behavior of the ink.

By pushing the tack-roller onto the ink film, the internal structure of the ink is destroyed, due to breaking the van-der-Waals bonds. When using 1 second contact time, the time available for these “broken structures” to build up again, is lower than when using 5 seconds contact time. Thus one measures higher tack-forces after longer holding times. The difference is more pronounced with more advanced setting times. This could result from the fact, that due to less viscous phase available, the tack-built-up-rate is quicker.

The tack-roller is pushed into the inked sample with a constant pressure. With higher viscosity, due to longer setting times, the ink cannot flow aside sufficiently well, as in the case of longer holding times. Thus a greater area of the tack-roller is covered, and the force to separate the tack roll increases. This is supported by the fact that more obvious tack-marks on the sample strip can be observed with longer hold times.

With help of a factorial trial following results were obtained with increasing contact time:

- The maximum force values increase significantly
- The beginning force values increase
- The coefficient of variance for force values decreases, which means that more reliable values are obtained.

One objective of the work carried out within the frame of the thesis was to find the ideal setting for future measurements

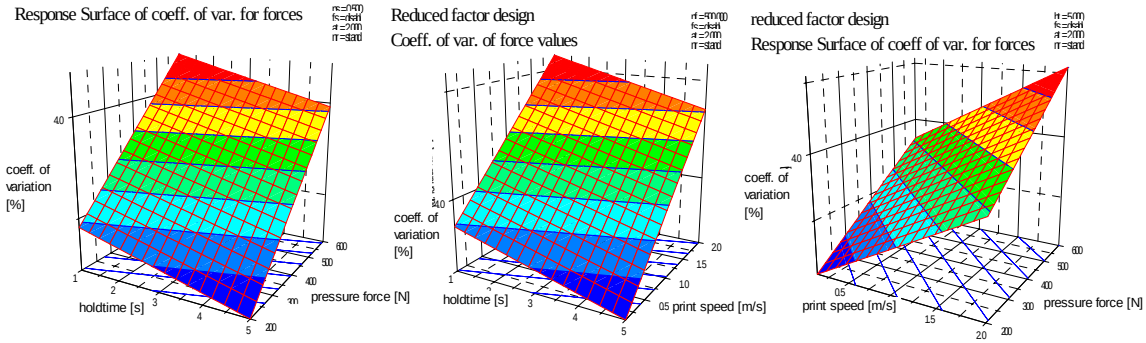

Fig. 10.23: Influence of parameters on the coefficient of variation

The recommended settings of the instrument supplier have been confirmed, i.e.:

- print speed 0,5 m/s
- hold time 5 s
- pressure force 500 N

10.3.5. Additional parameters tested:

The effects of changing further parameters were tested in order to understand the physical processes involved with ink tack development, and to find a ranking of the influencing parameters. A reduced factor trial with 6 variables and 20 experiments was made. Reduced factor trials can be utilized, when the overlapping effects are negligible. For the evaluation a computer program called Modde from the University of Umea was used. In addition to the previously tested parameters (holding time, print speed and pressure force), the following parameters were tested:

- The effect of a new, less used, nitril rubber covered tack-roll
- The effect of a longer application time. The application time is increased by leaving the ink for 20 minutes instead of 2 minutes on the ink distributor.

10.3.5.1 Increasing the ink distribution time:

The supplier of the instrument recommends not to use an ink that was too long a time on the ink distributor, because solvents and lighter oils may evaporate, or because an oxidation of some components of the ink might take place. [35, 36]. The supplier also recommends to shut down the ventilation device. The ink is constantly sheared and exposed to a big surface (1215 cm²).

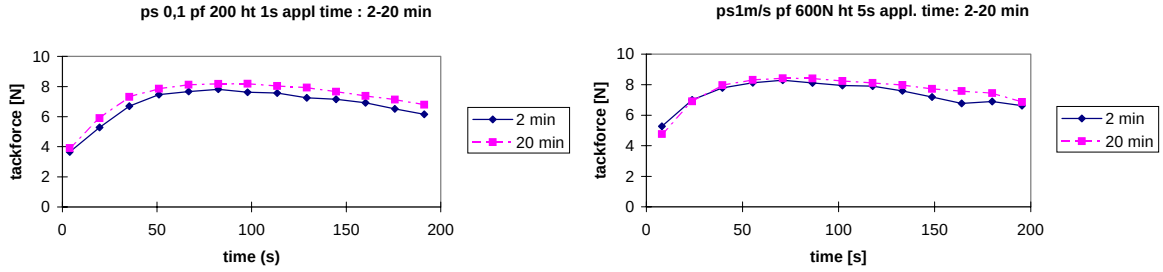

Fig. 10.24: Effect of longer distribution on the IGT color distributor.

The results show that a longer time on the ink distributor slightly increases all measured tack-force curves. The rise of the tack-force does not originate in a larger transferred amount of ink.

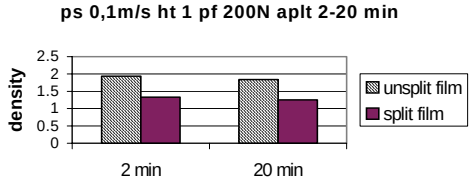

Fig. 10.25: Densities of a 2 and 20 minutes distributed ink

This can be seen from the densities of the ink films (Fig. 10.25). The densities remain almost constant. One possible explanation is the reaction of the ink with the oxygen or evaporation. Sheet-fed offset inks contain both mineral and vegetable oils. Therefore an oxidation or even polymerization of the inks cannot be excluded. Experiments like a rolling ball on an inked glass surface have shown, that after 30 min changes in the tackiness/viscosity of the ink can be detected [37]. In addition, experiments using the cryoscopic method showed that the molecular weight of the ink film rose from 1735 g/mol to 1864 g/mol after half an hour of exposure to air [37].

10.3.5.2 Influence of a new measuring disc surface:

The nitril rubber surface of a used disc is darker, smoother and glossier than that of a new disc, due to more extensive contact with ink and cleaning solvent.

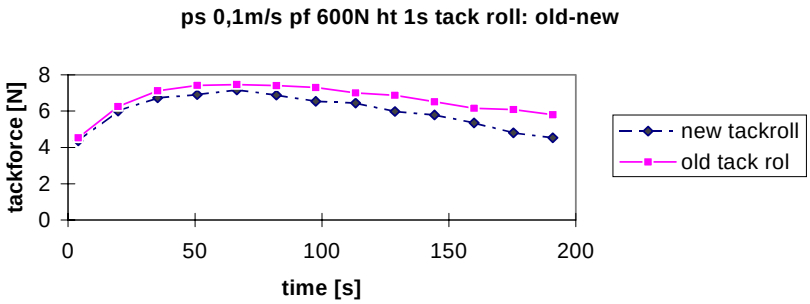

Fig 10.26: Difference between tack-force curves measured by an old and a new tack disc

When using a new tack-roll, one obtains tack-force values, that are lower than those, measured with an older standard roll. Since the surface roughness can have an impact due to a higher local gap between two separating plates, the greater roughness might contribute to lower measured forces.

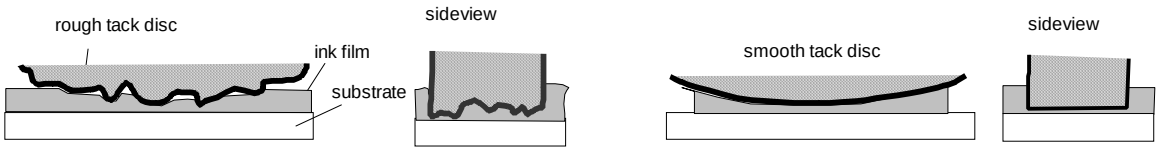

Fig. 10.27: Higher local gap due to increased roughness

10.3.5.3 Increasing the thickness of the measured sample:

The thickness of the substrate was increased by taping samples on samples using adhesive tape.

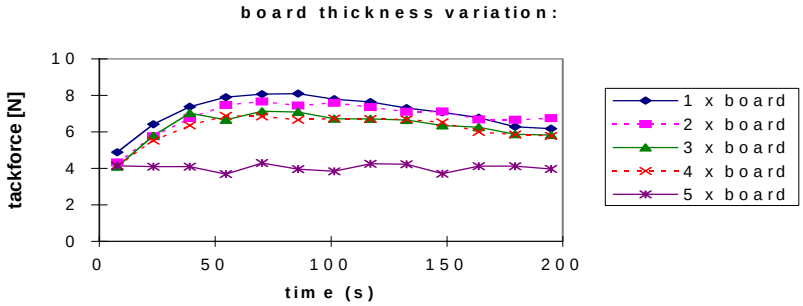

Fig. 10.28: Increase of sample thickness of board samples

With every additional sample the curve shifted down. With 5 samples taped over each other, the strip was 0,7 cm thick. This strip thickness exceeds the usual thickness of paper/board samples. With additional substrate thickness, the spring force needed to separate the tack-roller disc from the inked substrate, induces a lower force to the load cell. Thus lower forces with thicker samples are measured. However with less spring force available for the separation, the speed of ink flow decreases. Thus longer times are needed to separate the tack disc from the surface. One can see this from formula (9.23). If one generalizes this state:

Slower withdrawing of the inked film, i.e. slower print speed in real printing process diminishes the ink tack-force values.

If the separation time exceeds the set time interval in the machine, the light sensor does not recognize a separation. Thus the force measured to the end of the interval is registered, and in the extreme case of 5 samples taped above each other, a constant force will be measured (Fig. 10.28), [35].

10. 4 Ink parameter investigation:

10.4.1 Measurements with air as a fluid:

By using no ink on the substrate, one has only air with a very low viscosity present.

When testing the steel surface of the measuring sample carrier with air as the fluid, the results showed extreme variations ranging from 0,3 N to above 5 N.

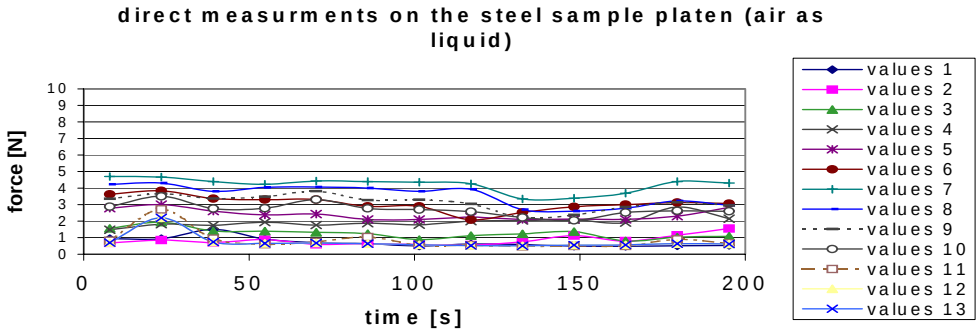

Fig. 10.29: Zero measurements with air on the pure steel surface of the sample carrier as a substrate

An explanation of these responses might be air which is trapped in the cavities of the rough steel surface and the soft nitril rubber tack disc. By pushing the tack disc to the steel surface air is pushed out of the cavity. The result is a lower pressure in the cavity, which causes a suction effect on the nitril rubber disc. This causes a higher force value when the separation process is started. This effect emphasizes once more the impact of the distance between the tack roller disc and the sample in eq.(9.23), as well as the importance of roughness.
From these results one can conclude, that flow to a great extend contributes to the phenomena of “ink-tack”.

10.4.2 Investigation of different commercial ink types:

On an SBB board sample (IG 260 g/m^2), one measured the influence of different offset inks. For the comparison commercial inks of the company `Hartmann Druckfarben´ were chosen. The colors used were [Hartmann product catalogue]:
Hartmann Star Glanz Cyan, a high tack-ink
Hartmann Multilith Cyan, a fast setting and low tack-ink
Hartmann Oekolith Cyan, a mineral oil free ink

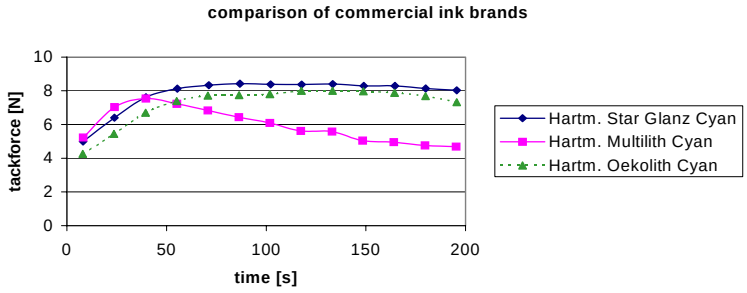

Fig. 10.30 Comparison of commercial ink types

The measurements confirmed the prediction of the supplier. The color Hartmann Oekolith is a mineral oil free color. Thus it can be assumed that vegetable oils are used as a carrier

phase. These vegetable oils separate more slowly from the ink due to greater molecular weight.

10.4.3 Investigation of different inks and varnish of one commercial type:

Four commercial inks of one type and one clear lacquer were measured in order to determine if differences in ink tack behavior prevail. The composition of these inks is unknown.

However, it is usually claimed that black inks in general contain pigments (carbon pigments), that are smaller than the pigments used for other shades.

Varnish is clear lacquer, which is used to give a print job a glossy appearance. Varnish has also the function to protect the surface. The composition of litho-varnishes is completely different from usual inks. Varnishes do not contain pigments. If one assumes that the basic composition of the inks are equal, the different pigments should contribute to the drying behavior.

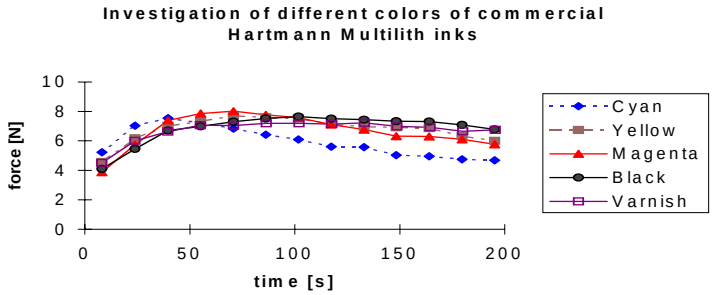

Fig. 10.31 Comparison of different colors of Hartmann Multilith with varnish

The black ink was the slowest drying ink. This could be due to the finer pigments that would cover the ink film more effectively. Thus solvents cannot be absorbed as fast as in a dispersion with larger pigments. To be sure, that the pigment size contributes to the drying behavior, one should conduct a sedimentation analysis of the pigments.

10.4.4 Application of the instrument as an inkometer:

One wants to investigate, whether ink tack development on a non absorbent mylar surface corresponds to the first values measured on coated board.

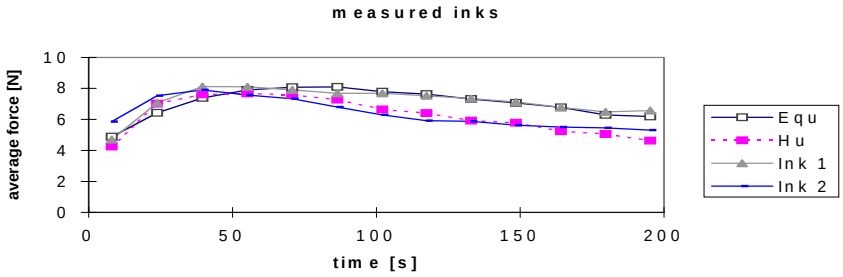

Fig.10.33.1: Application of the instrument as an inkometer

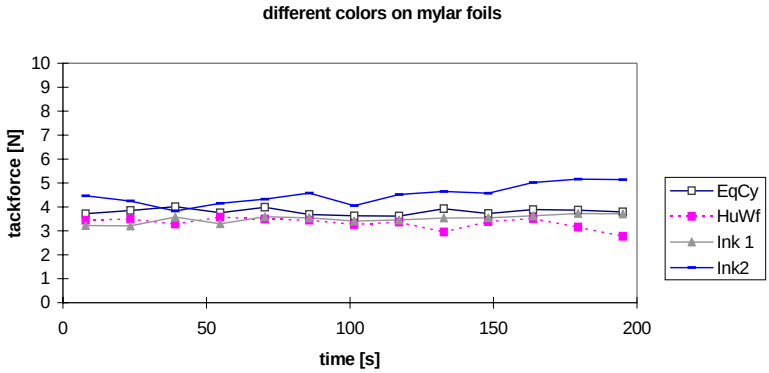

Fig. 10.33.2: Application of the instrument as a rheometer (inkometer)

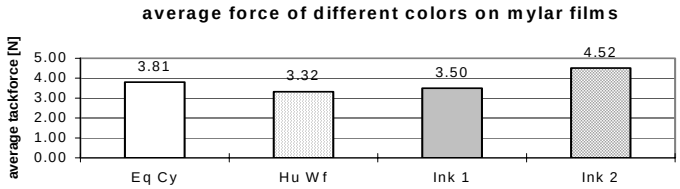

Fig. 10.34: Comparison of average force values

By calculating the average values, one finds that the average force values of a non absorbent foils are at the same order of magnitude as the first measured force values, measured on coated board. The following conclusions can be drawn:

The Ink-tack instrument can be used as a simple ink rheometer. Because ink-tack is not always correlated to viscosity [19, [28], the expression inco-meter or inco-scope is more appropriate.

10. 5 Investigation of different substrates on the ink-tack development:

10. 5.1 Description of the substrates used for the investigation:

Since ink-tack is a rather new field to be explored, little is known about the behavior of different substrates. Therefore a number of different substrates were tested.

Code	Paper/board type	Surface characteristics	PPS-roughness [µm]
SBB, ICA	Solid bleached board	Triple coated, high gloss, high smoothness	0,77
SBB, ICCG	Solid bleached board	Double coated, high gloss, high smoothness	0,8
SBB, ICCM	Solid bleached board	Double coated, matt, medium smoothness	1,09
SBB, ICG	Solid bleached board	Triple coated, medium gloss, medium smoothness	1,1
SBB, OICG	Solid bleached board	Double coated, medium gloss, medium smoothness, more clay than ICG	1,2
FBB 1	Folding box board	Double coated	1,27
FBB 2	Folding box board	Double coated	1,08
FBB 3	Folding box board	Double coated	1,45
FBB 4	Folding box board	Double coated	1,1
FP glossy	Fine paper	Double coated, glossy, contains more clay than FP matt, average pore radius = 0.03 µm, pore volume = 4.5 cm^3/m^2	0,9
FP matt	Fine paper	Double coated, matt, aver. Pore radius = 0.082 µm, pore volume = 6.37 cm^3/m^2	3
MWC 1	Wood containing	Coated	1,45
MWC 2	Wood containing	Coated	1,3
MWC 3	Wood containing	Coated	1,24
MWC 4	Wood containing	Coated, average pore radius = 0,044 µm, pore volume = 3 cm^3/m^2, designed for sheet-fed	1,48
MWC 5	Wood containing	Coated, matt, aver. pore radius = 0.065 µm, pore volume = 4.04 cm^3/m^2	3,12
MWC 6	Wood containing	Coated	1,44
MWC 7	Wood containing	Double coated, aver. pore radius = 0.055 µm, pore volume = 4.58 cm^3/m^2, designed for web fed	0,94
CC 1	Fully bleached board	Cast coated, very high smoothness and gloss	0,71

Table 10.1: Paper board substrates

In addition to the above mentioned substrates, also double coated model surfaces were evaluated, in which both the pigment type and the coat weight of the coating layers were altered. The composition of those model surfaces is listed in Table 10.2:

Code	precoating	topcoating	Topcoating weight	PPS roughness [µm]
E 1	Fine $CaCO_3$	Coarse $CaCO_3$	Thin	1,9
E 2	Fine $CaCO_3$	Coarse $CaCO_3$	Medium	2,08
E 3	Fine $CaCO_3$	Coarse $CaCO_3$	Thick	2,1
E 4	Coarse $CaCO_3$	Fine $CaCO_3$	Thin	1,54
E 5	Coarse $CaCO_3$	Fine $CaCO_3$	Medium	1,58
E 6	Coarse $CaCO_3$	Fine $CaCO_3$	Thick	1,69

Table 10.2: Model surfaces

Further tests were carried out on model mylar films coated with different latex types. The composition of these model surfaces is listed in table 10.3.

Code	Latex type	Tg [°C]	Degree of carboxylation	PPS roughness [µm]
SB high T	Styrene butadiene	27		2,15
SB low T	Styrene butadiene	-7		1,48
SA high T	Styrene acrylate	25		2,19
SB high C	Styrene butadiene	9	High	2,02
SB medium C	Styrene butadiene	8	Medium	1,7
SB low C	Styrene butadiene	13	Low	2,3

Table 10.3: Latex films

Further ink-tack tests were carried out on different polymer films, which often were the backsides of polymer laminated board.

Code	PPS roughness [µm]
PE + corona, glossy	3,73
PE + corona, rough	6,33
PE, rough	7,8
PP + corona glossy	4,17
PP, rough	7,79
PET, rough	9,14
PMP, rough	7,44

Table 10.4; Polymer films

Code	PPS roughness [µm]
Mylar film	0,6
Aluminum foil, glossy	0,5
Aluminum foil, rough	1,04

Table 10.5: Other films

10.5.2 General influence of the type of paper and board substrate:

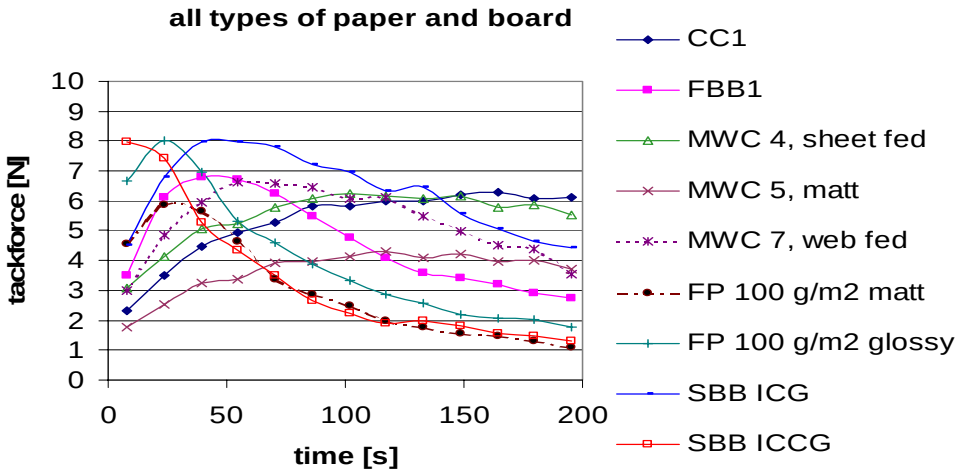

Fig. 10.36: General influence of the type of board and paper

In the above plot the greatest differences in ink-tack development between different paper/boards are presented. The overall tendency is, that smooth, solid bleached, boards and smooth fine papers develop fastest their ink-tack maximum, less smooth folding box boards and solid bleached boards and fine papers set slower, while less smooth MWC papers set slowly. Matt fine papers, the less smooth folding box board, and matt MWC papers develop lower maxima ink tack forces. Compared to other samples, the cast coated board CC1 is an exception, because it has an extreme slow ink setting rate with quite a low tack force maximum, despite a very low surface roughness. The reason for this may be the slow absorption rate, which gives a low viscous ink film. Viscosity is a variable that goes in linearly into the force balance, which can be seen from formula [9.23]. The absorption rate depends on the amount and size of the capillaries, which can be seen from formula [9.45].

SEM images from boards/papers with the most different ink tack development behavior were taken (see Appendix). These were:

- SBB ICCG
- SBB ICG
- CC 1

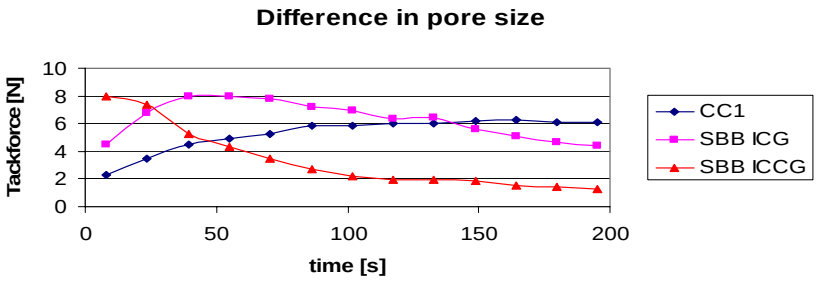

Fig. 10.36.1: Tack-force development curves of samples, where SEM images were obtained

Indeed the solid bleached board ICCG shows the finest surface structure. A large number of very small pores would be available to absorb the oils of an offset ink film. ICG shows a slightly rougher structure. The third, slowest setting, sample shows only a few very large available pores at the surface.
Thus the resulting pore structures determine the rate of ink tack build up, as can be seen from formula (9.45).

An attempt was made to correlate ink-tack development with measurements of the surface energy of the tested paper. The total energy consists of the terms acid-base energy and Lifshitz-van-der-Waals energy. The acid base energy can be split into acid and base energy terms.

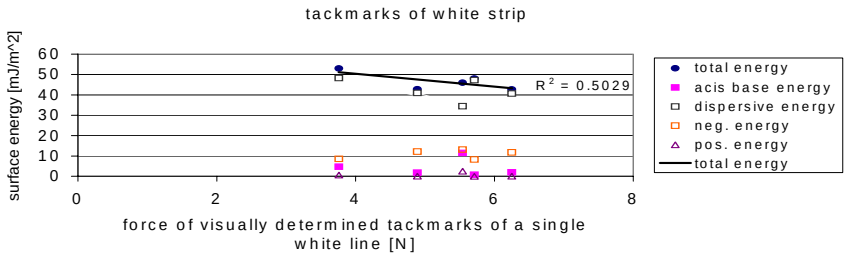

Fig 10.37.1: Surface energy values against pure adhesion force between an ink-film and the substrate

By determining the first contact angle values, obtained after 0 seconds through interpolation [see appendix], it can be seen, that the pure adhesion force between ink film and surface decreases with higher values of total surface energy, and higher values of acid-base energy (see fig. 10.37.1). Oil in offset inks has a low surface energy. Solubility usually increases with

more similar surface energies between ink-film and substrate. Thus for coated paper adhesion corresponds rather to the solubility properties of oils into the coating. This seems to be in agreement with the findings of [12].

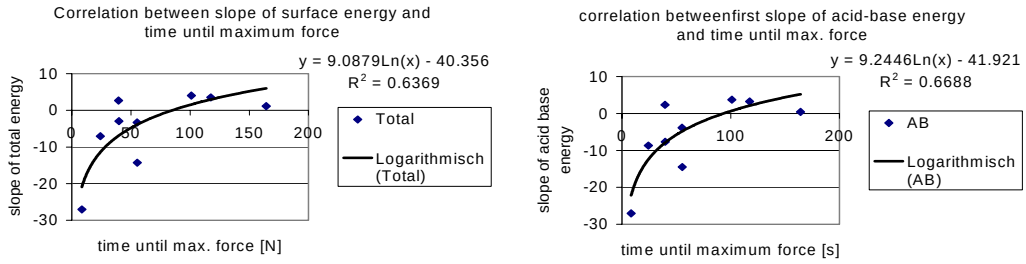

Fig. 10.37.2: Correlation between the slope of the evaluated surface energies in the first tenth seconds and the absorption time

The evaluated slope of the surface energies against the time curve shows a good correlation with the setting time of the ink (see fig. 10.37.2).
The slope is calculated as: (first measured surface energy value – second measured surface energy value) divided by (first time value corresponding with the first surface energy value – second time value corresponding with the second surface energy value).
With an increasing slope, the time until the maximum tack force is lengthened.

10.5.3 Dependence of printing in machine and cross direction for ink-tack development:

When paper and board is produced, fibers are oriented in the machine direction. Thus the direction can be described with machine direction (MD) and cross direction (CD). In the following chapter the dependence of printing in machine and cross direction for ink-tack is investigated.

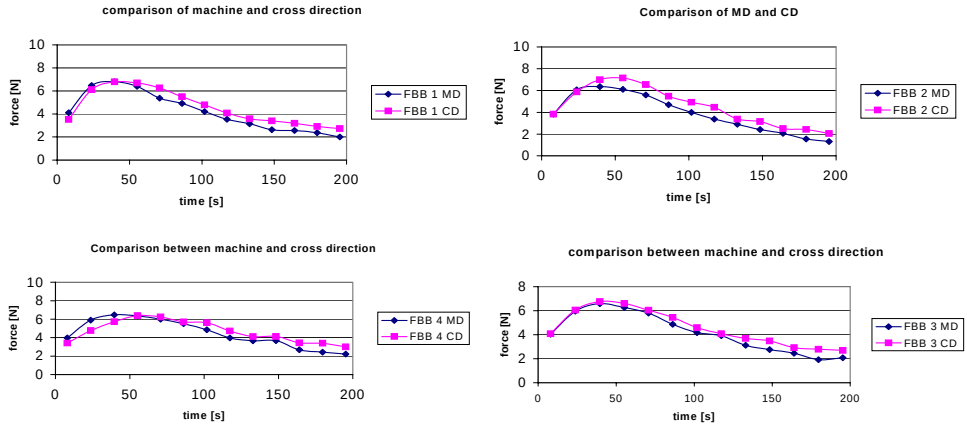

Fig. 10.38: Ink-tack development curves of folding box board samples printed in machine and cross direction

When comparing the ink-tack development curves of FBB samples printed in the machine and in the cross direction, one can clearly detect, that the ink-tack development of the in-machine-direction-printed sample always lies under the cross direction printed board. The cross direction printed samples curves look like curves from a board, printed with fewer ink. This was not the case, as densiometer values prove. When applying ink to the surface, ink flows into the lowered areas that lie parallel to the fiber direction of the board. Air can be pushed out when the ink is printed on the surface. It can be supposed that paper/board surface is better wetted by the ink, when printed in the machine direction. Thus the ink coats a larger surface and can set quicker. In cross direction printing, air can be trapped in the pores under the ink. This might explain the above curves (see fig. 10.38).

Substrate	Internal topography index MD	Internal topography index CD
FBB 1	20	31
FBB 2	33	44
FBB 3	29	32
FBB 4	31	42

Table 10.6: Structure measurement with a laser instrument, internally used by MoDo Iggesund, (the greater values correspond with greater roughness)

The roughness is always greater in the cross direction than in the machine direction. This is proved by measurement with a structure instrument, which measures the surface topography with a laser beam.

For solid bleached board, the ink-tack development does not follow the above pattern. A possible explanation for this is, that the baseboard has an influence on the structure of the coating. A solid bleached board has a more even surface, which can be covered more

effectively with coating. This corresponds to the findings of [43]. Thus the influence of the fiber direction of a bulky folding box baseboard shows more through.

10.5.4 Influence of surface roughness:

Roughness of coated paper/board is usually measured with a PPS roughness tester. High values represent a higher roughness. Due to eq.(9.23) roughness indirectly affects the film thickness. A rough sample achieves a channel effect, through which a fluid can be more easily pressed. In extreme cases air can be trapped in the valleys of the surface topography, and air can flow into the gap, thus lowering the measured tack-force (see also Fig. 10.28).

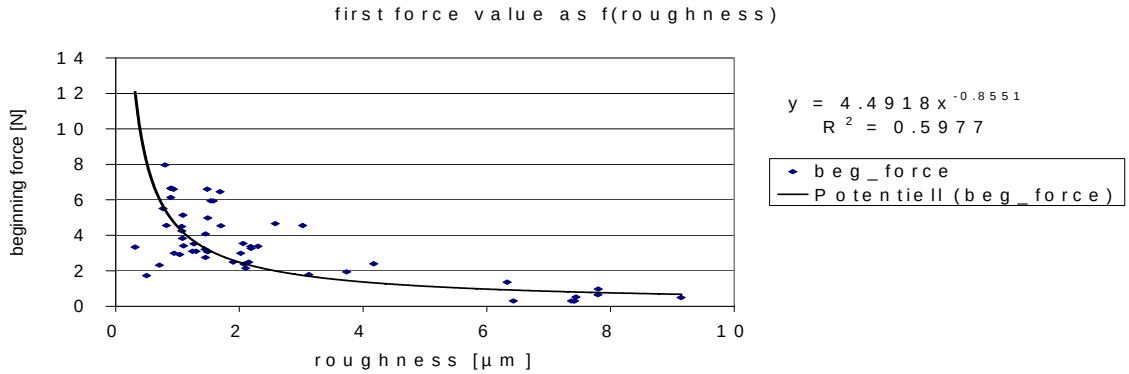

Fig. 10.39: Correlation between the first measured force value of the ink tack development curve and the roughness

From the above graph (see Fig.10.39), one can see that there is a correlation between the first measured value of the tack force development curve and the roughness, that is similar to a function $1/h^3$, see formula [9.23].
It can be stipulated that the first measured value is predominantly determined by the flow of the ink.

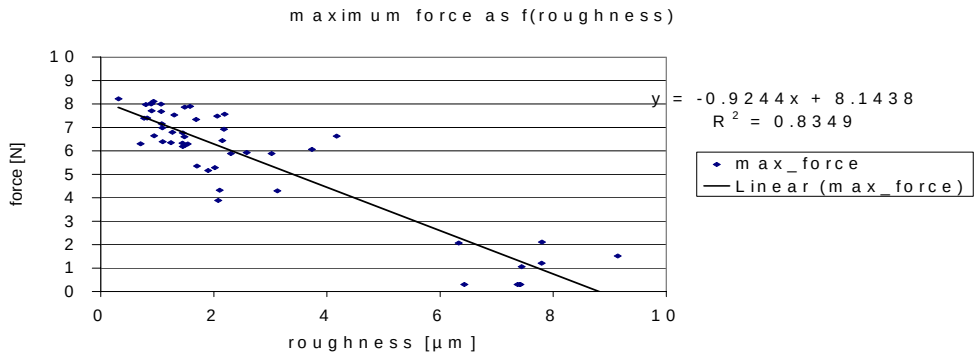

Fig. 10.40: Correlation between the maximum force and the roughness

A linear correlation exists between roughness and maximum force value. Tackmarks at the maximum force are usually a white strip with a lighter shade around the line. So the flow of ink is apparent (see also Fig. 10.5).

The single white line represents the adhesion failure of the ink at the surface of the substrate. The force value, corresponding with this tack mark is probably determined by the by the wetting of the ink.
The difference in force between those two kind of tack marks is only up to 30 % of the force value of the one with the lighter environment. So the adhesion to the surface contributes predominantly to the maximum force.

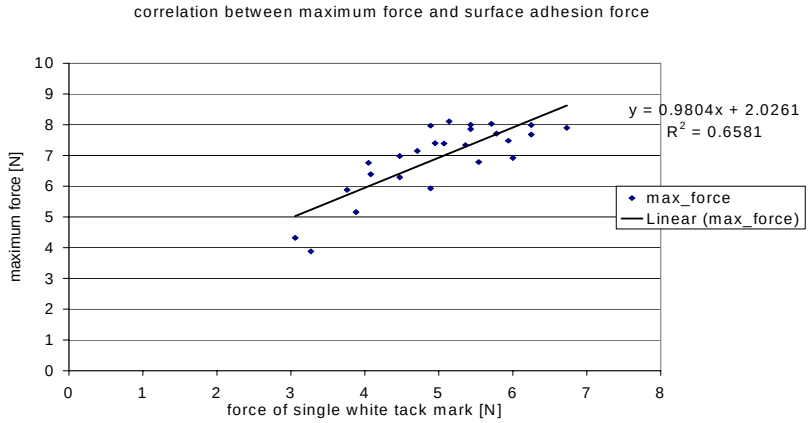

Fig. 10.41: Correlation between the maximum force and force measured at a single white tack mark

This can be seen from the above graph, if one considers the force measured at the last visually detectable tack mark of a single white line as the surface adhesion force.
The adhesion force is due to formula (9.33) determined by the contact area. So one could understand the linear correlation between roughness and maximum force values.

A good correlation exists between the maximum force value and the beginning force value.

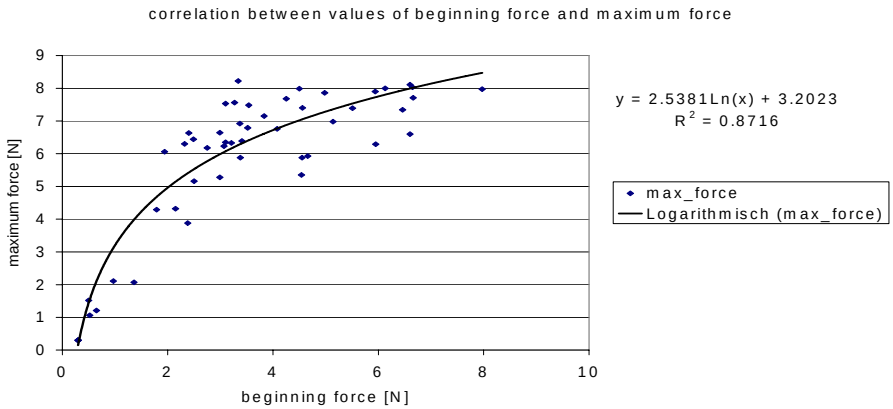

Fig. 10.42: Good correlation between beginning force and maximum force.

If one generalizes this correlation one can state:

The greater the first measured value, the greater will the maximum force value be.

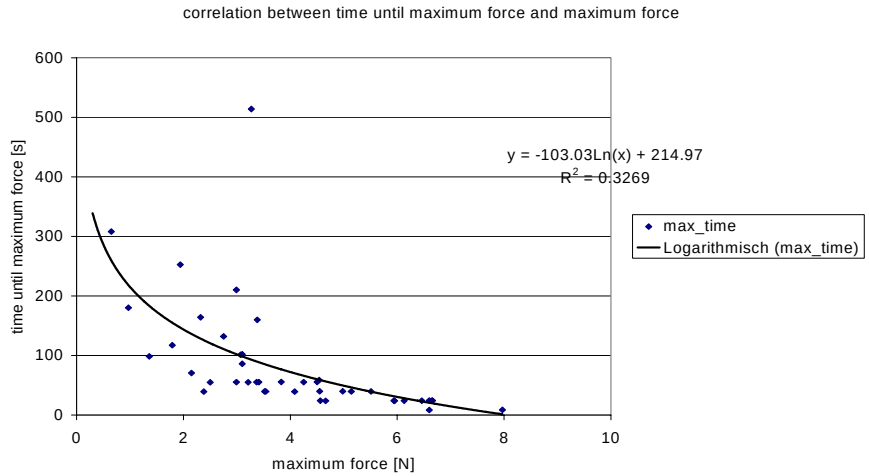

Fig. 10.43: Correlation between time until maximum force and maximum force value

Usually a tack-force curve with low beginning force needs a longer time until the maximum of force is reached. Some correlation can be obtained as can be seen in figure 10.43. The correlation coefficient is not very high, so other factors should have an influence also. The time until the maximum is determined by the rate capillary absorption. So the pore size and the pore amount to the surface can be supposed to be important parameters.

The last measured force of the ink force development curve does not correlate well with the surface roughness. This value seems to be determined by other factors.

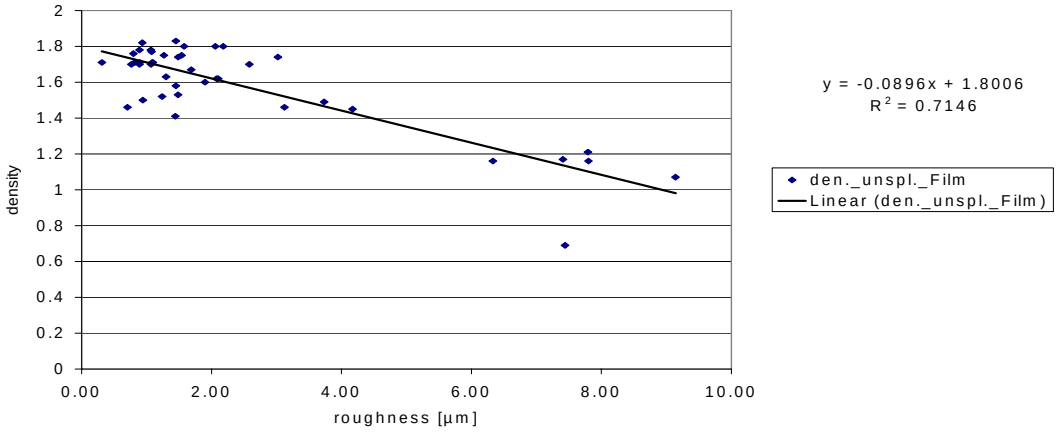

Fig. 10.44: Correlation between density of unsplit printed ink film and the roughness

The figure above shows the linear relation between the surface roughness and the print density. It seems that with increasing roughness the ink does not cover the surface efficiently. The applied ink amount remained the same.

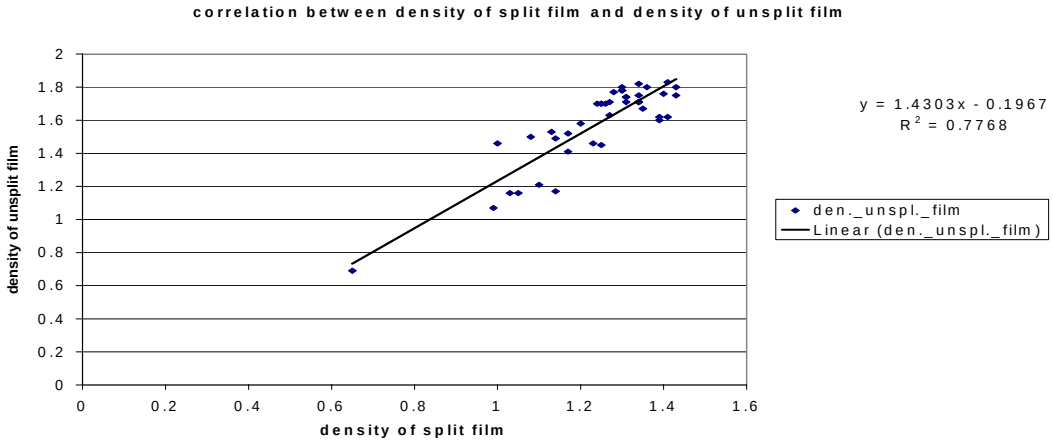

Fig. 10.45: Correlation between optical density of a split and an unsplit ink film

This seems to be confirmed by the above graph. The optical density of the first film split, which takes part after about 8-9 seconds and the density of an unsplit ink film correlate well. A high density in the first film split should be the result of a quick absorption of the applied ink film. Ink absorption increases for better wetted surfaces.

10.5.5 Influence of the porosity of coating layer:

Experiments on model surfaces with different pigment sizes and different thick coating layers were carried out.

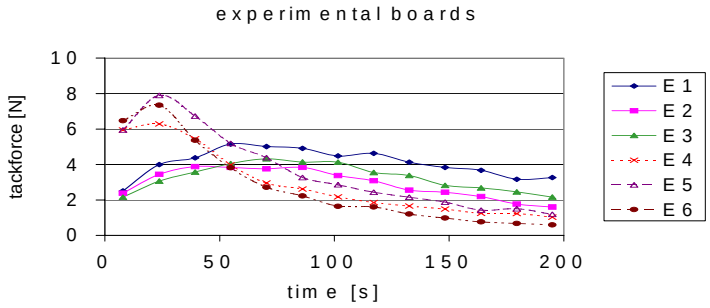

Fig. 10.46: Tack-force development graphs on model surfaces with different pigments in different coating thickness (see also table 10.2)

Out of the above figure one can see, that with a fine $CaCO_3$ in the top coating layer (experimental board 4,5,6) the maximum force is reached faster in comparison to a coarse pigment in the top coating (experimental board 1,2,3). This is assumed to be the result of smaller pore radii that absorb the carrier phase of an ink more efficiently. The tack force maximum is much higher due to more effective ink covering and wetting of the substrate

surface. The resulting gap should be smaller and as stated in equation (9.23) separation forces should rise.

As expected the optical densities of the printed unsplit film were lower for rougher surfaces. It can also be seen, that rough surfaces seem to develop lower maximum forces after long time. This can at least be stated, when the same pigment are used.

It is not the case, when comparing matt and glossy finepapers:

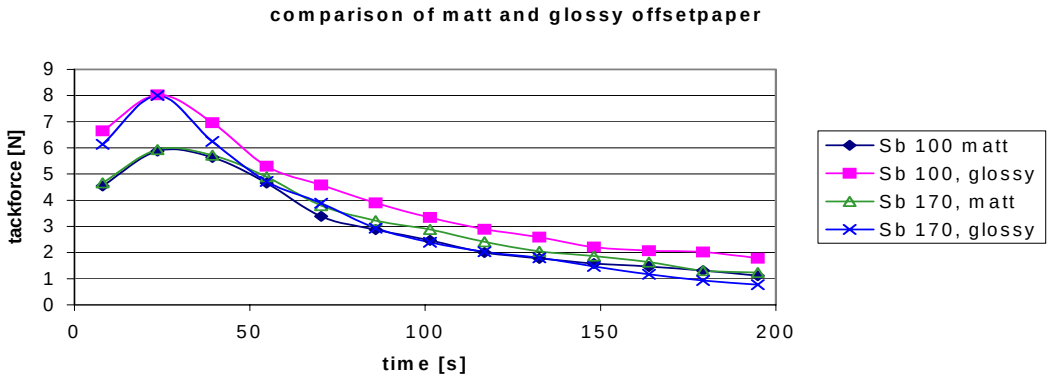

Fig. 10.47: Comparison of matt and glossy commercial offsetpaper

From the above graph, it can be concluded, that the time at which maximum force is reached is independent of the paper surface. This might be explained by the fact that glossy papers often contain higher amount of clay pigments and the total pore volume in the coating layer might be low (see table 10.1). Clay pigments cover the surface more effectively and the total pore volume present in the coating layer might be low (see also Fig.5.4). This is especially the case, when the paper is calendered. Thus a less pore volume would be available for the fluid to be absorbed. This results in a more retarded ink drying. This might explain why the time needed to reach the maximum force can be similar, though the surface roughness is entirely different. This in return means, that both surface roughness and absorption properties influence on the location in time of the point of maximum force.

Mercury porosimetric measurements (see table 10.1) confirm that the glossy version has much finer pores than the matt version. The matt version develops a lower tack-force maximum and the declining force curve is lower than the of the glossy version. This could result from the larger pore volume. During testing one could detect that sometimes coating particles were torn out of the surface by the tacking ink (ink picking). This could result from the lower binder content usually applied in paper.

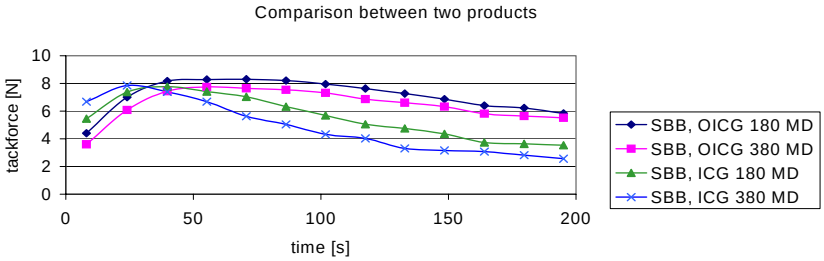

Fig. 10.48: Comparison between two products

The influence of pigment composition in the coating layer on tack development can also be seen in the above figure.10.48. The product SBB OICG has a higher amount of clay pigments in the coating. As can be seen the time at which the maximum force is reached is longer for SBB OICG, despite the fact, that the surface roughness is comparable. So again, the time until the maximum force is controlled both by the porous structure of the coating layer and the roughness of the surface.

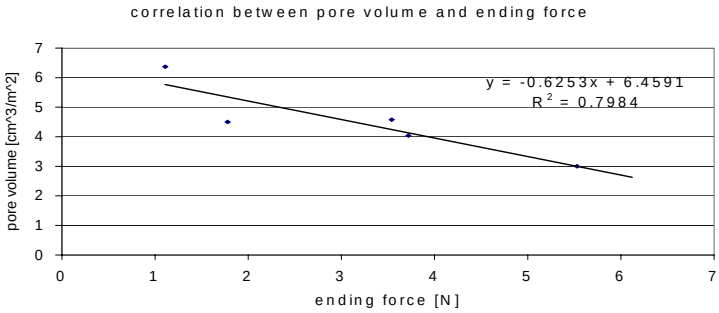

Fig. 10.49: Good correlation between the ending force and the total amount of pore volume

The ending force seems to correlate quite well with the total amount of pore volume (see table 10.1 and tack-force curves in the appendix). This seems to confirm the statements from the inventor of the apparatus, who claimed that the latter half of the ink force development curve is influenced by the total amount of pores in the substrate. However more experiments have to be carried out to fully confirm these findings.

10.5.6 The role of latex type on the tack-force development:

To investigate on the influence of the latex-type in the coating, experiments were carried out with different types of latices, that were applied on a mylar film with a laboratory coater.

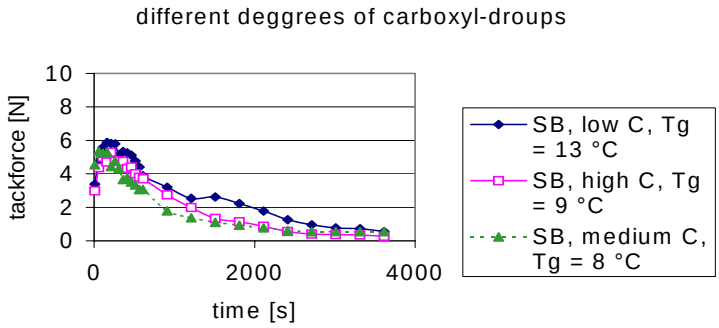

Fig. 10.50: Comparison of tack development curves for latices with different degrees of carboxylation

The above curves show, that the degree of carboxylation of the latices does not seem to influence much on the ink-tack development. It is however very interesting to notice a clear development of tack-forces with time. This would indicate that not only a porous substrate can absorb the oil phase from an applied ink, but also latices can absorb oils, probably through swelling.

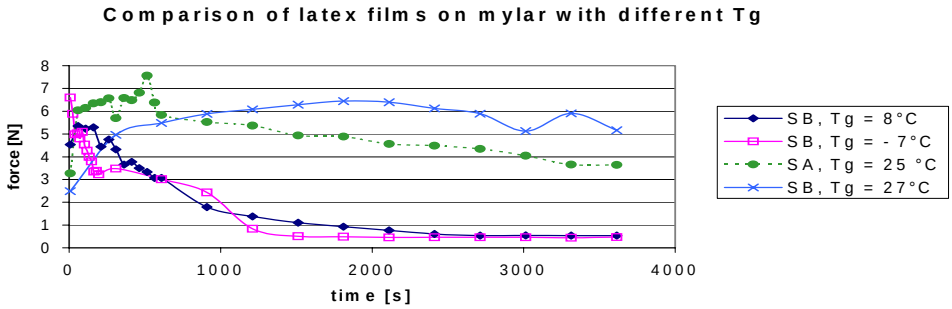

Fig. 10.51: Comparison of latices with different glass transition temperatures.

In contrast to the degree of carboxylation, the glass transition temperature seems to have a much higher effect on the development of ink tack. A latex with a high glass transition temperature takes long time to develop tack (3 hours for a latex with a glass transition temperature of 27°C), while a latex with a low temperature reaches it's tack-force maximum within 8 seconds. As stated earlier a latex probably absorbs the ink carrier phase by swelling. The swellability is determined by the configuration of the latex. Styrene butadiene latices with low Tg usually contain more butadiene. This might explain the above findings as butadiene, due to it's less bulkier structure contributes to swellability of a latex.

Usually a more closed pore structure is obtained with a higher amount of latex in coating colors. This would lead to a lower absorption of mineral oil components of the ink. Thus ink setting should be delayed. In the case of the latex with a glass transition temperature of –7°C, the latex might itself contribute to the absorption of oils. So the oil phase in the ink film is being absorbed, both through capillary absorption and swelling. This would confirm the experiments, carried out by Triantafillopoulos et Al [11].

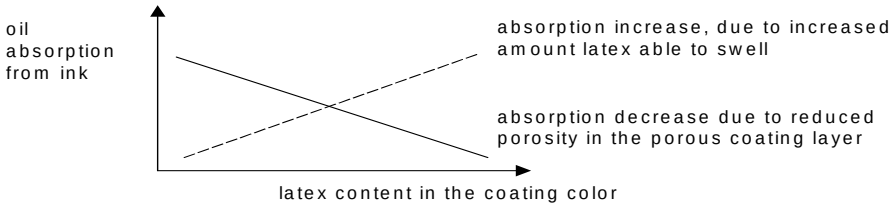

Fig. 10.51.1: Possible influence of latex amount in the coating color on the oil absorption

10.5.7 Ink drying and setting on polymer and aluminum films:

Experiments were made by measuring the ink-tack development of ink applied on different polymer laminated boards.

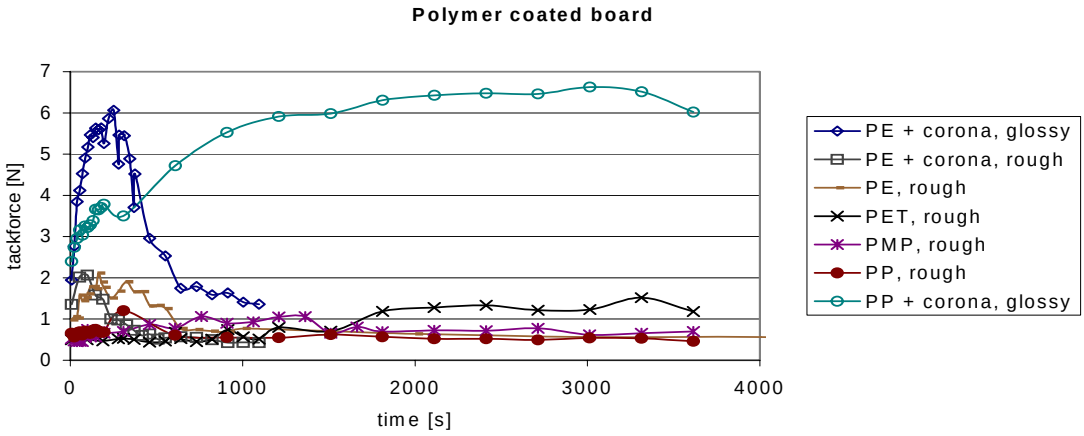

Fig. 10.53: Ink setting (swelling) and drying on polymer-coated board samples

One can clearly distinguish the pattern, that for rough surfaces tack force is always on a low level. For PE coatings a maximum is found. A corona treated surface is develops faster the tack maximum than a non corona treated surface. For a glossy corona treated surface a high tack-force maximum is obtained. With a glossy corona-treated PE surface ink and dries and is absorbed quicker than a glossy corona-treated PP surface. An explanation may be that PE is a slim molecule with small branches (H-atoms). It has a lower glass transition temperature than PP. The Tg of PE is - 110°C, while for PP the glass transition temperature is around –10°C. Thus PE has a better ability to swell and to absorb mineral oils from the ink. PP has methyl-groups as branch-groups, which, due to their larger size results in a higher glass

transition temperature. Polypropylene chains can join together more effectively and thus form a polymer with a higher amount of crystallinity. The ability to swell is therefore very low for PP. It would be interesting to test the now commercially available syndiotactic version of PP, which has a lower Tg and probably a better swellability.

A corona treatment usually causes the formation of unsaturated (C=C) and carbonyl (>C=O) groups which are considered to increase surface energy [38]. Thus the interaction between the mineral oils of the ink and the surface increases, leading to a better absorption of the oils. The roughness and the surface energy seems to be predominant parameters governing the tack-force development. PET, PMP and PP surfaces have lower surface energy, than corona treated polymer surfaces.

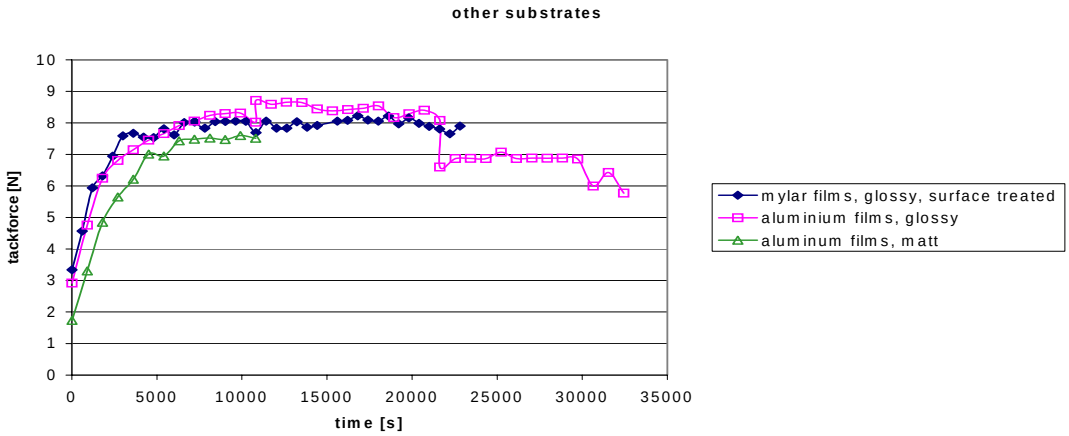

Fig 10.54: Ink-tack development on mylar- and rough and glossy aluminum films

Long time experiments have been carried out on mylar and aluminum films. None of the films do absorb ink components. Thus ink drying occurs only through slow evaporation of oil components to the surrounding air. This may be the reason for a similar tack development of all curves in Fig. 10.54.

It can be assumed, that in this case ink tack rises through evaporation, oxidation and polymerization.

It is interesting to see, that the tack force values of a matt aluminum foil constantly lie under the tack force values of a glossy aluminum film. The shape of the tack force curve remains the same.

Thus it can be stated:

For a constant oil absorption rate, the roughness has a diminishing effect on ink tack forces (see also Fig. 10.27 and fig 10.28).

10.6 A modification of the test:

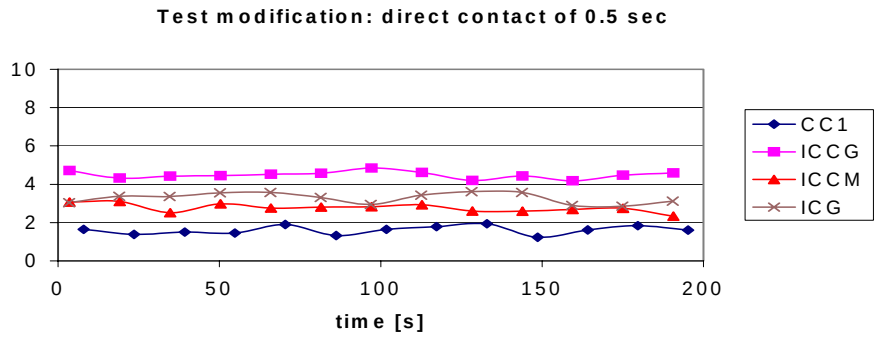

Fig. 10.55: Tack-forces obtained by a modification in the testing procedure.

By inking the nitril covered tack measurement roller and carrying out the test on an unprinted test strip, one obtains conditions closer to those prevailing a real printing press (see Fig. 9.10). The contact time between tack roller and sample is set to 0,5 s. With this procedure a small fresh ink film is always applied to the substrate surface and a half second later the tack roller separates.

In a sheet fed offset press one prints with a speed of about 8000 sheets per hour. This would result in about 0,5 s contact time of a blanket printing cylinder and a substrate, which is the above chosen time.

The above curves prove that even for such short contact times great differences in the tack force can be observed. The above tack force values correlate in the ranking well with the first values obtained in a regular ink tack test (see Fig. 10.36.1). Some of the problems like delamination and set-off can be foreseen in this experiment.

Thus it can be stated that the initial ink tack force might correlate to capillary absorption (see also the SEM images in the appendix)

11 Outlook

During testing one can observe, that the measured weight of transferred ink varies so much, that one can not use it as a control parameter. This variation is probably due to evaporation of the solvent used in the experiments. Thus more rubber printing discs would be useful in order to allow for a complete evaporation of the solvents.

The instrument is not provided with a manual, which would be useful in future.

The testing instrument has many parts that can age. The inking discs, the tack disk and the springs are parts that change their properties after time. Thus proper maintenance of the instrument would be useful.

It would be useful to export more than one file at a time from the computer data base. A crank for the pressure force winding spring would be more convenient.

It is very important to have a sufficient air evacuation device installed, since the cleaning solvents are harmful 16].

The instrument has the disadvantage that it measures a static force, i.e. a force between a sample and a roller, which are not rotating. In a real printing condition, also a dynamic component is present, i.e. the withdrawing of an inked sheet from a rotating blanket. The instrument does not consider the compressibility of the substrate, nor the initial ink tack. A device, similar to the S.D. Warren load cell, that would allow to take above effects in consideration is presented in the figure below.

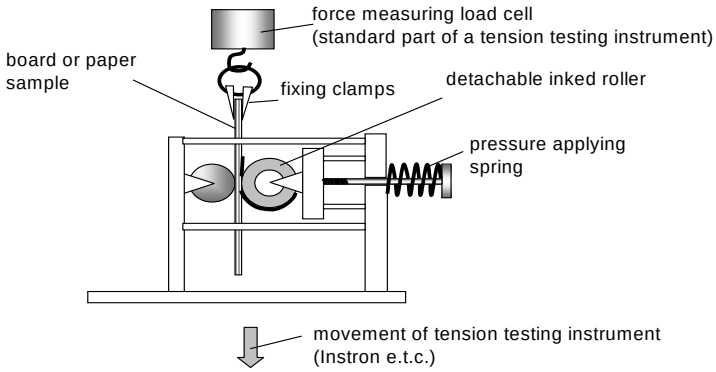

Fig. 11.1: Proposal for a simple ink tack measurement instrument usable on a standard tension testing Machine

This device could be mounted on a standard tension testing instrument like an Instron tension tester.

The time of setting correlates with the binder amount in the remaining ink film. This can be determined with infrared spectroscopy [40]. Since the binder amount should have a main contribution to ink tack [19], it would be interesting to correlate some of tack development tests (see Fig. 10.36.1) with IR spectroscopic measurements of the binder phase in the top coating.

12 Summary:

Roughness seems to be the predominant factor for tack force development. A rough surface is not effectively wetted, so the absorption of oils is less sufficient. Moreover a rough surface causes local gaps that mechanically enable an easier film split.
A smoother surface is better wetted. Thus ink components are better absorbed. The rate of oil absorption depends on the capillar absorption, probably due to solubility of the binder in the oil phase and the solubility of the oil phase in the coating.
A surface with a high amount of very fine pores absorb the ink very quickly, leaving the tacky binder phase at the surface.
Capillary absorption seems to determine the first initial ink tack value.
The first measured tack value is determined by the separation force due to a flow phenomenon
A high first measured tack-force value is often followed by a high maximum tack force value
The maximum force value is determined by the adhesion of the ink layer to the surface
The time until the maximum force value is reached, is determined by the roughness and by the pigment selection.
The last measured force value is probably determined by the total pore volume in the coating.

The delamination problem for very smooth, finely porous, thick and compressible substrates can to be understood, by considering Fig. 9.10. and Fig. 10.55.
Initial ink tack and delamination could be lowered by

- Lower print speeds
- Lower printing pressures
- Lower paper/board thicknesses
- Rougher rubber blankets
- Rougher substrate surfaces
- The choice of pigments (larger pigments or pigments with a higher aspect ratio that produce a less porous surface with greater pore radii)
- Probably the amount and type of latex used in the coating color
- Choice of ink (i.e. the choice of binder, oil carrier phase and pigment type, viscosity of the ink)

For non porous substrate surfaces, ink tack forces rise with higher surface energies of the substrates.

13 Acknowledgements:

I would like to thank the following people for their support:

Prof. Dr. J. Petermann from the University of Dortmund of the Department of Chemical Engineering, chair of Material Science, Polymers and Compounds, for the opportunity to carry out my thesis in Sweden and for his advise,

My tutor from the company side, Dr. Philippe Letzelter, Manager of the Centre of Excellence for Surface Treatment in MoDo Iggesund, for his advise, help during my project, and proof-reading my report,

Bertil Wallon for the contact angle tests, scanning important photographs, his kind advise during my first contact with the instrument and for his permanent encouragement,

Edward Seyler, the instrument supplier, for kind advise in all question dealing with the apparatus,

Inga-Märta Grundström for her advise and help with practical procedures of tests with the apparatus

Emilia Liiri Broden for her advice and passing over her experience about offset colors.

MoDo research and development for providing me with additional test results.

Viola Lindstöm of the MoDo library for providing me with all literature I ordered

Lars-Eric Persson of MoDo research for providing me with mercuri porisometic tests

Johan Granås for kind advice and proof-reading my report,

Dr. Erki Latti for his advice about surface energy

Anders Skoglund for his advise in all statistical and many other problems

Johanna Österberg for her kind advice in statistics and helping me with the program Modde.

Lisetti Gidlund from MoDo research for UBM roughness tests

Ann Mari Eriksson, Anita Wahlstöm, Torsten Myrgren, Per-Arne Berg, Anna-Lena Ström, Susanna Yoki, Bernt Andersson, Johann Nordlund, Prof. Dr. Anders Brundin, Bernt Andersson, Elisabeth Persson, Kailash Paitnak, Esco Pakkinen, Birgitta Wallin, Michael Karathanasis for their great encouragement, kind advice and important information.

My family for proof-reading and their great encouragement during my studies.

References:

[1] H. J. Saarelma and P. T. Oittinen, Fundamentals of Printing Technology, [Helsinki University of Technology, Laboratory of Graphic Arts Technology, 1994]

[2] G. H. Hutchinson, Advance in the technology of water-based inks and coatings for the printing and packaging industries. Croda International Inks Federation [Journal of Oil and Color Chemical Association, 1985]

[3] R. H. Leach, C. Armstrong, J. F. Brown, M. J. Mackenzie, L. Randall and H. G. Smith, The Printing Ink Manual, Fourth Edition [Chapman & Hall, 1991]

[4] C. D. Norgate, Coates Lorilleux International Ltd, [Journal of Oil and Color Chemical Association, Recent developments in printing of newspapers in Europe and their effect on printing ink technology, 1989]

[5] E. L. Broden, Litteraturstudie över skillnader mellan ark- och rulloffset, med betoning på tryckfärger, [Rapport nr 4636, MoDo Forskning och Utveckling, 1996]

[6] J-C. Sirost and P. Cole, Coates Lorilleux, The study of rheology and physics of interfaces as an aid to the offset process

[7] From paperboard to product, Paperboard Reference Manual, Iggesund Paperboard AB, (latest edition).

[8] J. M. Reck, L. Dulog, Stabilisierung von Rutilpigment-Dispersionen durch Blockcopolymere in organischen Medien, [Farbe + Lack, 99. Jahrgang 2/1993]

[9] Gunnar Olsson, Bestrykning, Skogsindustrins Utbildning i Markaryd AB, [Yrkesbok Y-308, 1994]

[10] E. L. Broden, The importance of surface composition for printability, Part 4. Graphical evaluation of the surfaces, Offset Printing, [MoDo research amd development, project 446000, 1997]

[11] N. Triantafillopoulos, D. Lee, D.Philip, Einfluß des Strichs auf das Wegschlagen beim Offsetdruck, [Wochenblatt für Papierfabrikation 4, 1997]

[12] R.L. Van Gilder, R. D. Purfeerst, Commercial Six-Color Press Printing and the Rate of Ink-tack Build as related to the Latex Polymer Solubility Parameter.

[13] Hollemann .Wiberg, Lehrbuch der anorganischen Chemie, [de Gruyter, 91.-100. Auflage, Berlin.New York, 1985]

[14]. G. Witke, Farbstoffchemie, [Studienbücher Chemie, Verlag Diesterweg, Otto Salle Verlag, Verlag Sauerländer, 2. Auflage 1984]

[15] C. H. Hare, The basic composition of paint, [Surface Coatings International, 1995]

[16] R. H. E. Munn, Resin developments for tomorrow's inks, [journal of oil and color assoc., 1990]

[17] P. Decker, Theoretische Überlegungen zum Verhalten von Druckfarbe im Spalt zweier Walzen, [Druck Print 12/1973]

[18] P. Oittinen, .,J. Kainulainen, J., Mickels, J., Rheological Properties, Setting and Smearing of Offset News Inks, [Graphic Arts in Finland 21, 1992]

[19] J. S. Aspler, NMR Spectroscopy, Polymer Motion and “Tack” of Model Printing Inks, [Polymer Engineering And Science, September 1992, Vol. 32, No. 18]

[20] C. Testa, Developments in rheology for lithographic ink varnishes, [journal of oil and color association (11), 1992]

[21] D. U. Ott, G. Eulitz, Neue organische Pigmente für wasserverdünnbare Druckfarben, [Farbe + Lack 3/1989]

[22] K. Strauß, Strömungsmechanik, eine Einführung für Verfahrensingenieure, VCH Verlag, Weinheim. New York ,Basel ,Cambridge, 1991

[23] M.J. Stefan, Versuche über die scheinbare Adhäsion, [Sitz. Kais. Akad. Wien, Math. Nat. Klasse A69, S.713 – 735, 1874]

[24] O. Reynolds, On the Theory of Lubriciation and ist Application to Mr. Beauchamp Tower‘s Experiments, including an Experimental Determination of the Viscosity of Olive Oil, [Proceedings of the Royal Society of London/ Series A, Mathematical and physical sciences, recieved. 1885, read 1886]

[25] DIN 16519, Prüfung von Drucken und Druckfarben, Herstellung von Norm-Druckproben für optische Messungen, August 1985

[26] J. Clarke, Pigment dispersion and rheology modifications usind carboxylated acrylic polymers in water-borne coatings, [Surface Coatings International, (7) 1994]

[27] G. Turcotte, Yield stress measurements in paints, [Surface Coatings International, 1994]

[28] M. Has, H. Wordel, Charakterisierung der Farbzügigkeit von Offsetdruckfarben, [Applied Rheology, Oktober 1996]

[29] U. Scheufelen, Eigenschaften von synthetischem Papier aus Folien und synthetischem Zellstoff, [Diss. 78/--69, Fachbereich Maschinenbau an der Technischen Hochschule Darmstadt, 1978]

[30] Nils Pauler, M. Sjögren, MoDo Forskning och utveckling, Färgsettningsstudier med Prüfbau laboratorietryckpress, [Rapport nr 4620 Tryckbarhet, 1995]

[31] P.A.C. Gane, E.N. Seyler, Tack development: An Analysis of Ink/paper Interaction in Offset Printing] 1994 International Printing and Grafic Arts Conference.

[32] S. Finke, Versuchsanleitungen zum Anfänger-Praktikum in Physik, [Fachbereich Physik, Universität Dortmund, 22. Auflage September 1990]

[33] I. N. Bronstein, K. A. Semendjajew, [Taschenbuch der Mathematik, Verlag Harri Deutsch, Thun und Frankfurt/ Main, 1989]

[34] H. Schubert, Kapillarität in porösen Feststoffsystemen, S.104, [Springer-verlag Berlin Heidelberg, New York, 1982]

[35] Telephone call to Eward Seyler, suplplier of the ink-tack-instrument

[36] N. Plowman Sandreuter, The impact of Paper Properties on the Success of In-Line Aqueous Coutings, [International Printing & Graphics Arts Conference, 1996]

[37] A. Voet, Ink and Paper in the Printing Process, [Interscience Publishers, New York, London, 1952]

[38] A.J. Kinloch, Adhesion and adhesives, [science and technology, Chapman and Hall, 1986]

[39] P. H. Sørensen, Tack of a printed ink film and ist relation to the properties of ink and paper surface [Advances in printing science and technology, Oxford Pergamon, Press 1961]

[40] M. Wickman, M. Sundin, A new method for direct measurment of ink setting on coated paper, [Institute for Surface Chemistry, Box 5607, S-114 86 Sockholm, Sweden, 1994]

[41] R. J. Dickson, P. Lepoutre, Mechanical interlocking in coating adhesion to paper [Tappi Journal, Vol. 80, NO. 11, Nov. 1997]

[42] J. H. Taylor, A. Zettlemoyer, Hypothesis on the mechanics of ink splitting during printing, [Tappi, , Vol. 41, No.12, December 1958]

[43] G. Novak, I. Malesic, Streichrohpapier als einer der wichtigsten Faktoren für die Qualität von gestrichenen Papieren, [Das Papier, Heft 3, 1993]

Appendix:

A.1 Investigating the spring force:

The load cell in the apparatus measures a maximum tack-force of 10 N. This force is induced by the spring that can exceed to a distance of 0,7 cm. The spring constant is measured in order to confirm the correct measured forces. One uses the formulas:

$F = C \cdot x$ and
$F = m \cdot \ddot{x}$

Combining the formulas one receives:

$$C = \frac{m\,\ddot{x}}{x}$$

With

$\ddot{x}$ = g = 9,81 m/s^2 and

x = 0,007 m,

m = 1,283 kg

a spring constant of C = 1797,66 kg/s^2 is recieved.

The maximum possible spring force is then:

F_{max} = 10,5 N

The maximum of the measurement range is 10 N. The apparatus measures correct forces.

A.2 Evaluation of the Navier-Stokes equations for rectangular bodies:

If the bodies are two rectangular bodies that are separated from each other, the cartesian form of the Navier-Stokes equations can be used:

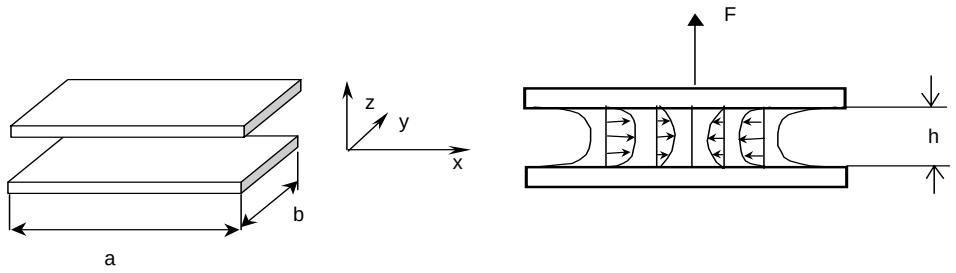

Fig. Liquid between two separating plane surfaces

For other geometries the solution is more difficult. In cartesian coordinates the Navier-Stokes-equations are:

$$\rho\cdot\left(\frac{\partial v_x}{\partial t}+v_x\frac{\partial v_x}{\partial x}+v_y\frac{\partial v_x}{\partial y}+v_z\frac{\partial v_x}{\partial z}\right)=-\frac{\partial p}{\partial x}+\mu\left(\frac{\partial^2 v_x}{\partial x^2}+\frac{\partial^2 v_x}{\partial y^2}+\frac{\partial^2 v_x}{\partial z^2}\right) \tag{A1}$$

$$\rho\cdot\left(\frac{\partial v_y}{\partial t}+v_x\frac{\partial v_y}{\partial x}+v_y\frac{\partial v_y}{\partial y}+v_z\frac{\partial v_y}{\partial z}\right)=-\frac{\partial p}{\partial y}+\mu\left(\frac{\partial^2 v_y}{\partial x^2}+\frac{\partial^2 v_y}{\partial y^2}+\frac{\partial^2 v_y}{\partial z^2}\right) \tag{A2}$$

$$\rho\cdot\left(\frac{\partial v_z}{\partial t}+v_x\frac{\partial v_z}{\partial x}+v_y\frac{\partial v_z}{\partial y}+v_z\frac{\partial v_z}{\partial z}\right)=-\frac{\partial p}{\partial z}+\mu\left(\frac{\partial^2 v_z}{\partial x^2}+\frac{\partial^2 v_z}{\partial y^2}+\frac{\partial^2 v_z}{\partial z^2}\right) \tag{A3}$$

The fluid's speed in the x and y- direction is much greater than in z – direction.

So only those terms have to be considered. The Navier- Stokes equations simplify then to:

$$\eta\frac{\partial^2 v_x}{\partial z^2}=\frac{\partial p}{\partial x} \tag{A4}$$

$$\eta\frac{\partial^2 v_y}{\partial z^2}=\frac{\partial p}{\partial y} \tag{A5}$$

$$\frac{\partial p}{\partial z}=0 \tag{A6}$$

The continuity equation is:

$$\nabla\cdot\underset{\sim}{v}\ \underset{\sim}{=}\frac{\partial v_x}{\partial x}+\frac{\partial v_y}{\partial y}+\frac{\partial v_z}{\partial z}=0 \tag{A7}$$

With

$$v_z << v_x, v_y$$

$$\frac{\partial v_z}{\partial z} >> \frac{\partial v_x}{\partial x}, \frac{\partial v_y}{\partial y}$$

And

integration the above equation on the z-component gives:

$$\int_0^h \frac{\partial v_z}{\partial z}\partial z=-\int_0^h\left(\frac{\partial v_x}{\partial x}+\frac{\partial v_y}{\partial y}\right)\partial z \tag{A8}$$

The boundary conditions are:

$$z=0: v_z=v_x=v_y=0$$

$$z=h: v_z=-u;\ v_x=v_y=0$$

$$y=0; y=b: p=p_0$$

$$x=0; x=a: p=p_0$$

Integrating the x-component of the Navier-Stokes equation on the z-component: gives:

$$\eta \int_0^z \frac{\partial^2 v_x}{\partial z^2} \partial z = \eta \frac{\partial v_x}{\partial z} = \frac{\partial p}{\partial x}(z + C_1) \tag{A9}$$

$$\eta v_x = \frac{\partial p}{\partial x}\left(\frac{z^2}{2} + C_1 z + C_2\right) \tag{A10}$$

Putting in the boundary conditions one gets:

$$\eta v_x = \frac{\partial p}{\partial x}\frac{z}{2}(z - h) \tag{A11}$$

Integrating the y-component in a similar way the following solution is obtained:

$$\eta v_y = \frac{\partial p}{\partial y}\frac{z}{2}(z - h) \tag{A12}$$

Taking the integrated form of the continuity equation:

$$\int_0^h \frac{\partial v_z}{\partial z} \partial z = -\int_0^h \left(\frac{\partial v_x}{\partial x} + \frac{\partial v_y}{\partial y}\right) \partial z \tag{A13}$$

And putting the last equations into the solution, the following form is obtained:

$$\begin{aligned} -u &= -\frac{\partial}{\partial x}\int_0^h \frac{1}{2\eta} z(z-h)\frac{\partial p}{\partial x}\partial z - \frac{\partial}{\partial y}\int_0^h \frac{1}{2\eta} z(z-h)\frac{\partial p}{\partial y}\,\partial z \\ &= -\frac{1}{2\eta}\frac{\partial}{\partial x}\left[\frac{h^3}{3} - \frac{h^3}{2}\right]\frac{\partial p}{\partial x} - \frac{\partial}{\partial y}\frac{1}{2\eta}\left[\frac{h^3}{3} - \frac{h^3}{2}\right]\frac{\partial p}{\partial y} \\ &= \frac{h^3}{6 \cdot 2\eta}\left(\frac{\partial^2 p}{\partial x^2} + \frac{\partial^2 p}{\partial y^2}\right) \end{aligned} \tag{A14}$$

$$\Leftrightarrow \frac{\partial^2 p}{\partial x^2} + \frac{\partial^2 p}{\partial y^2} = -\frac{12\eta u}{h^3} \tag{A15}$$

The last differential equation is called Poisson equation. For a square area the solution is quite difficult. It is much easier to approximate the area by an ellipse. Moreover can the elliptical shape be found at the tack marks on the tested paper and board samples.

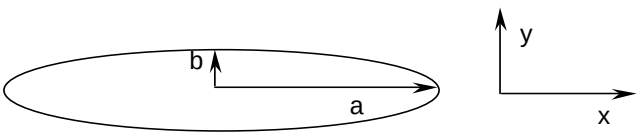

Fig. elliptical area with the pressure $p - p_0$

The equation for the ellipse is:

$$\frac{x^2}{a^2}+\frac{y^2}{b^2}=1 \tag{A16}$$

$$\frac{x^2}{a^2}+\frac{y^2}{b^2}-1=0 \tag{A17}$$

The solution of the ellipse is approached with the form that has to fulfill:

$$k\cdot\left(\frac{x^2}{a^2}+\frac{y^2}{b^2}-1\right)=p-p_0=\Delta p \tag{A18}$$

By differentiating this approach to the x and y coordinate, one gets

$$\frac{\partial p^2}{\partial x^2}=k\left(\frac{2}{a^2}\right) \tag{A19}$$

$$\frac{\partial p^2}{\partial y^2}=k\left(\frac{2}{b^2}\right) \tag{A20}$$

Putting this into the differential equation, one gets for k:

$$k=-6\cdot\eta\frac{u}{h^3}\cdot\frac{a^2b^2}{a^2+b^2} \tag{A21}$$

So the solution for the differential equation is:

$$-6\eta\frac{u}{h^3}\frac{a^2b^2}{a^2+b^2}\cdot\left(\frac{x^2}{a^2}+\frac{y^2}{b^2}-1\right)=p-p_0 \tag{A22}$$

The maximum of the force is

$$F=\int_0^a\int_0^b p_{(x,y)}\,\partial x\,\partial y \tag{A23}$$

$$F_{max}=-2\eta\frac{u}{h^3}\frac{a^3b^3}{a^2+b^2} \tag{A24}$$

The force needed to separate the plates rises linear with the viscosity, cubical with a decreasing gap and to the forth exponent of the area that is covered.

A.3 Evaluation of a 2^3 factor design with effects: hold time, pressure force and print speed:

Maximum force:

	1	a	b	ab	c	ac	bc	abc
max force [N]:	7.82	7.45	8.34	8.37	7.46	7.68	8.33	8.3

effects [%]:

print speed	A	-0.038	SS A	0.0028	MSA	0.0028
hold time	B	0.7325	SS B	1.0731	MSB	1.0731
pressure force	C	-0.052	SS C	0.0055	MSC	0.0055
ps + ht	AB	0.0375	SS AB	0.0028	MSAB	0.0028
ps + pf	AC	0.295	SS AC	0.1741	MSAC	0.1741
ht + pf	BC	0.0125	SS BC	0.0003	MSBC	0.0003
ps + ht + pf	ABC	-0.162	SS ABC	0.0528	MSABC	0.0528

		MSR	0.0575
significance:	F	$F_{0.95}$	7.71
faktor A:	0.0489	***not significant***	
faktor B:	18.664	***significant !!!***	
faktor C:	0.0959	***not significant***	
faktor AB:	0.0489	***not significant***	
faktor AC:	3.0271	***not significant***	
faktor BC:	0.0054	***not significant***	
faktor ABC:	0.9185	***not significant***	

Max. force time:

	1	a	b	ab	c	ac	bc	abc
max force time [s]:	82.391	51.129	86.512	102.33	66.742	66.73	70.961	70.961

effects [%]:

print speed	A	-3.864	SS A	29.861	MSA	29.861
hold time	B	15.943	SS B	508.36	MSB	508.36
pressure force	C	-11.74	SS C	275.75	MSC	275.75
ps + ht	AB	11.773	SS AB	277.21	MSAB	277.21
ps + pf	AC	4.9158	SS AC	48.329	MSAC	48.329
ht + pf	BC	-11.72	SS BC	274.62	MSBC	274.62
ps + ht + pf	ABC	-11.77	SS ABC	276.92	MSABC	276.92

		MSR	219.27
significance:	F	$F_{0.95}$	7.71
faktor A:	0.1362	***not significant***	
faktor B:	2.3184	***not significant***	
faktor C:	1.2576	***not significant***	
faktor AB:	1.2642	***not significant***	
faktor AC:	0.2204	***not significant***	
faktor BC:	1.2524	***not significant***	
faktor ABC:	1.2629	***not significant***	

Slope in the beginning:

	1	a	b	ab	c	ac	bc	abc
slope [N/s]:	0.1039	0.1205	0.1023	0.1072	0.1094	0.1281	0.0929	0.1094

effects [%]:

print speed	A	0.0142	SS A	0.0004	MSA	0.0004
hold time	B	-0.013	SS B	0.0003	MSB	0.0003
pressure force	C	0.0015	SS C	4E-06	MSC	4E-06
ps + ht	AB	-0.003	SS AB	2E-05	MSAB	2E-05
ps + pf	AC	-0.005	SS AC	6E-05	MSAC	6E-05
ht + pf	BC	-0.005	SS BC	5E-05	MSBC	5E-05
ps + ht + pf	ABC	0.0024	SS ABC	1E-05	MSABC	1E-05

		MSR	4E-05
significance:	F	$F_{0.95}$	7.71
faktor A:	11.075	***significant !!!***	
faktor B:	8.6238	***significant !!!***	
faktor C:	0.1165	***not significant***	
faktor AB:	0.6611	***not significant***	
faktor AC:	1.6077	***not significant***	
faktor BC:	1.4189	***not significant***	
faktor ABC:	0.3124	***not significant***	

Coefficiant of Variation of force:

	1	a	b	ab	c	ac	bc	abc
Coeff.of Var.of for.:	5.2	2.11	3.78	3.56	3.18	6.18	1.93	4.27

effects [%]:

print speed	A	0.5075	SS A	0.5151	MSA	0.5307
hold time	B	-0.783	SS B	1.2246	MSB	2.9994
pressure force	C	0.2275	SS C	0.1035	MSC	0.0214
ps + ht	AB	0.5525	SS AB	0.6105	MSAB	0.7455
ps + pf	AC	1.1	SS AC	2.42	MSAC	11.713
ht + pf	BC	-0.798	SS BC	1.272	MSBC	3.236
ps + ht + pf	ABC	-0.883	SS ABC	1.5576	MSABC	4.8523

		MSR	1.465
significance:	F	$F_{0.95}$	7.71
faktor A:	0.3622	***not significant***	
faktor B:	2.0473	***not significant***	
faktor C:	0.0146	***not significant***	
faktor AB:	0.5088	***not significant***	
faktor AC:	7.9949	***significant !!!***	
faktor BC:	2.2088	***not significant***	
faktor ABC:	3.3121	***not significant***	

Transferred ink:

	1	a	b	ab	c	ac	bc	abc
transferred ink [g]:	0.0072	0.0059	0.0071	0.007	0.0061	0.0066	0.0065	0.006

effects [%]:

print speed	A	-3E-04	SS A	2E-07	MSA	2E-07
hold time	B	0.0002	SS B	9E-08	MSB	9E-08
pressure force	C	-5E-04	SS C	6E-07	MSC	6E-07
ps + ht	AB	4E-05	SS AB	3E-09	MSAB	3E-09
ps + pf	AC	0.0003	SS AC	2E-07	MSAC	2E-07
ht + pf	BC	-3E-04	SS BC	2E-07	MSBC	2E-07
ps + ht + pf	ABC	-5E-04	SS ABC	6E-07	MSABC	6E-07

		MSR	2E-07
significance:	F	$F_{0.95}$	7.71
faktor A:	0.9802	***not significant***	
faktor B:	0.364	***not significant***	
faktor C:	2.3109	***not significant***	
faktor AB:	0.0146	***not significant***	
faktor AC:	0.8864	***not significant***	
faktor BC:	0.6358	***not significant***	
faktor ABC:	2.4631	***not significant***	

Beginning force:

	1	a	b	ab	c	ac	bc	abc
beginning force [N]:	3.65	3.65	4.78	4.08	4.53	3.32	5.15	5.28

effects [%]:

print speed	A	-0.445	SS A	0.396	MSA	0.396
hold time	B	1.035	SS B	2.1425	MSB	2.1425
pressure force	C	0.53	SS C	0.5618	MSC	0.5618
ps + ht	AB	0.16	SS AB	0.0512	MSAB	0.0512
ps + pf	AC	0.3625	SS AC	0.2628	MSAC	0.2628
ht + pf	BC	0.255	SS BC	0.1301	MSBC	0.1301
ps + ht + pf	ABC	0.51	SS ABC	0.5202	MSABC	0.5202

		MSR	0.2411
significance:	F	$F_{0.95}$	7.71
faktor A:	1.6429	***not significant***	
faktor B:	8.8874	***significant !!!***	
faktor C:	2.3305	***not significant***	
faktor AB:	0.2124	***not significant***	
faktor AC:	1.0902	***not significant***	
faktor BC:	0.5395	***not significant***	
faktor ABC:	2.1579	***not significant***	

Density:

	1	a	b	ab	c	ac	bc	abc
density:	1.94	1.81	1.93	1.93	1.69	1.85	1.85	1.76

effects [%]:

print speed	A	-0.015	SS A	0.0005	MSA	0.0005
hold time	B	0.045	SS B	0.0041	MSB	0.0041
pressure force	C	-0.115	SS C	0.0264	MSC	0.0264
ps + ht	AB	-0.03	SS AB	0.0018	MSAB	0.0018
ps + pf	AC	0.05	SS AC	0.005	MSAC	0.005
ht + pf	BC	-0.01	SS BC	0.0002	MSBC	0.0002
ps + ht + pf	ABC	-0.095	SS ABC	0.0181	MSABC	0.0181

		MSR	0.0063
significance:	F	$F_{0.95}$	7.71
faktor A:	0.0719	***not significant***	
faktor B:	0.6467	***not significant***	
faktor C:	4.2236	***not significant***	
faktor AB:	0.2874	***not significant***	
faktor AC:	0.7984	***not significant***	
faktor BC:	0.0319	***not significant***	
faktor ABC:	2.8822	***not significant***	

Coefficiant of variance of density of unsplit film:

	1	a	b	ab	c	ac	bc	abc
Co.of var.of den.:	1.39	0.3	0.31	0.15	0.23	0.25	0.07	0.63

effects [%]:

print speed	A	-0.168	SS A	0.0561	MSA	0.012
hold time	B	-0.253	SS B	0.1275	MSB	0.0001
pressure force	C	-0.243	SS C	0.1176	MSC	1E-05
ps + ht	AB	0.3675	SS AB	0.2701	MSAB	0.03
ps + pf	AC	0.4125	SS AC	0.3403	MSAC	0.0561
ht + pf	BC	0.3625	SS BC	0.2628	MSBC	0.0276
ps + ht + pf	ABC	-0.098	SS ABC	0.019	MSABC	0.0435

		MSR	0.2231
significance:	F	$F_{0.95}$	7.71
faktor A:	0.0539	***not significant***	
faktor B:	0.0005	***not significant***	
faktor C:	6E-05	***not significant***	
faktor AB:	0.1345	***not significant***	
faktor AC:	0.2516	***not significant***	
faktor BC:	0.1238	***not significant***	
faktor ABC:	0.1951	***not significant***	

Average slope

	1	a	b	ab	c	ac	bc	abc
aver. slope	0.005	-0.006	0.0077	0.0084	-0.003	0.0003	0.0042	-0.002

effects [%]:

print speed	A	-0.003	SS A	2E-05	MSA	2E-05
hold time	B	0.0054	SS B	6E-05	MSB	6E-05
pressure force	C	-0.004	SS C	3E-05	MSC	3E-05
ps + ht	AB	0.0006	SS AB	8E-07	MSAB	8E-07
ps + pf	AC	0.0027	SS AC	1E-05	MSAC	1E-05
ht + pf	BC	-0.003	SS BC	2E-05	MSBC	2E-05
ps + ht + pf	ABC	-0.005	SS ABC	6E-05	MSABC	6E-05

		MSR	2E-05
significance:	F	$F_{0.95}$	7.71
faktor A:	1.052	***not significant***	
faktor B:	2.5283	***not significant***	
faktor C:	1.3096	***not significant***	
faktor AB:	0.0341	***not significant***	
faktor AC:	0.6281	***not significant***	
faktor BC:	0.8836	***not significant***	
faktor ABC:	2.4542	***not significant***	

End force:

	1	a	b	ab	c	ac	bc	abc
end force value	6.15	4.51	7.71	7.22	5.8	5.38	7.33	6.62

effects [%]:

print speed	A	-0.815	SS A	1.3285	MSA	1.3285
hold time	B	1.76	SS B	6.1952	MSB	6.1952
pressure force	C	-0.115	SS C	0.0265	MSC	0.0265
ps + ht	AB	0.215	SS AB	0.0925	MSAB	0.0925
ps + pf	AC	0.7375	SS AC	1.0878	MSAC	1.0878
ht + pf	BC	-0.375	SS BC	0.2812	MSBC	0.2812
ps + ht + pf	ABC	-0.36	SS ABC	0.2592	MSABC	0.2592

		MSR	0.4302
significance:	F	$F_{0.95}$	7.71
faktor A:	3.0881	***not significant***	
faktor B:	14.401	***significant !!!***	
faktor C:	0.0615	***not significant***	
faktor AB:	0.2149	***not significant***	
faktor AC:	2.5287	***not significant***	
faktor BC:	0.6538	***not significant***	
faktor ABC:	0.6025	***not significant***	

Density of split film:

	1	a	b	ab	c	ac	bc	abc
density of split film:	1.33	1.23	1.3	1.32	1.11	1.23	1.18	1.11

effects [%]:

print speed	A	-0.008	SS A	0.0001	MSA	0.0001
hold time	B	0.0025	SS B	1E-05	MSB	1E-05
pressure force	C	-0.138	SS C	0.0378	MSC	0.0378
ps + ht	AB	-0.017	SS AB	0.0006	MSAB	0.0006
ps + pf	AC	0.02	SS AC	0.0008	MSAC	0.0008
ht + pf	BC	-0.028	SS BC	0.0015	MSBC	0.0015
ps + ht + pf	ABC	-0.077	SS ABC	0.012	MSABC	0.012

		MSR	0.0037
significance:	F	$F_{0.95}$	7.71
faktor A:	0.0301	***not significant***	
faktor B:	0.0033	***not significant***	
faktor C:	10.126	***significant !!!***	
faktor AB:	0.164	***not significant***	
faktor AC:	0.2142	***not significant***	
faktor BC:	0.405	***not significant***	
faktor ABC:	3.2167	***not significant***	

Coefficiant of variance of density of split film:

	1	a	b	ab	c	ac	bc	abc
C of Var. of spl. f.	5.12	2.68	3.89	3.87	5.46	1.46	1.47	5.44

effects [%]:

print speed	A	-0.622	SS A	0.775	MSA	0.775
hold time	B	-0.013	SS B	0.0003	MSB	0.0003
pressure force	C	-0.433	SS C	0.3741	MSC	0.3741
ps + ht	AB	2.5975	SS AB	13.494	MSAB	13.494
ps + pf	AC	0.61	SS AC	0.7442	MSAC	0.7442
ht + pf	BC	0.0075	SS BC	0.0001	MSBC	0.0001
ps + ht + pf	ABC	1.3875	SS ABC	3.8503	MSABC	3.8503

		MSR	4.5222
significance:	F	$F_{0.95}$	7.71
faktor A:	0.1714	***not significant***	
faktor B:	7E-05	***not significant***	
faktor C:	0.0827	***not significant***	
faktor AB:	2.984	***not significant***	
faktor AC:	0.1646	***not significant***	
faktor BC:	2E-05	***not significant***	
faktor ABC:	0.8514	***not significant***	

Evaluation of a reduced 2^6 factor design with effects: print speed, hold time, pressure force, new tack roller, additional film split and distribution time.

	new roll	apl. time	film split disabl.	print speed	pressure force	hold time
eff. coeff. of var. force val.	-2.12	1.72	-1.68	1.33	-0.34	-0.21
conf. Int. (±)	2.22	2.22	2.22	2.56	1.58	1.58
effect beginning force	0.24	0.04	-1.76	-1.10	0.25	1.22
conf. Int. (±)	0.48	0.48	0.48	0.55	0.34	0.34
			significant	**significant**		**significant**
effect beginning slope	-0.0070	0.0032	0.0350	0.0360	-0.0060	-0.0170
conf. Int. (±)	0.0170	0.0170	0.0170	0.0190	0.0120	0.0120
				significant		**significant**
effect time till max. force	-5.54	10.25	36.71	2.97	-4.73	-0.38
conf. Int. (±)	19.16	19.16	19.16	22.10	13.65	13.65
			significant			
effect maximum force	-0.34	0.17	0.274	-0.085	-0.240	0.674
conf. Int. (±)	0.27	0.27	0.268	0.309	0.191	0.191
	significant		**significant**		**significant**	**significant**
effect density	-0.033	0.022	0.353	-0.023	-0.044	-0.016
conf. Int. (±)	0.127	0.127	0.127	0.146	0.090	0.090
effect coeff. var. density	0.877	-1.170	-2.760	1.70	1.59	0.75
conf. Int. (±)	2.68	2.680	2.660	3.08	1.91	1.90
			significant			
effect average slope	0.005	0.001	0.014	-0.001	-0.002	0.003
conf. Int. (±)	0.007	0.007	0.007	0.008	0.005	0.005
			significant			
effect ending force	-0.763	0.510	1.340	-0.711	-0.194	1.460
conf. Int. (±)	0.770	0.770	0.770	0.888	0.548	0.548
			significant			**significant**
effect transferred ink	-0.0014	-0.0005	-0.0003	0.0005	0.0004	0.00002
conf. Int. (±)	0.001	0.0012	0.0012	0.0013	0.0008	0.00083
	significant					

A.4 Contact angle measurments courtesly used from MoDo research.

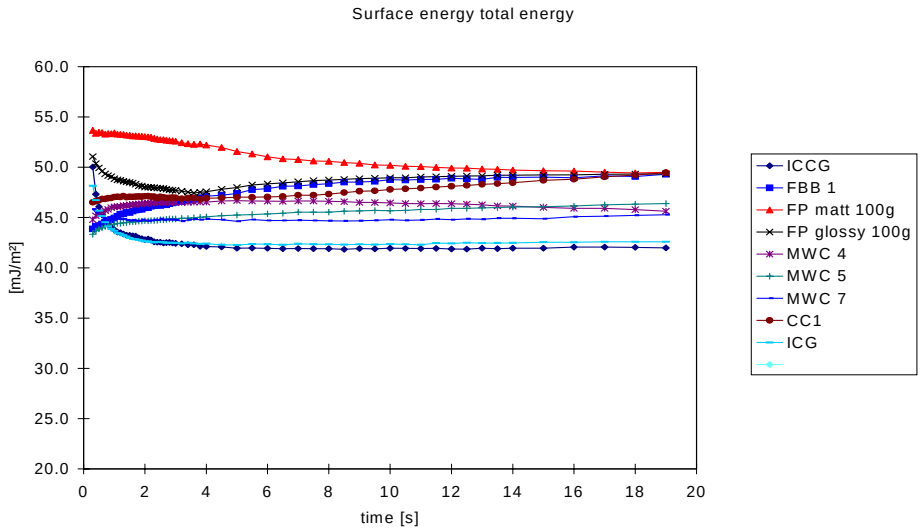

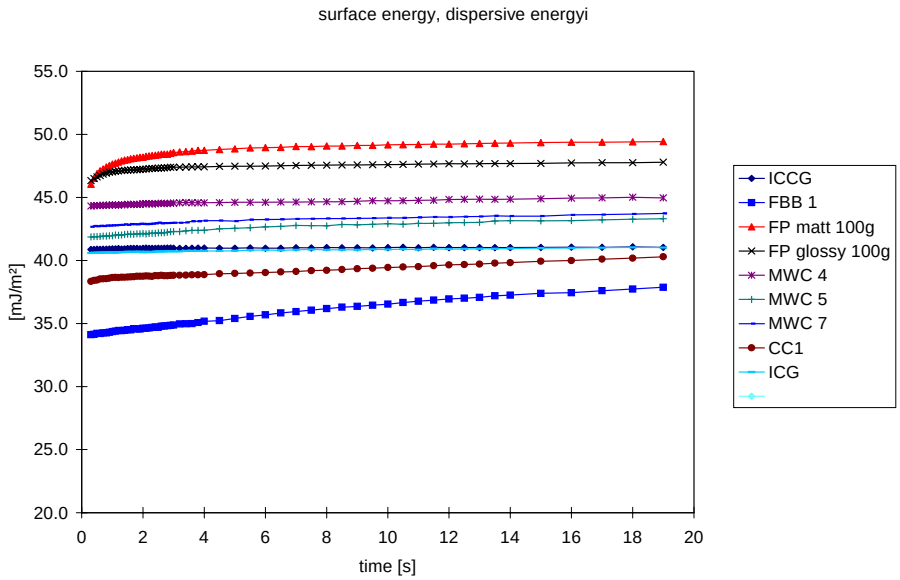

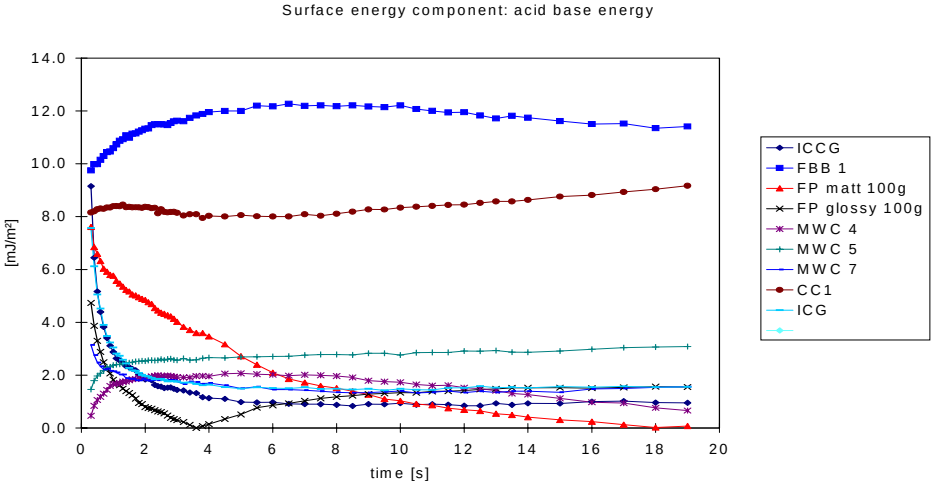

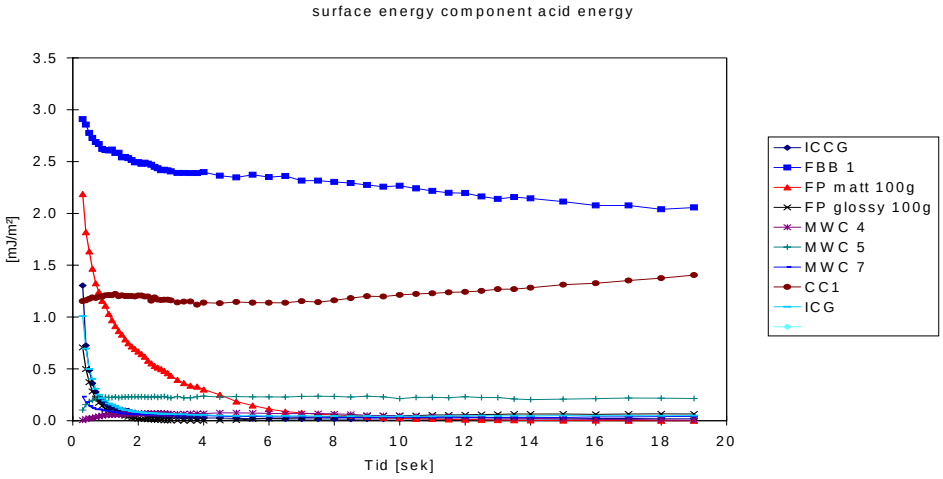
surface energy component acid energy
[mJ/m²]
Tid [sek]
ICCG
FBB 1
FP matt 100g
FP glossy 100g
MWC 4
MWC 5
MWC 7
CC1
ICG

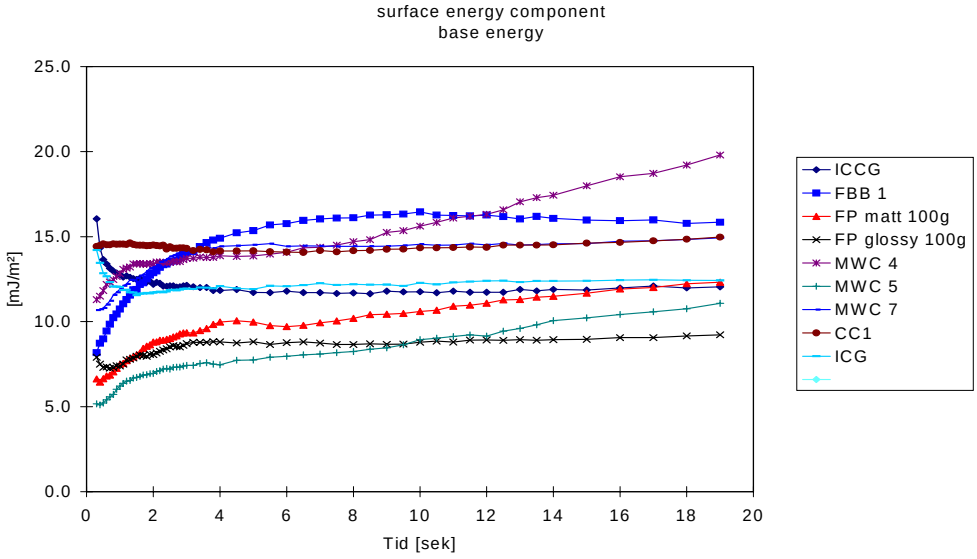
surface energy component
base energy
[mJ/m²]
Tid [sek]
ICCG
FBB 1
FP matt 100g
FP glossy 100g
MWC 4
MWC 5
MWC 7
CC1
ICG

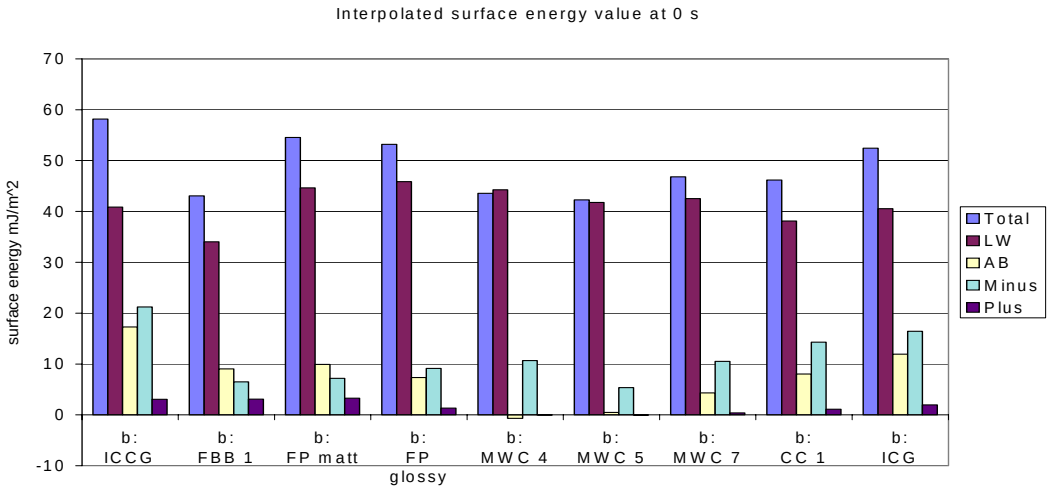
Interpolated surface energy value at 0 s
surface energy mJ/m^2
b: ICCG
b: FBB 1
b: FP matt
b: FP glossy
b: MWC 4
b: MWC 5
b: MWC 7
b: CC 1
b: ICG
Total
LW
AB
Minus
Plus

A.5 PPS roughness tests [µm], tack marks [N]:

substrate	PPs_roughness [µm]	tackm. w. str. + lighter surr. area [N]	tackm. white strip [N]	difference marks [N]
SBB ICA	0.77	6.41	5.07	1.34
SBB ICCM	1.09	6.13	4.47	1.66
SBB ICCG	0.80	7.41	4.89	2.52
SBB ICG 180	1.49	6.46	5.43	1.03
SBB ICG 260	1.07	7.38	6.25	1.13
SBB ICG 260 some week	1.07	7.38	6.25	1.13
SBB ICG 380	0.90	7.32	5.78	1.54
FP matt 100	3.02	5.4	3.76	1.64
FP glossy 100	0.89	8.03	5.71	2.32
FP glossy 130	0.93	8.11	5.14	2.97
FP matt 170	2.58	5.93	4.89	1.04
FP glossy 170	0.89	8	5.43	2.57
FP matt 200	2.06	7.41	5.94	1.47
FP glossy 240	0.82	7.19	4.95	2.24
FP matt 300	2.18	6.98	6	0.98
MWC 1	1.45	6.25		
MWC 2	1.30	6.45		
MWC 3	1.24	6.04		
MWC 4	1.48	5.96		
MWC 5	3.12	4.16		
MWC 6	1.44	6.12		
MWC 7	0.94	6.16		
FBB 1	1.27	6.66	5.54	1.12
FBB 2	1.08	6.8	4.71	2.09
FBB 3	1.45	6.29	4.05	2.24
FBB 4	1.10	5.92	4.08	1.84
CC 1	0.71	6.12		
E Baseboard	7.41			
E 1	1.90	4.95	3.88	1.07
E 2	2.08	3.75	3.27	0.48
E 3	2.10	4.33	3.06	1.27
E 4	1.54	6.29	4.47	1.82
E 5	1.58	7.9	6.73	1.17
E 6	1.69	7.34	5.36	1.98
SB Tg 13°C low c	2.30			
SB Tg 9°C high c	2.02			
SB Tg 8°C medium c	1.70			
SB Tg -7°C	1.48			
SA Tg 25°C	2.19			
SB Tg 27°C	2.15			
PE+cor, glossy	3.73			
PE+cor, rough	6.33			
PE, rough	7.80			
PET, rough	9.14			
PMP, rough	7.44			
PP, rough	7.79			
PP + cor, glossy	4.17			
Mylar film	0.31			
Aluminum foil glossy	1.04			
Aliminum foil, matt	0.50			
Base FP	7.37			
Data copy	7.42			
OCR basepaper	6.43			

A.6 SEM images of ICCG

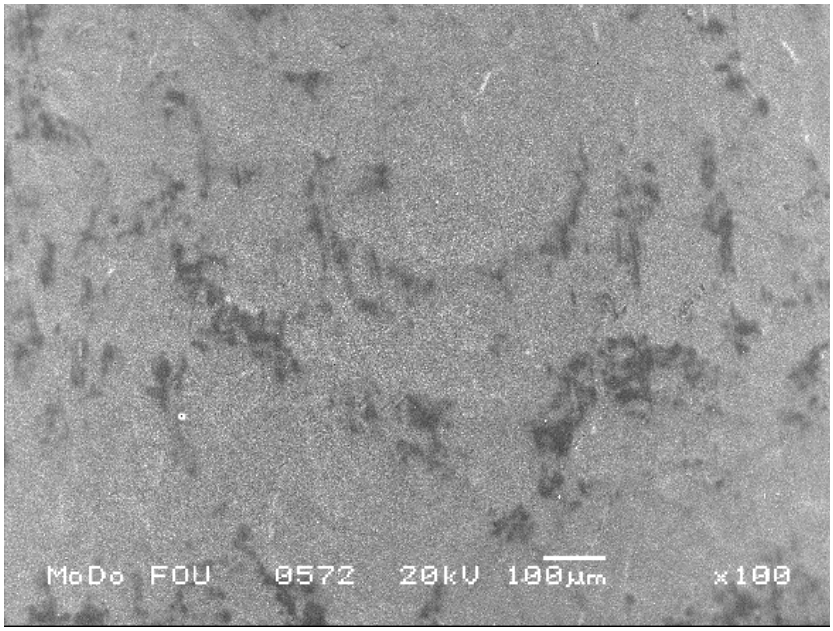

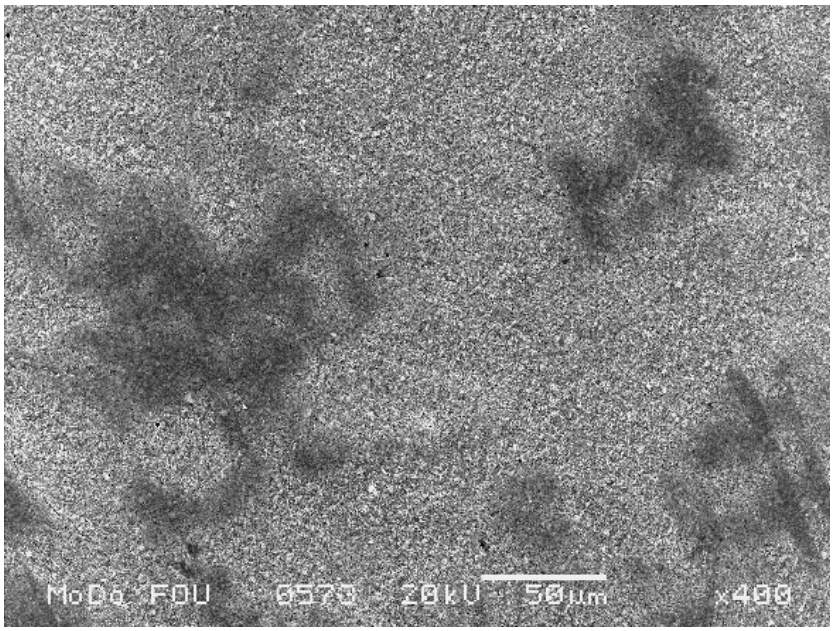

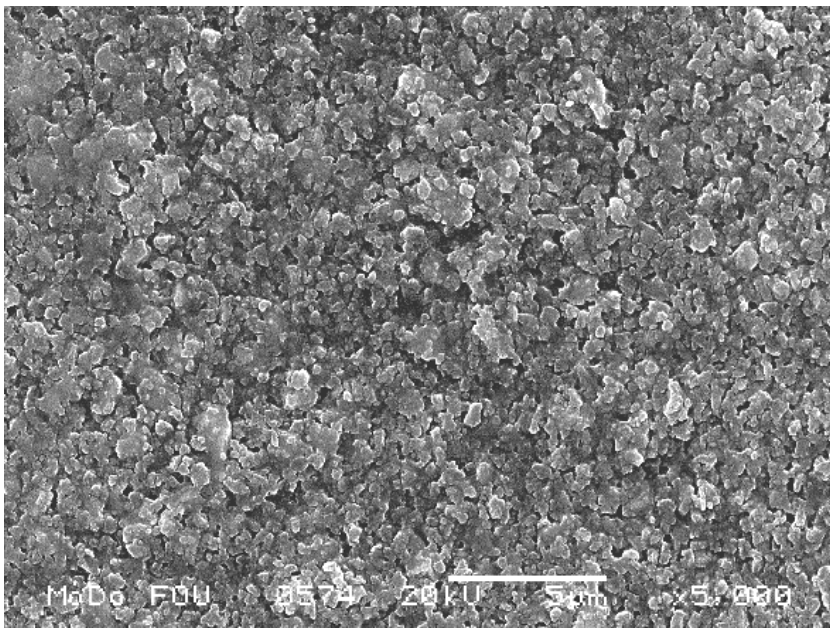

SEM images ICG

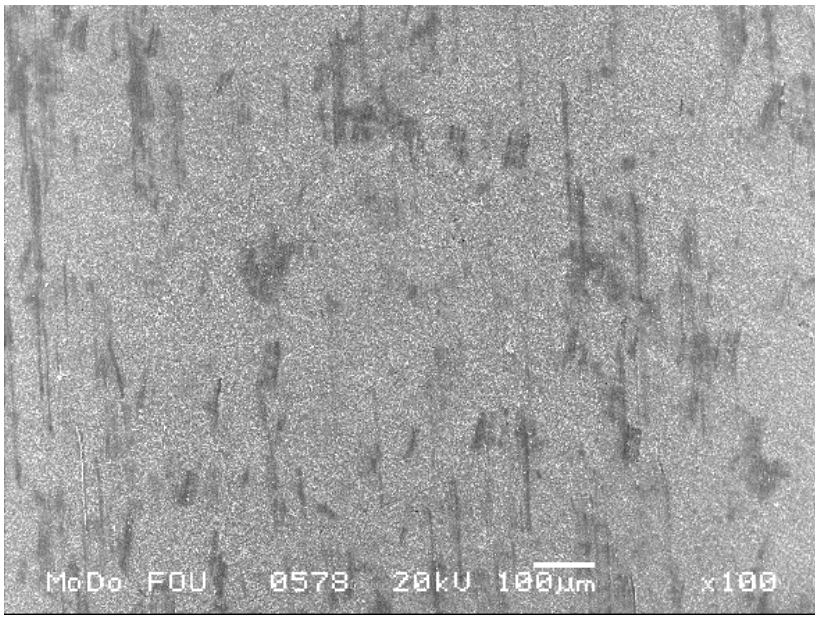

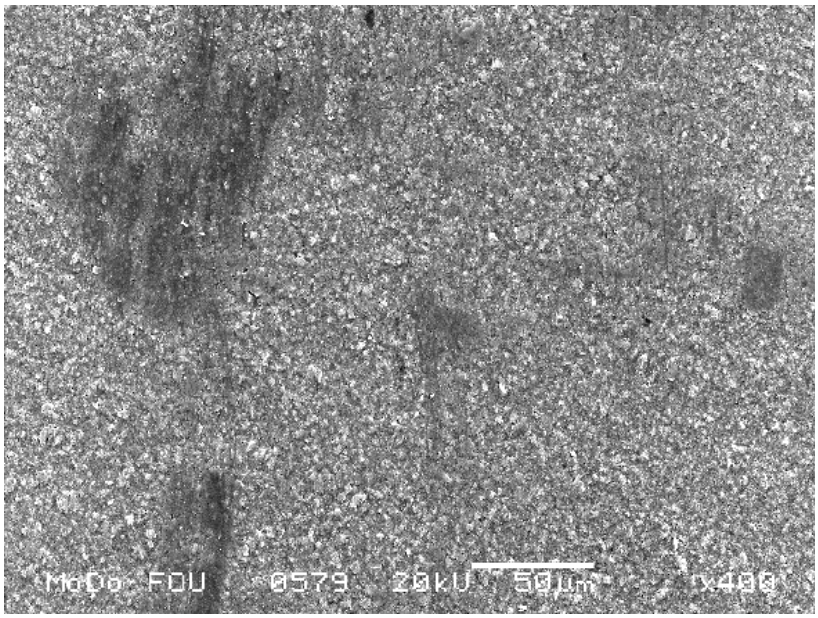

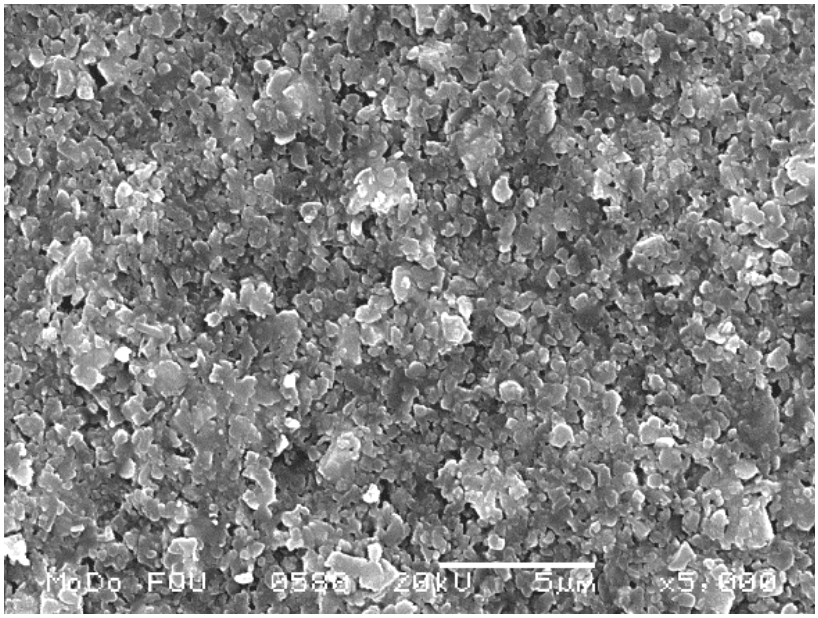

SEM images CC 1

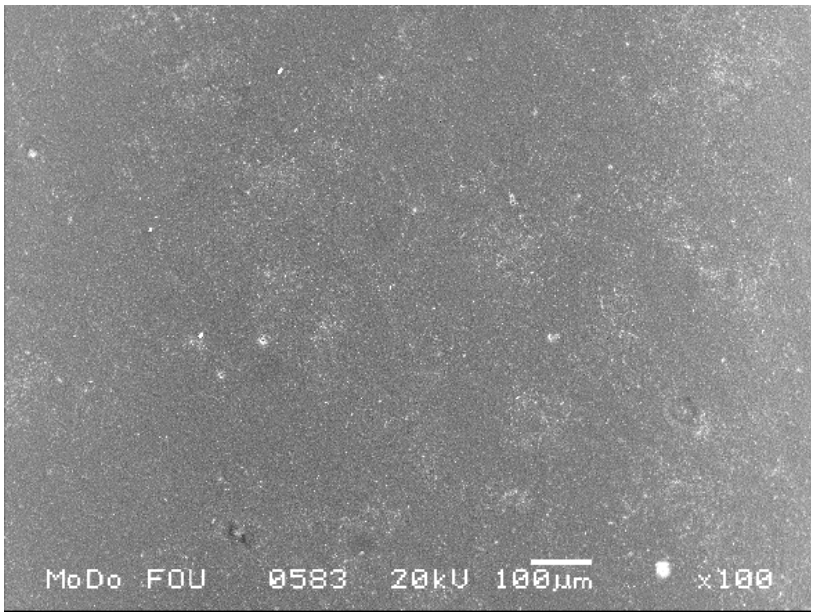

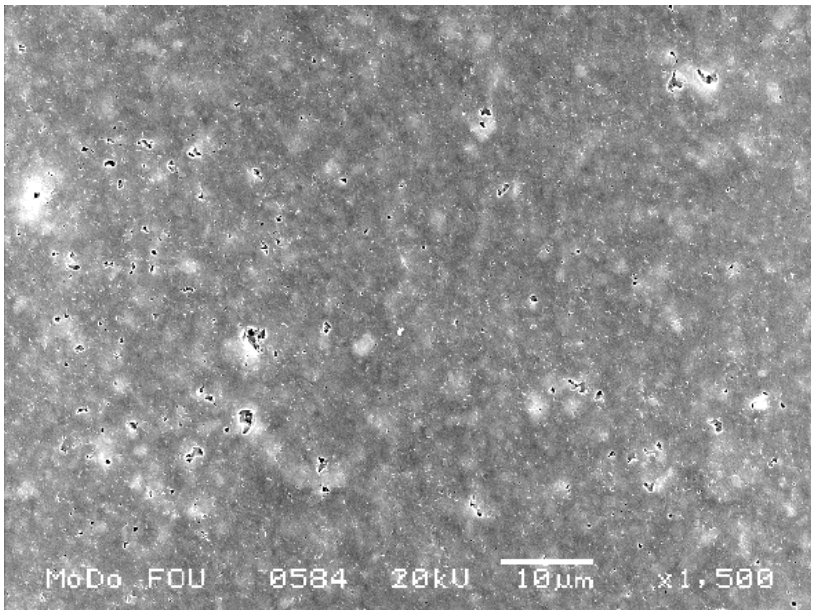

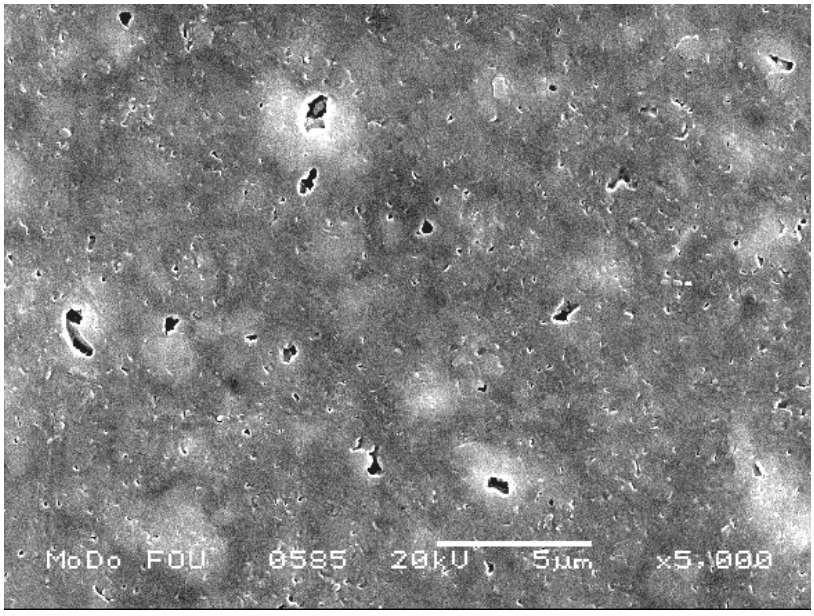

A.7 Declaration:

I declare that I performed my thesis independently. All references I used as a help, are referred to.

Sven Keiter, Iggesund 05. 02.1998

A.8 Tack-force development-curves of a 2^3 trial factor design:

Print speed: 0,1 m/s; holding time: 1 s; pressure force: 200 N

Data of average curve:

	time [s]	force [N]	Slope [N/s]
Max. ford	82.391	7.62	
beginning:		3.65	0.10388
average:			0.00504
end:		6.15	

	curve 1	curve 2	curve 3	average
transf. ink [g]:	0.0075	0.007	0.0071	0.0072
transf. ink [g/m²]	1.39	1.30	1.31	1.33

		C.of Var.[%]:
aver. density of split film:	1.33	5.12
av. density of unspl. film:	1.94	3.03
av. coef. of var. of force values [%]:		5.20372

mach. param. serie 1

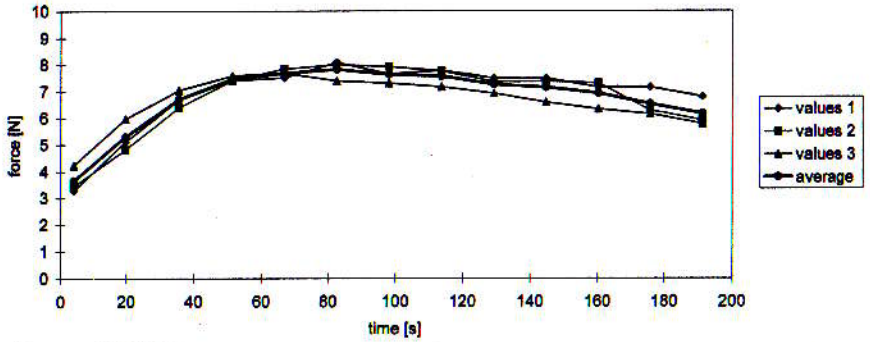

Print speed: 1 m/s; holding time: 1 s; pressure force:200 N

Data of average curve:

	time [s]	force [N]	Slope [N/s]
Max.:	51.129	7.45	
beginning:		3.65	0.12053
average:			-0.006
end:		4.51	

	curve 1	curve 2	curve 3	average
transf. ink [g]:	0.0094	0.0064	0.0065	0.00743
transf. ink [g/m²]	1.74	1.19	1.20	1.38

		C.of Var.[%]:
aver. density of split film:	1.23	2.68
av. density of unspl. film:	1.81	3.23
av. coef. of var. of force values [%]:		2.11311

machine param. serie a

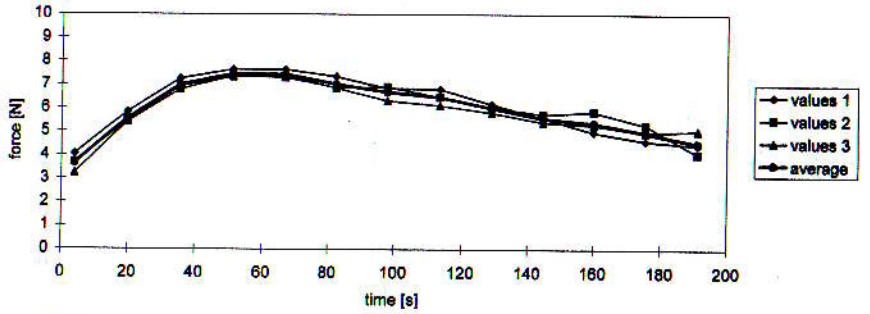

Print speed: 0.1 m/s; holding time: 5 s; pressure force: 200 N

Data of average curve:

	time [s]	force [N]	Slope [N/s]
Max.:	88.512	8.34	
beginning:		4.78	0.10228
average:			0.00766
end:		7.71	

	curve 1	curve 2	curve 3	average
transf. ink [g]:	0.0076	0.0068	0.0069	0.0071
transf. ink [g/m²]	1.41	1.26	1.28	1.31

		C.of Var.[%]:
aver. density of split film:	1.30	3.89
av. density of unspl. film:	1.93	3.39
av. coef. of var. of force values [%]:		3.77835

machine param. serie b

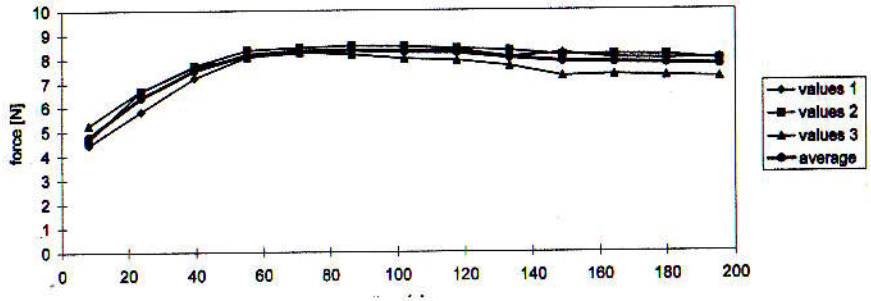

Print speed: 1 m/s; holding time: 5 s; pressure force: 200 N

Data of average curve:

	time [s]	force [N]	Slope [N/s]
Max.:	102.33	8.37	
beginning:		4.08	0.10724
average:			0.00843
end:		7.22	

	curve 1	curve 2	curve 3	average
transf. ink [g]:	0.0074	0.0076	0.008	0.007
transf. ink [g/m²]	1.37	1.41	1.11	1.30

		C.of Var.[%]:
aver. density of split film:	1.32	3.87
av. density of unspl. film:	1.93	3.00
av. coef. of var. of force values [%]:		3.56119

machine param. serie ab

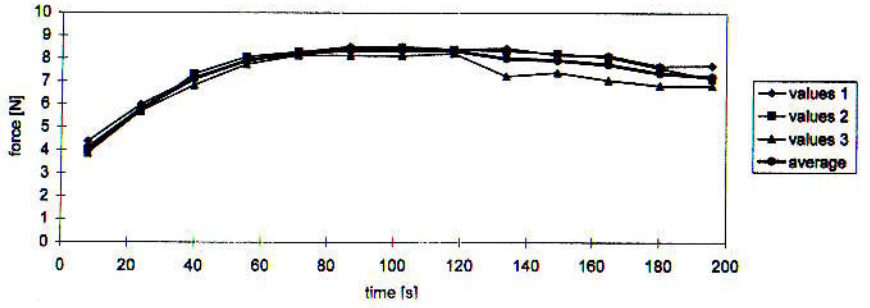

Tack-force development-curves of a 2^3 trial factor design:

Print speed: 0.1 m/s; holding time: 1 s; pressure force: 600 N

Data of average curve:

	time [s]	force [N]	Slope [N/s]
Max.:	66.742	7.46	
beginning:		4.53	0.10941
average:			-0.0026
end:		5.80	

	curve 1	curve 2	curve 3	average
transf. ink [g]:	0.0066	0.0057	0.0059	0.00607
transf. ink [g/m²]	1.22	1.06	1.09	1.12

		C.of Var.[%]:
aver. density of split film:	1.11	5.46
av. density of unspl. film:	1.69	5.01
av. coef. of var. of force values [%]:		3.18

machine param. ser. c

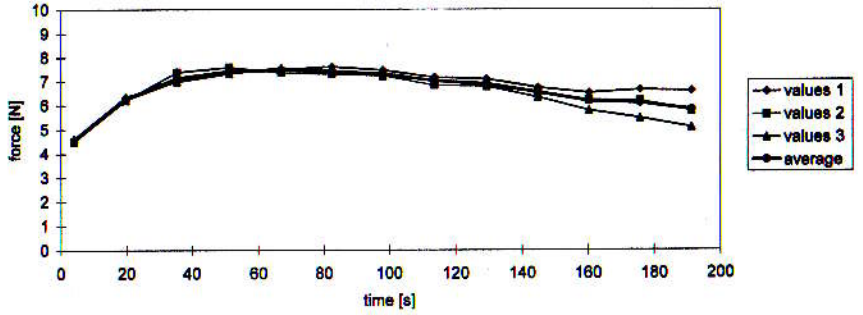

Print speed: 1 m/s; holding time: 1 s; pressure force: 600 N

Data of average curve:

	time [s]	force [N]	Slope [N/s]
Max.:	66.73	7.68	
beginning:		3.32	0.12807
average:			0.00026
end:		5.38	

	curve 1	curve 2	curve 3	average
transf. ink [g]:	0.0064	0.0067	0.0066	0.00657
transf. ink [g/m²]	1.19	1.24	1.22	1.22

		C.of Var.[%]:
aver. density of split film:	1.23	1.46
av. density of unspl. film:	1.85	2.51
av. coef. of var. of force values [%]:		6.17569

machine param. serie ac

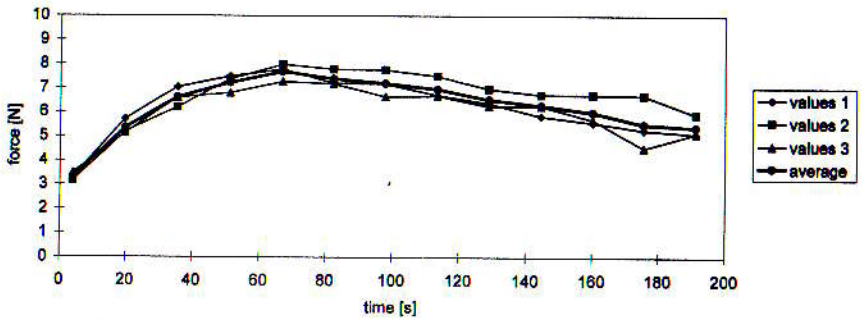

Print speed: 0.1 m/s; holding time: 5 s; pressure force: 600 N

Data of average curve:

	time [s]	force [N]	Slope [N/s]
Max.:	70.961	8.33	
beginning:		5.15	0.09289
average:			0.00424
end:		7.33	

	curve 1	curve 2	curve 3	average
transf. ink [g]:	0.0077	0.0045	0.0073	0.0065
transf. ink [g/m²]	1.43	0.83	1.35	1.20

		C.of Var.[%]:
aver. density of split film:	1.18	1.47
av. density of unspl. film:	1.85	1.97
av. coef. of var. of force values [%]:		1.92983

machine param. serie bc

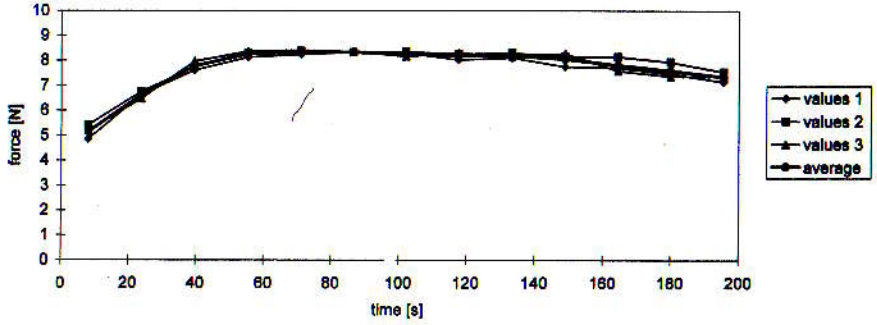

Print speed: 1 m/s; holding time: 5 s; pressure force: 600 N

Data of average curve:

	time [s]	force [N]	Slope [N/s]
Max.:	70.961	8.30	
beginning:		5.28	0.10938
average:			-0.0022
end:		6.62	

	curve 1	curve 2	curve 3	average
transf. ink [g]:	0.0053	0.007	0.0057	0.006
transf. ink [g/m²]	0.98	1.30	1.06	1.11

		C.of Var.[%]:
aver. density of split film:	1.11	5.44
av. density of unspl. film:	1.67	6.83
av. coef. of var. of force values [%]:		4.27047

machine param. serie abc

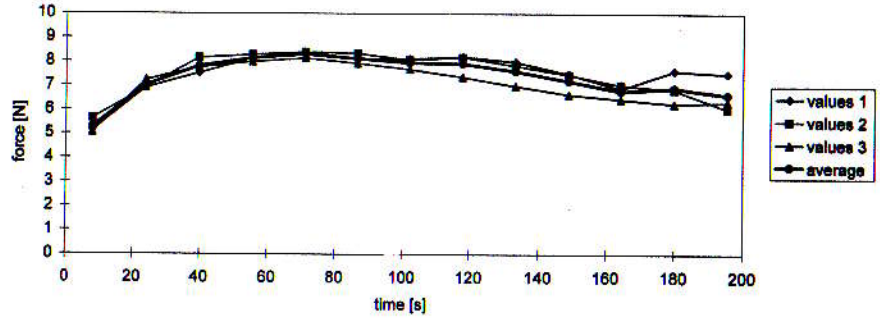

Central point experiments used for a reduced 2^6 factor design

Print speed: 0,5 m/s; holding time: 1 s; pressure force: 200 N

Data of average curve:

	time [s]	force [N]	Slope [N/s]
Max. force val.:	82.281	7.68	
beginning:		3.07	0.13666
average:			0.00394
end:		5.89	

	curve 1	curve 2	curve 3	average
transf. ink [g]:	0.0067	0.0067	0.007	0.0068
transf. ink [g/m²]	1.24	1.24	1.30	1.26

		C.of Var.[%]:
aver. density of split film:	1.30	5.23
av. density of unspl. film:	1.92	3.85
av. coef. of var. of force values [%]:		3.43034

mach. param. serie 1

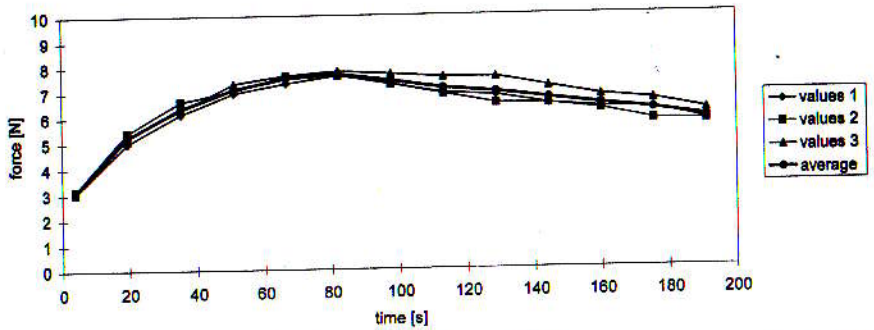

Print speed: 2 m/s; holding time: 5 s; pressure force: 200 N

Data of average curve:

	time [s]	force [N]	Slope [N/s]
Max.:	71.18	6.34	
beginning:		4.17	0.14623
average:			-0.0004
end:		6.41	

	curve 1	curve 2	curve 3	average
transf. ink [g]:	0.0057	0.0058	0.0078	0.00643
transf. ink [g/m²]	1.06	1.07	1.44	1.19

		C.of Var.[%]:
aver. density of split film:	1.10	6.05
av. density of unspl. film:	1.76	8.17
av. coef. of var. of force values [%]:		7.07084

machine param. serie ab

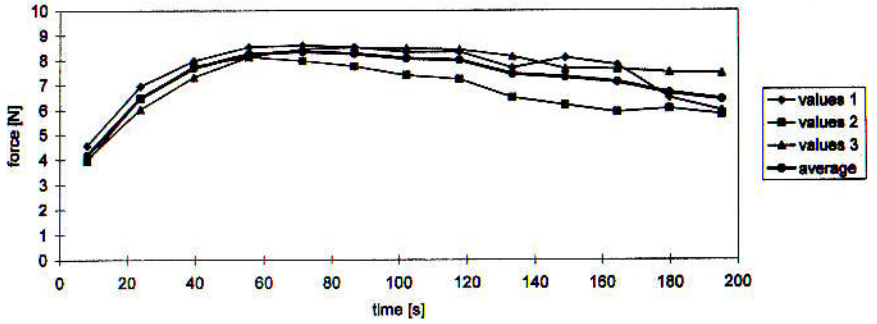

Print speed: 0.5 m/s; holding time: 5 s; pressure force: 600 N

Data of average curve:

	time [s]	force [N]	Slope [N/s]
Max.:	70.957	8.22	
beginning:		4.83	0.11941
average:			-0.0012
end:		6.50	

	curve 1	curve 2	curve 3	average
transf. ink [g]:	0.0068	0.0068	0.011	0.0082
transf. ink [g/m²]	1.26	1.26	2.04	1.52

		C.of Var.[%]:
aver. density of split film:	1.21	8.45
av. density of unspl. film:	1.76	7.96
av. coef. of var. of force values [%]:		3.38906

machine param. serie bc

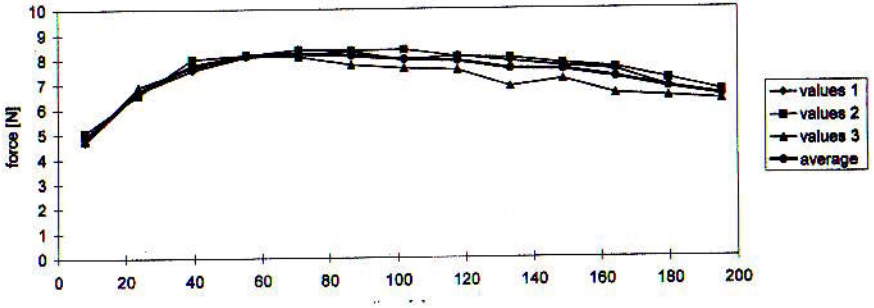

Print speed: 2 m/s; holding time: 1 s; pressure force: 600 N

Data of average curve:

	time [s]	force [N]	Slope [N/s]
Max.:	97.992	7.74	
beginning:		2.61	0.12808
average:			0.00916
end:		6.20	

	curve 1	curve 2	curve 3	average
transf. ink [g]:	0.0086	0.0077	0.0065	0.0076
transf. ink [g/m²]	1.59	1.43	1.20	1.41

		C.of Var.[%]:
aver. density of split film:	1.24	5.79
av. density of unspl. film:	1.91	5.42
av. coef. of var. of force values [%]:		5.19948

machine param. serie ac

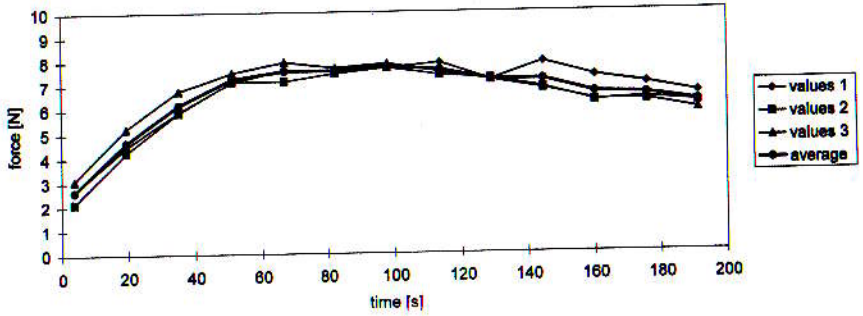

Corner point experiments for a reduced 2^6 factor design:

Print speed: 1 m/s; hold time: 1 s; pres. force: 200 N; add. filmsplit. roll en., apl. time 2 min; stand. tackroll

Data of average curve:

	time [s]	force [N]	Slope [N/s]
Maxf.:	35.48	7.53	
beginning:		5.25	0.10051
average:			-0.0178
end:		3.79	

	curve 1	curve 2	curve 3	average
transf. ink [g]:	0.0047	0.005	0.009	0.00623
transf. ink [g/m²]	0.87	0.93	1.67	1.15

		coef. of var.[%]:
aver. density of split film:	0.96	4.10
av. density of unspl. film:	1.37	4.49
av. coef. of var. of force values [%]:		4.16089

machine param. serie 1

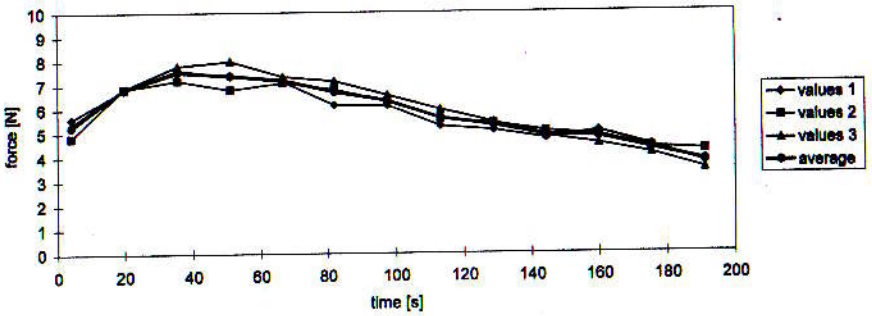

Print speed: 1 m/s; hold time: 5 s; pres. force: 600 N; add. filmsplit. roll dis., apl. time 20 min; stand. tackroll

Data of average curve:

	time [s]	force [N]	Slope [N/s]
Maxf.:	70.961	8.42	
beginning:		4.76	0.13555
average:			-0.0003
end:		6.86	

	curve 1	curve 2	curve 3	average
transf. ink [g]:	0.0045	-	0	0.00225
transf. ink [g/m²]	0.83	-	0.00	0.42

		coef. of var.[%]:
aver. density of split film:	1.22	2.05
av. density of unspl. film:	1.78	3.08
av. coef. of var. of force values [%]:		2.39707

machine param. serie 3

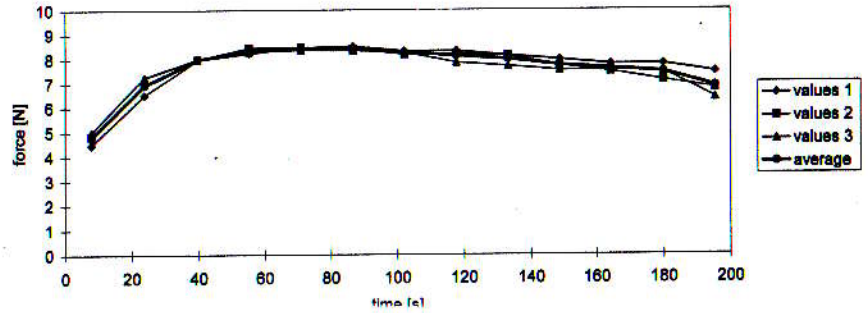

Print speed: 0,1 m/s; hold time: 5 s; pres. force: 200 N; add. filmsplit. roll en., apl. time 20 min; new tackroll

Data of average curve:

	time [s]	force [N]	Slope [N/s]
Maxf.:	39.66	8.28	
beginning:		7.21	0.05215
average:			-0.012
end:		5.98	

	curve 1	curve 2	curve 3	average
transf. ink [g]:	0.0047	0.0039	0.0039	0.00417
transf. ink [g/m²]	0.87	0.72	0.72	0.77

		coef. of var.[%]:
aver. density of split film:	1.19	6.19
av. density of unspl. film:	1.47	6.25
av. coef. of var. of force values [%]:		6.71368

machine param. serie 2

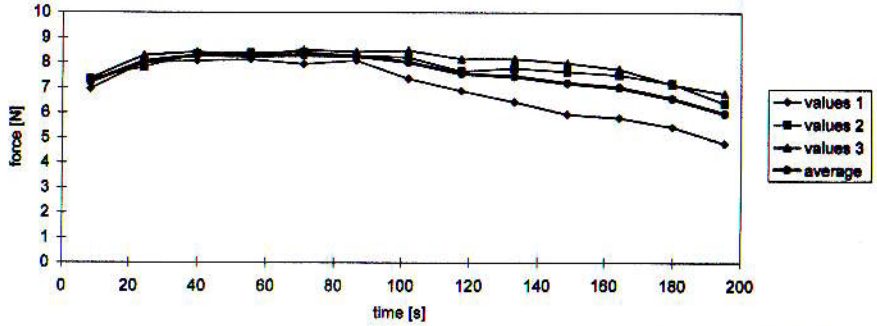

Print speed: 0,1 m/s; hold time: 1 s; pres. force: 200 N; add. filmsplit. roll dis., apl. time 20 min; stand. tackroll

Data of average curve:

	time [s]	force [N]	Slope [N/s]
Maxf.:	98.094	8.19	
beginning:		3.91	0.12595
average:			0.00519
end:		6.79	

	curve 1	curve 2	curve 3	average
transf. ink [g]:	0.0041	0.004	0	0.0027
transf. ink [g/m²]	0.76	0.74	0.00	0.50

		coef. of var.[%]:
aver. density of split film:	1.25	2.16
av. density of unspl. film:	1.84	1.61
av. coef. of var. of force values [%]:		5.84124

machine param. ser. 4

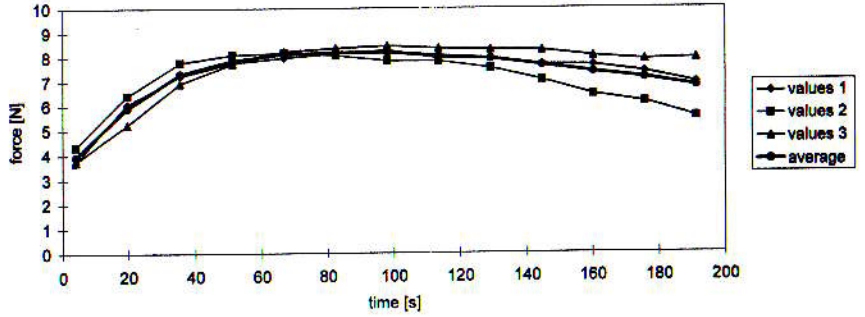

Experiment used for a reduced 2^6 factor design:

Print speed: 1 m/s; hold time: 5 s; pres. force: 200 N; add. filmsplit. roll dis., apl. time 2 min; new tackroll

Data of average curve:

	time [s]	force [N]	Slope [N/s]
Maxf.:	70.961	8.11	
beginning:		4.76	0.10381
average:			0.00105
end:		6.57	

	curve 1	curve 2	curve 3	average
transf. ink [g]:	0.0045	0.0049	0.005	0.0048
transf. ink [g/m²]	0.83	0.91	0.93	0.89

		coef. of var.[%]:
aver. density of split film:	1.19	2.75
av. density of unspl. film:	1.77	2.42
av. coef. of var. of force values [%]:		3.39358

machine param. serie 5

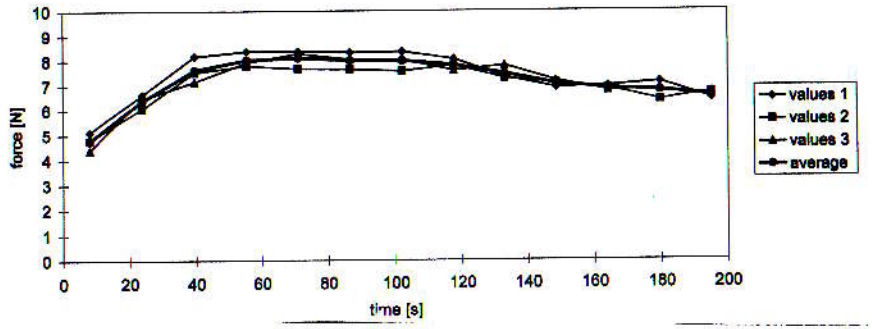

Print speed: 0,1 m/s; hold time: 1 s; pres. force: 600 N; add. filmsplit. roll dis., apl. time 2 min; new tackroll

Data of average curve:

	time [s]	force [N]	Slope [N/s]
Max.:	66.508	7.17	
beginning:		4.36	0.10466
average:			-0.0086
end:		4.53	

	curve 1	curve 2	curve 3	average
transf. ink [g]:	-	0.0045	-	0.0045
transf. ink [g/m²]	-	0.83	-	0.83

		coef. of var.[%]:
aver. density of split film:	1.15	5.63
av. density of unspl. film:	1.74	6.37
av. coef. of var. of force values [%]:		9.49358

machine param. serie 6

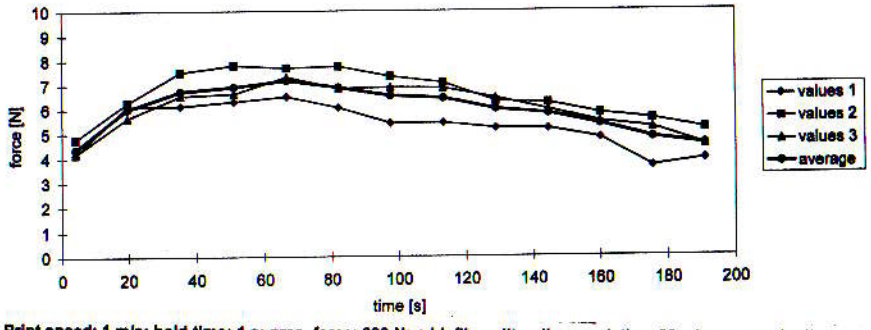

Print speed: 0,1 m/s; hold time: 5 s; pres. force: 600 N; add. filmsplit. roll en., apl. time 2 min; stand. tackroll

Data of average curve:

	time [s]	force [N]	Slope [N/s]
Max.:	39.652	7.88	
beginning:		6.87	0.05185
average:			-0.009
end:		6.15	

	curve 1	curve 2	curve 3	average
transf. ink [g]:	0.0054	0.0054	0.0058	0.00553
transf. ink [g/m²]	1.00	1.00	1.07	1.02

		coef. of var.[%]:
aver. density of split film:	1.34	5.38
av. density of unspl. film:	1.50	8.07
av. coef. of var. of force values [%]:		4.98765

machine param. serie 7

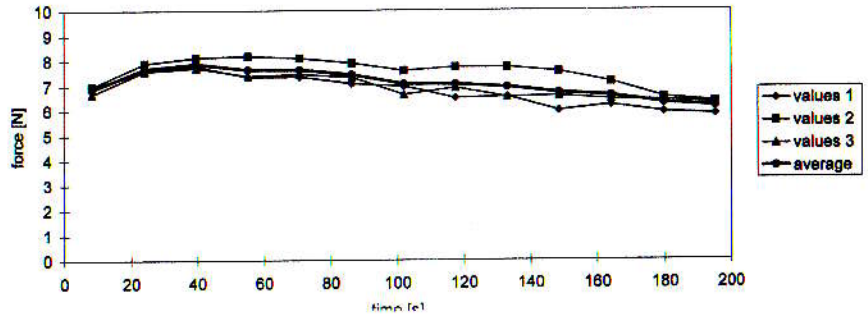

Print speed: 1 m/s; hold time: 1 s; pres. force: 600 N; add. filmsplit. roll en., apl. time 20 min; new tackroll

Data of average curve:

	time [s]	force [N]	Slope [N/s]
Max.:	50.92	6.82	
beginning:		5.25	0.09693
average:			-0.0179
end:		3.71	

	curve 1	curve 2	curve 3	average
transf. ink [g]:	0.0048	0.0056	0.0064	0.0056
transf. ink [g/m²]	0.89	1.04	1.19	1.04

		coef. of var.[%]:
aver. density of split film:	1.12	6.94
av. density of unspl. film:	1.53	8.13
av. coef. of var. of force values [%]:		4.79609

mach. param. serie 8

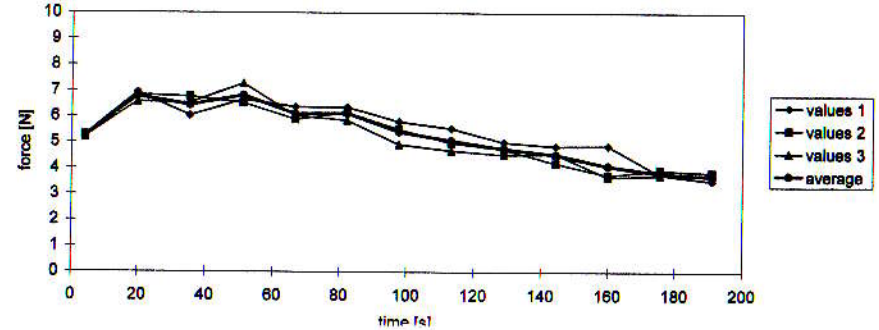

Tack force development curves for the ink investigation, commercial offset inks of different brands:

SBB ICG with Hartmann Multilith Cyan

Data of average curve:

	time [s]	force [N]	Slope [N/s]
Max.:	39.61	7.54	
beginning:		5.23	0.114555
average:			-0.013657
end:		4.69	

	curve 1	curve 2	curve 3	average
transf. ink [g]:	0.007	0.0061	0.0065	0.00653
transf. ink [g/m²]:	1.30	1.13	1.20	1.21

	C.of Var.[%]:	
av. density of split film:	1.22	3.25
av. density of unspl. film:	1.76	3.23
av. var. of force values of curve [%]:		3.15

Hartmann Multilith Cyan on SBB ICG

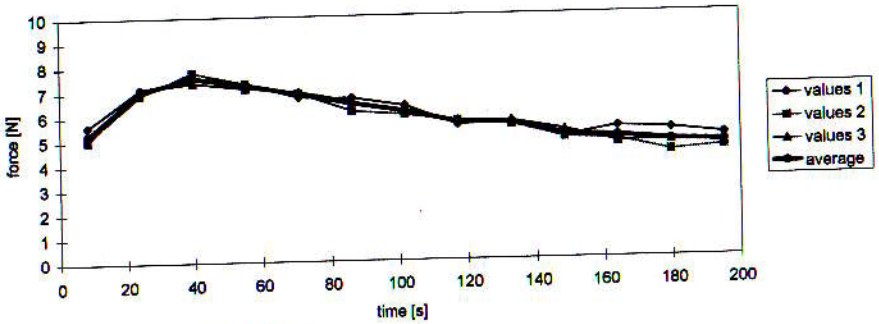

SBB ICG with Hartmann Oekolith Cyan

Data of average curve:

	time [s]	force [N]	Slope [N/s]
Max.:	133.25	8.00	
beginning:		4.25	0.076139
average:			0.010902
end:		7.32	

	curve 1	curve 2	curve 3	average
transf. ink [g]:	0.0075	0.006	0.007	0.00683
transf. ink [g/m²]:	1.39	1.11	1.30	1.27

	C.of Var.[%]:	
av. density of split film:	1.50	3.55
av. density of unspl. film:	2.11	3.42
av. var. of force values of curve [%]:		3.57

Hartmann Oekolith Cyan on SBB ICG

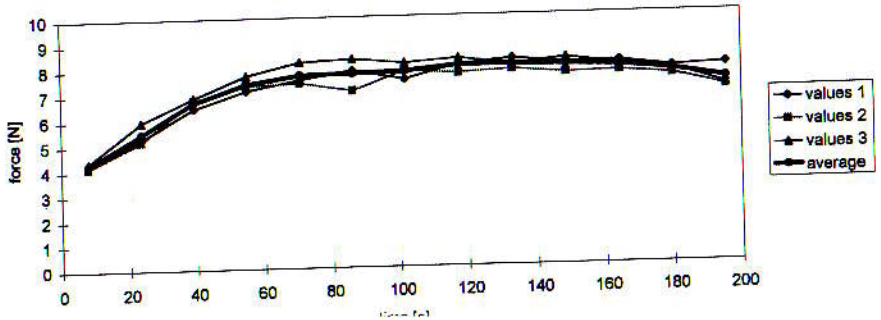

SBB ICG with Hartmann Star Glanz Cyan

Data of average curve:

	time [s]	force [N]	Slope [N/s]
Max.:	86.77	8.42	
beginning:		4.99	0.090107
average:			0.009482
end:		8.03	

	curve 1	curve 2	curve 3	average
transf. ink [g]:	0.0066	0.0061	0.0065	0.0064
transf. ink [g/m²]:	1.22	1.13	1.20	1.19

	C.of Var.[%]:	
av. density of split film:	1.33	2.69
av. density of unspl. film:	1.91	2.47
av. var. of force values of curve [%]:		1.87

Hartmann Star Glanz Cyan on SBB ICG

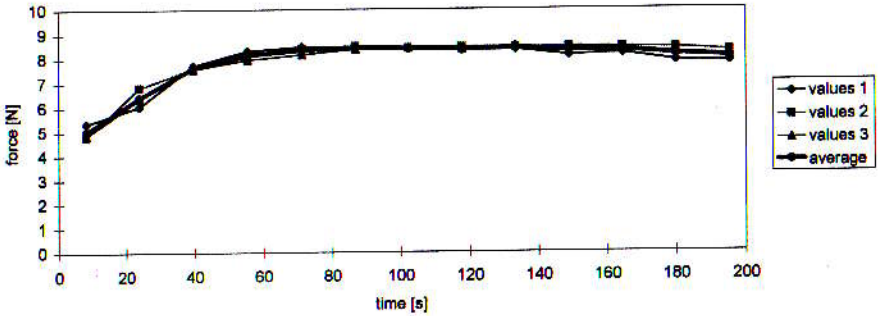

Investigation of the color influence of commercial offset inks of one ink brand + a varnish:

SBB ICG with Hartmann Multilith Magenta

Data of average curve:

	time [s]	force [N]	Slope [N/s]
Max.:	70.91	8.02	
beginning:		3.88	0.119004
average:			0.000107
end:		5.77	

	curve 1	curve 2	curve 3	average
transf. ink [g]:	0.0074	0.0074	0.0074	0.0074
transf. ink [g/m²]:	1.37	1.37	1.37	1.37

		C.of Var.[%]:
av. density of split film:	1.26	3.89
av. density of unspl. film:	1.77	3.85
av. var. of force values of curve [%]:		3.88

Hartmann Multilith Magenta on SBB ICG

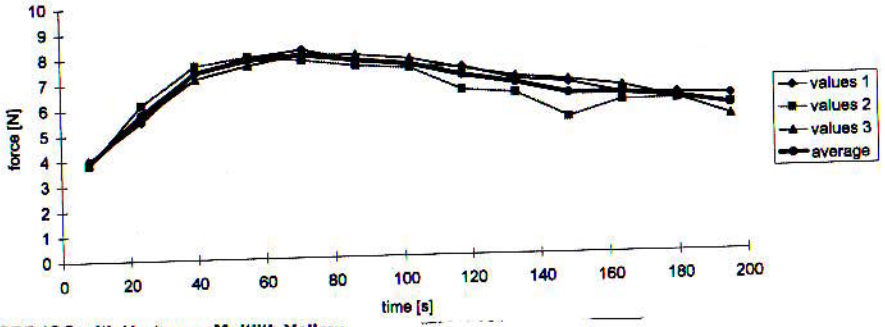

SBB ICG with Hartman Multilith Black

Data of average curve:

	time [s]	force [N]	Slope [N/s]
Max. force val.:	102	7.65	
beginning:		4.09	0.086077
average:			0.00776
end:		6.78	

	curve 1	curve 2	curve 3	average
transf. ink [g]:	0.006	0.0068	0.0065	0.00643
transf. ink [g/m²]:	1.11	1.26	1.20	1.19

		C.of Var.[%]:
av. density of split film:	1.51	2.79
av. density of unspl. film:	2.12	4.13
av. var. of force values of curve	3.56078	

Hartmann Multilith Black on SBB ICG

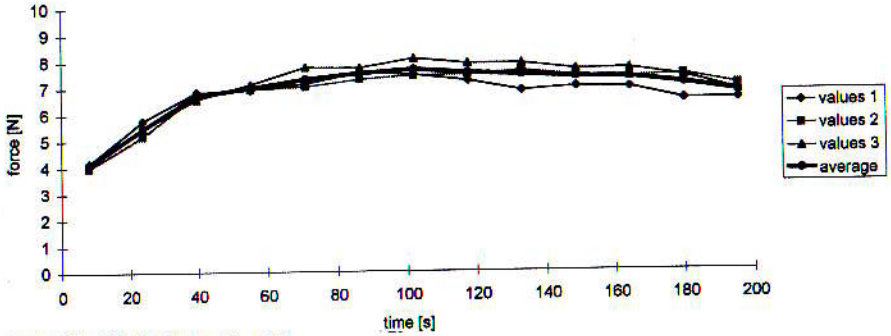

SBB ICG with Hartmann Multilith Yellow

Data of average curve:

	time [s]	force [N]	Slope [N/s]
Max.:	70.75	7.70	
beginning:		4.57	0.101111
average:			-0.001033
end:		6.00	

	curve 1	curve 2	curve 3	average
transf. ink [g]:	0.0067	0.009	0.0074	0.0077
transf. ink [g/m²]:	1.24	1.67	1.37	1.43

		C.of Var.[%]:
av. density of split film:	1.02	3.99
av. density of unspl. film:	1.39	2.48
av. var. of force values of curve [%]:		4.32

Hartmann Multilith Yellow with SBB ICG

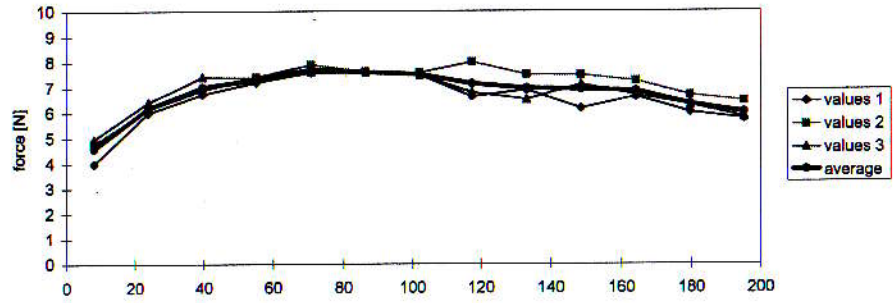

SBB ICG with Hartmann Varnish

Data of average curve:

	time [s]	force [N]	Slope [N/s]
Max.	133.25	7.22	
beginning:		4.50	0.095027
average:			0.004351
end:		6.75	

	curve 1	curve 2	curve 3	average
transf. ink [g]:	0.0075	0.007	0.006	0.00683
transf. ink [g/m²]:	1.39	1.30	1.11	1.27

		C.of Var.[%]:
av. density of split film:	1.28	4.63
av. density of unspl. film:	1.86	3.77
av. var. of force values of curve [%]:		5.18

Hartmann Varnish on SBB ICG

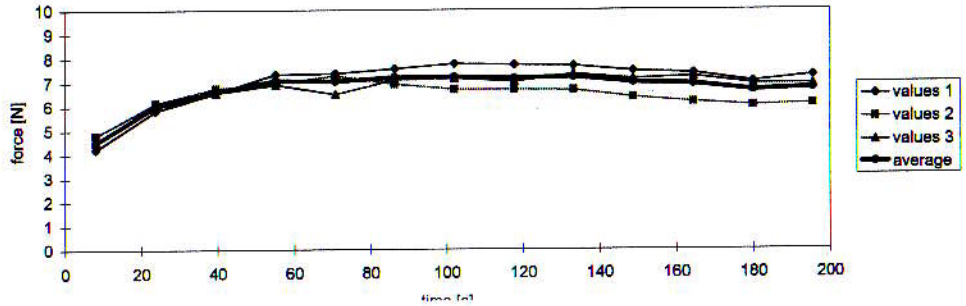

Investigation of the inks applied on mylar films

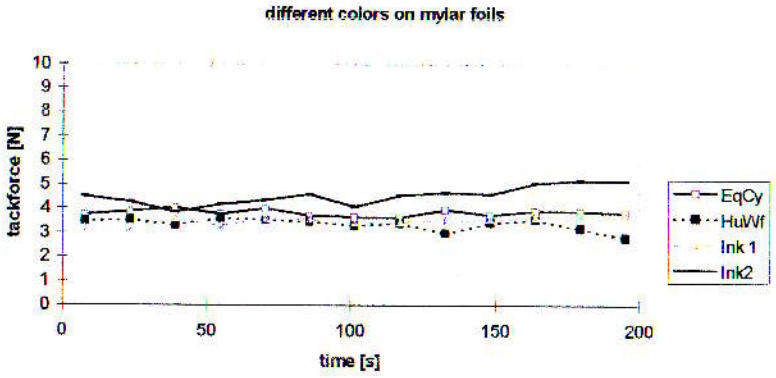

Fig. 10.33.2: Application of the instrument as a rheometer (inkometer)

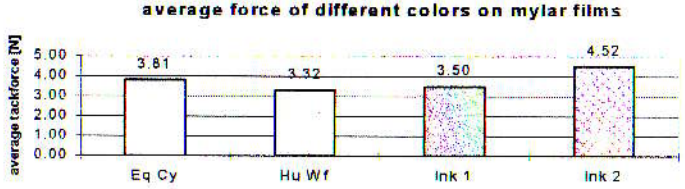

SBB ICG with Equinox Cyan

Data of average curve:

	time [s]	force [N]	Slope [N/s]
Max.:	86.44	8.10	
beginning:		4.88	0.097819
average:			-0.00139
end:		6.18	

	curve 1	curve 2	curve 3	average
transf. ink [g]:	0.0072	0.0068	0.0065	0.00683
transf. ink [g/m²]:	1.33	1.26	1.20	1.27

		C.of Var.[%]:
av. density of split film:	1.25	3.13
av. density of unspl. film:	1.79	2.77
av. var. of force values of curve [%]:		2.75

Equinox Cyan on SBB ICG

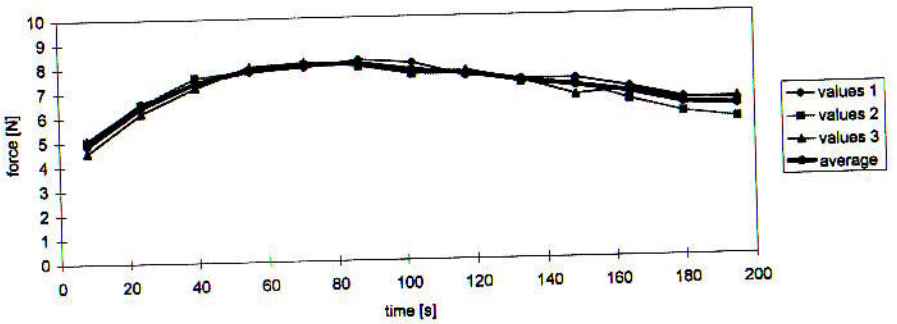

SBB ICG with Huber Wegschlagfarbe 520068 Cyan

Data of average curve:

	time [s]	force [N]	Slope [N/s]
Max.:	55.2	7.68	
beginning:		4.25	0.174894
average:			-0.013924
end:		4.63	

	curve 1	curve 2	curve 3	average
transf. ink [g]:	0.0074	0.0075	0.0076	0.0075
transf. ink [g/m²]:	1.37	1.39	1.41	1.39

		C.of Var.[%]:
av. density of split film:	1.25	3.84
av. density of unspl. film:	1.70	3.50
av. var. of force values of curve [%]:		4.96

Huber Wegschlagfarbe 520068 Cyan with SBB ICG

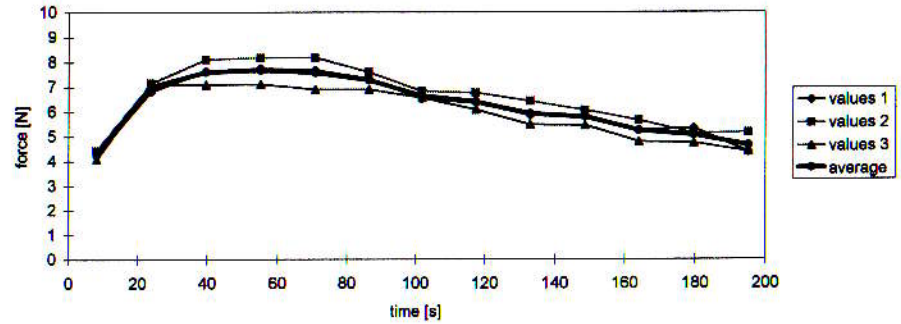

Substrate investigation, latices: with different degree of carboxyl groups

Styrene- butadiene-latex on mylar films, Tg = 13°C, low carboxyl degree:

Data of average curve:

	time [s]	force [N]	Slope [N/s]
Max.:	159.8	5.88	
beginning:		3.38	0.0265792
end:		0.546	

	average
transf. ink [g]:	0.00593
transf. ink [g/m²]:	1.10

		C.of Var.[%]:
aver. density of split film:	-	-
av. density of unspl. film:	-	-
av. coef. of var. of force values [%]:		13.2669

SB latex Tg = -13°C, low c

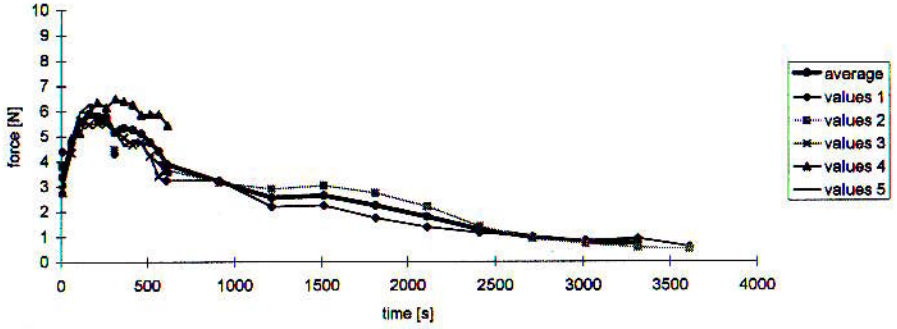

Styrene-butadiene-latex on mylar films, Tg = 9°C, high carboxyl-degree:

Data of average curve:

	time [s]	force [N]	Slope [N/s]
Max.:	210.25	5.28	
beginning:		2.99	0.0272425
end:		0.267	

	average
transf. ink [g]:	0.00677
transf. ink [g/m²]:	1.25

		C.of Var.[%]:
aver. density of split film:	-	-
av. density of unspl. film:	-	-
av. coef. of var. of force values [%]:		46.1038

SB latex TG 9°C, high c

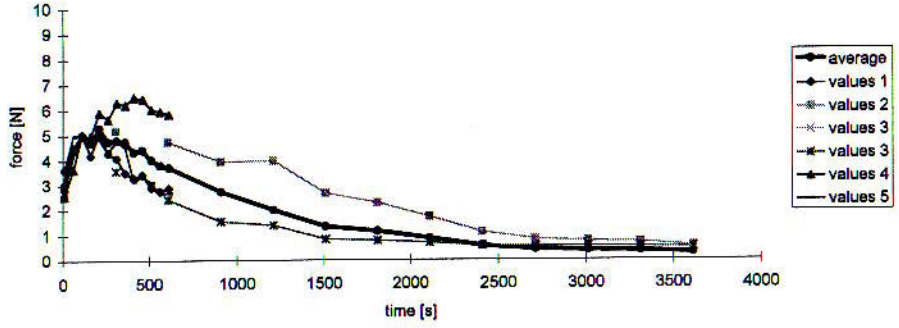

Styrene-butadiene-latex on mylar-films, Tg 8°C, medium carboxyl-degree:

Data of average curve:

	time [s]	force [N]	Slope [N/s]
Max.:	58.602	5.35	
beginning:		4.54	0.0160656
end:		0.536	

	average
transf. ink [g]:	0.00733
transf. ink [g/m²]:	1.36

		C.of Var.[%]:
aver. density of split film:	-	-
av. density of unspl. film:	-	-
av. coef. of var. of force values [%]:		14.971

SB latex ,Tg 8°C, medium c

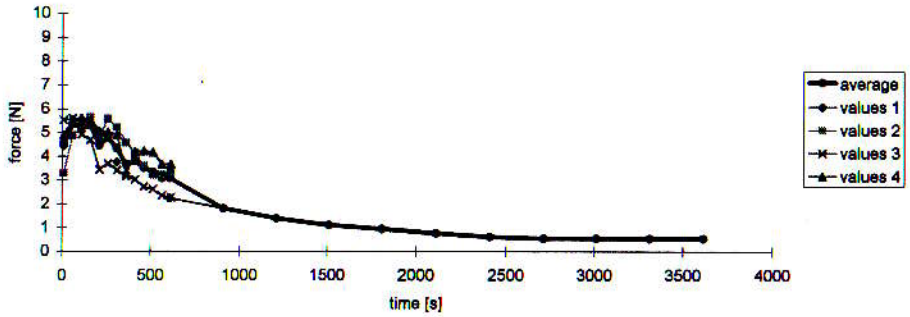

Substrate investigation of latices with different glass transition temperatures:

Styrene-butadiene-latex on mylar films, Tg = 27°C:

Data of average curve:

	time [s]	force [N]	Slope [N/s]
Max.:	1811	6.44	
beginning:		2.49	0.0082395
average:			6.05E-05
end:		5.17	

	curve 1	curve 2	curve 3	average
transf. ink [g]:	0.0066	0.0064	0.0064	0.00647
transf. ink [g/m²]:	1.22	1.19	1.19	1.20

		C.of Var.[%]:
aver. density of split film:	-	-
av. density of unspl. film:	-	-
av. coef. of var. of force values [%]:		11.3004

SB latex, Tg 27°C:

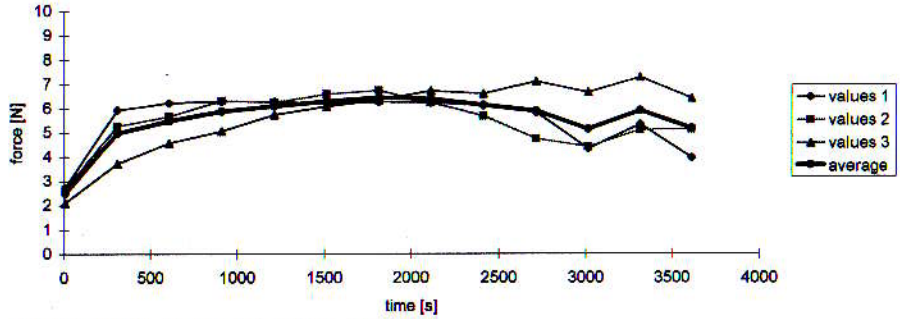

Styrene-acrylate-latex on mylar films, Tg 25°C:

Data of average curve:

	time [s]	force [N]	Slope [N/s]
Max.:	514	7.56	
beginning:		3.27	0.0547057
end:		3.6446667	

	average
transf. ink [g]:	0.00713
transf. ink [g/m²]:	1.32

		C.of Var.[%]:
aver. density of split film:	-	-
av. density of unspl. film:	-	-
av. coef. of var. of force values [%]:		8.17222

SA latex Tg 25°C

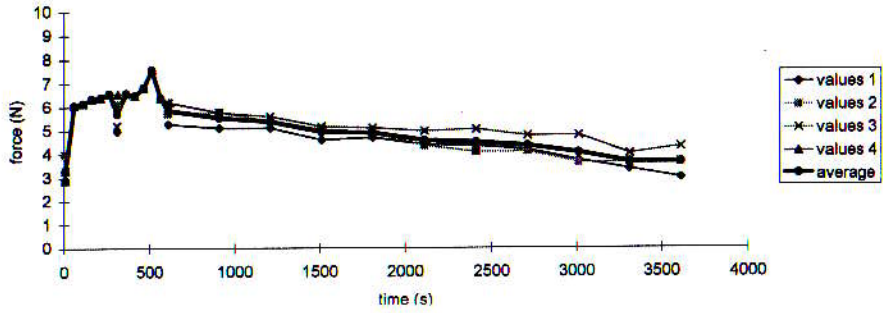

Styrene-butadiene-latex on mylar films, Tg = -7°C:

Data of average curve:

	time [s]	force [N]	Slope [N/s]
Max.:	8.29	6.60	
beginning:		6.60	-
average:			-
end:		3.22	

	curve 1	curve 2	curve 3	average
transf. ink [g]:	0.0073	0.0071	0.0076	0.00733
transf. ink [g/m²]:	1.35	1.31	1.41	1.36

		C.of Var.[%]:
aver. density of split film:	-	-
av. density of unspl. film:	-	-
av. coef. of var. of force values [%]:		7.30767

SB latex TG - 7°C

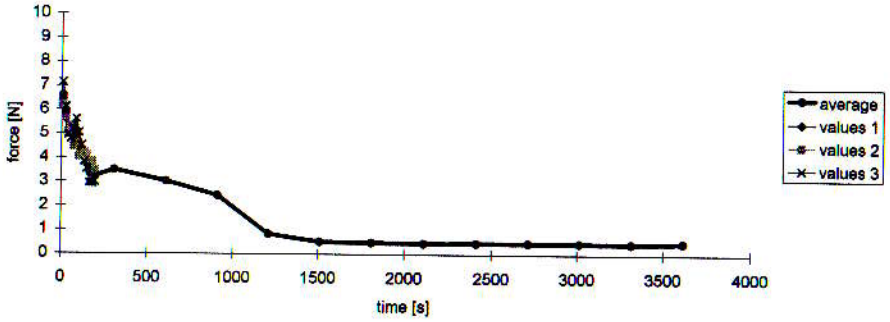

Substrate investigation of Polymer films : PE

Polymer coated board PE + corona, glossy:

Data of average curve:

	time [s]	force [N]	Slope [N/s]
Max.:	252,71	6.06	
beginning:		1.94	0.052616
end:		2.528	

	average
transf. ink [g]:	0.0073667
transf. ink [g/m²]:	1.36

		C.of Var.[%]:
aver. density of split film:	1.14	4.03
av. density of unspl. film:	1.49	1.89
av. coef. of var. of force values [%]:		5.70827

PE + corona glossy

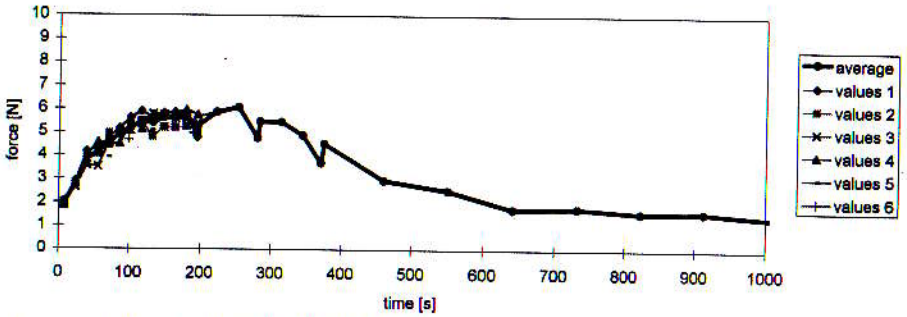

Polymer coated board, PE rough, without corona:

Data of average curve:

	time [s]	force [N]	Slope [N/s]
Max.:	180	2.11	
beginning:		0.97	0.00545
end:		0.389	

	average
transf. ink [g]:	0.00722857
transf. ink [g/m²]:	1.34

		C.of Var.[%]:
aver. density of split film:	1.03	4.53
av. density of unspl. film:	1.16	4.82
av. coef. of var. of force values [%]:		13.8974

PE rough, no corona:

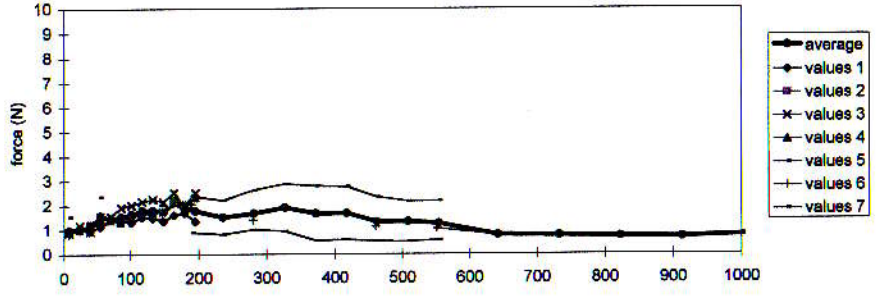

Polymer coated board, PE+ corona, rough surface:

Data of average curve:

	time [s]	force [N]	Slope [N/s]
Max.:	98.5	2.07	
beginning:		1.36	0.0145008
end:		0.4265	

	average
transf. ink [g]:	0.0074
transf. ink [g/m²]:	1.37

		C.of Var.[%]:
aver. density of split film:	1.05	4.71
av. density of unspl. film:	1.16	5.82
av. coef. of var. of force values [%]:		11.717

PE + corona rough surface:

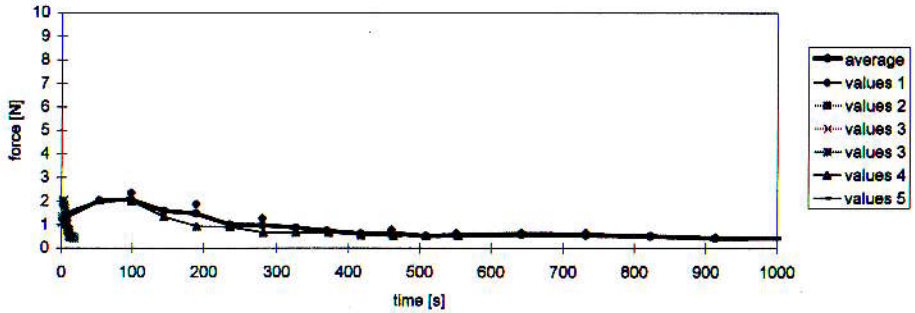

Substrate investigation of polymer films, PP, PMP, PET:

Polymer coated board, PP + corona, glossy:

Data of average curve:

	time [s]	force [N]	Slope [N/s]
Max.:	3013.7	6.63	
beginning:		2.40	0.021811
average:			-
end:		6.02	

	average
transf. ink [g]:	0.0070889
transf. ink [g/m²]:	1.31

		C.of Var.[%]:
aver. density of split film:	1.25	11.13
av. density of unspl. film:	1.45	4.17
av. coef. of var. of force values [%]:	-	

PP + corona glossy

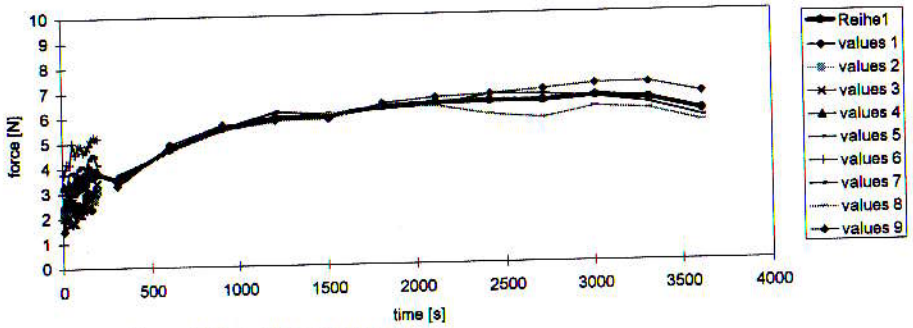

Polymer coated board, PP rough, no corona:

Data of average curve:

	time [s]	force [N]	Slope [N/s]
Max.:	308.24	1.21	
beginning:		0.65	-
average:			-
end:		0.46	

	average
transf. ink [g]:	0.00715
transf. ink [g/m²]:	1.32

		C.of Var.[%]:
aver. density of split film:	1.10	2.76
av. density of unspl. film:	1.21	1.54
av. coef. of var. of force values [%]:	-	

PP rough

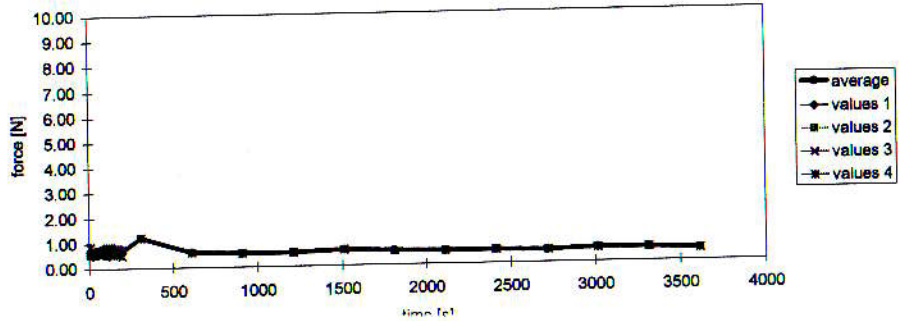

Polymer coated board, PMP, rough surface, no corona:

Data of average curve:

	time [s]	force [N]	Slope [N/s]
Max.:	760	1.06	-
beginning:		0.52	-
end:		0.808	

	average
transf. ink [g]:	0.00625
transf. ink [g/m²]:	1.16

		C.of Var.[%]:
aver. density of split film:	0.65	8.22
av. density of unspl. film:	0.69	5.39
av. coef. of var. of force values [%]:	-	

PMP rough:

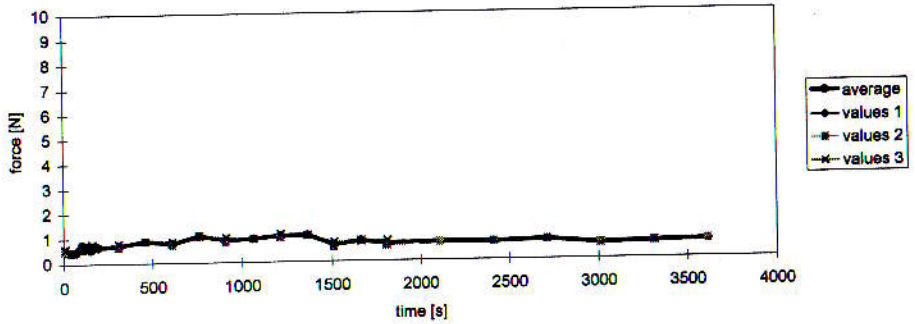

Polymer cpated board, PET rough surface, no corona:

Data of average curve:

	time [s]	force [N]	Slope [N/s]
Max.:	3314	1.52	
beginning:		0.50	-
average:			-
end:		1.18	

	curve 1	curve 2	curve 3	average
transf. ink [g]:	0.007	0.0068	0.0069	0.0069
transf. ink [g/m²]:	1.30	1.26	1.28	1.28

		C.of Var.[%]:
aver. density of split film:	0.99	4.05
av. density of unspl. film:	1.07	6.90
av. coef. of var. of force values [%]:	-	

PET rough, no corona:

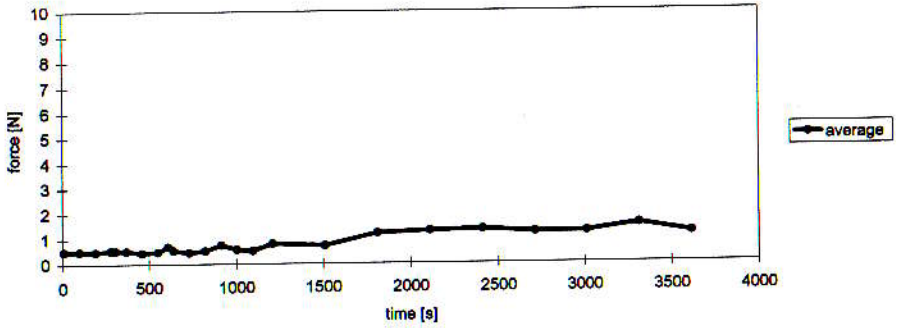

Substrate investigation, long time experiments carried out on aluminum and mylar films:

Aluminium foil, matt:

Data of average curve:

	time [s]	force [N]	Slope [N/s]
Max. force	-	-	
beginning:		1.73	0.00174
average:			-
end:		7.51	

	curve 1	curve 2	curve 3	average
transf. ink [g]:	0.005	0.006	0.006	0.0058
transf. ink [g/m²]:	0.93	1.11	1.17	1.07

		C.of Var.[%]:
aver. density of split film:	-	-
av. density of unspl. film:	-	-
av. coef. of var. of force values [%]:		9.682

Aluminium matt

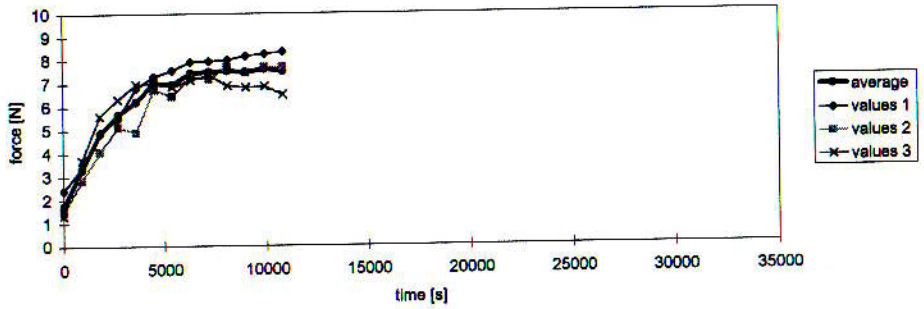

Aluminum foil, glossy:

Data of average curve:

	time [s]	force [N]	Slope [N/s]
Max. force	-	-	
beginning:		2.92	0.00203
average:			-
end:		5.77	

	curve 1	curve 2	curve 3	average
transf. ink [g]:	0.006	0.0056	0.006	0.0059
transf. ink [g/m²]:	1.11	1.04	1.11	1.09

		C.of Var.[%]:
aver. density of split film:	-	-
av. density of unspl. film:	-	-
av. coef. of var. of force values [%]:		3.662

Aluminium glossy

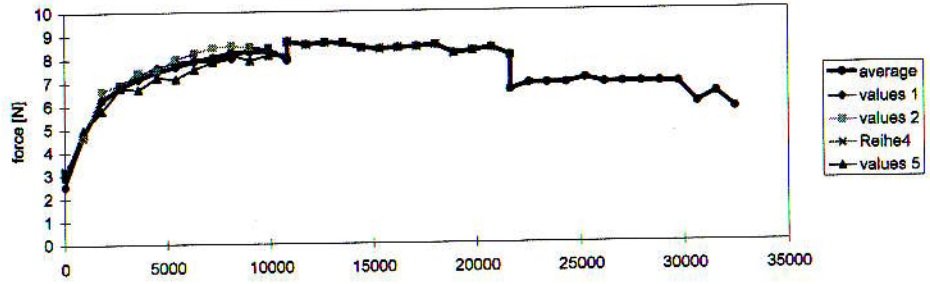

Mylar films, surface treated:

Data of average curve:

	time [s]	force [N]	Slope [N/s]
Max. force	16809	8.22	
beginning:		3.34	0.00205
average:			
end:		7.90	

	curve 1	curve 2	curve 3	average
transf. ink [g]:	0.0074	0.0074	0.007	0.0073
transf. ink [g/m²]:	1.37	1.37	1.30	1.35

		C.of Var.[%]:
aver. density of split film:	1.34	3.05
av. density of unspl. film:	1.71	3.17
av. coef. of var. of force values [%]:		

Mylar

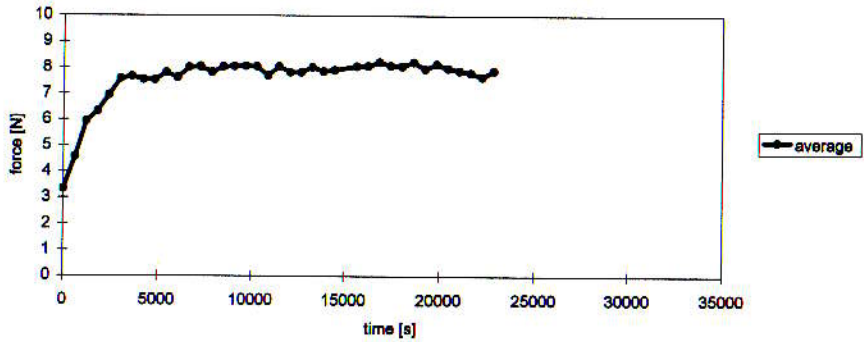

Substrate Investigation of glossy offset fine paper:

Fine paper 100 g/m², glossy, cross direction:

Data of average curve:

	time [s]	force [N]	Slope [N/s]
Max.:	24.2	8.03	
beginning:		6.65	0.08579
average:			-0.0366
end:		1.78	

	curve 1	curve 2	curve 3	average
transf. ink [g]:	0.0082	0.0072	0.0081	0.00783
transf. ink [g/m²]	1.52	1.33	1.50	1.45

		C.of Var.[%]:
aver. density of split film:	1.30	1.83
av. density of unspl. film:	1.78	2.20
av. coef. of var. of force values [%]:		21.3093

Fine paper 100 g/m² glossy, cross direction:

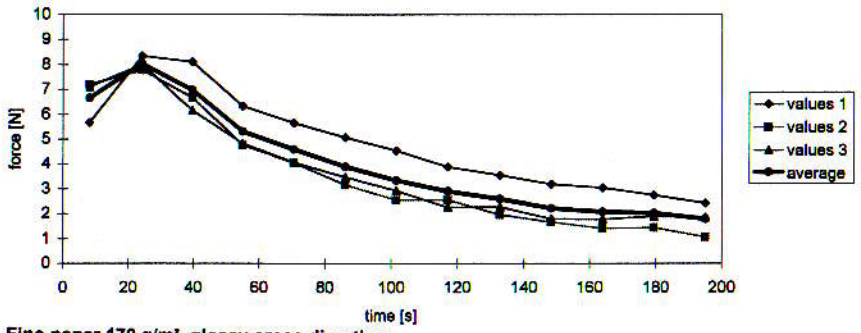

Fine paper 170 g/m², glossy cross direction:

Data of average curve:

	time [s]	force [N]	Slope [N/s]
Max.:	24	8.00	
beginning:		6.13	0.11808
average:			-0.0423
end:		0.77	

	curve 1	curve 2	curve 3	average
transf. ink [g]:	0.0073	0.0072	0.0085	0.00767
transf. ink [g/m²]	1.35	1.33	1.57	1.42

		C.of Var.[%]:
aver. density of split film:	1.25	3.84
av. density of unspl. film:	1.70	3.33
av. coef. of var. of force values [%]:		20.4202

Fine paper, 170 g/m² glossy, cross direction:

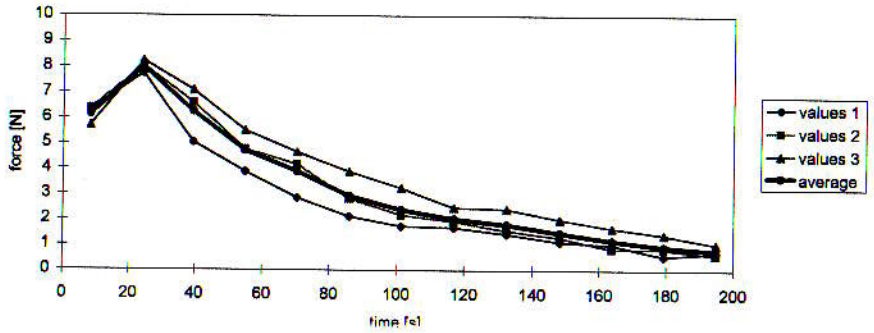

Fine paper 130 g/m², glossy cross direction:

Data of average curve:

	time [s]	force [N]	Slope [N/s]
Max.:	24.2	8.11	
beginning:		6.60	0.09445
average:			-0.0385
end:		1.53	

	curve 1	curve 2	curve 3	average
transf. ink [g]:	0.0079	0.0071	0.0084	0.0078
transf. ink [g/m²]	1.46	1.31	1.56	1.44

		C.of Var.[%]:
aver. density of split film:	1.34	3.73
av. density of unspl. film:	1.82	3.21
av. coef. of var. of force values [%]:		22.5912

Fine paper 130 g/m² glossy cross direction:

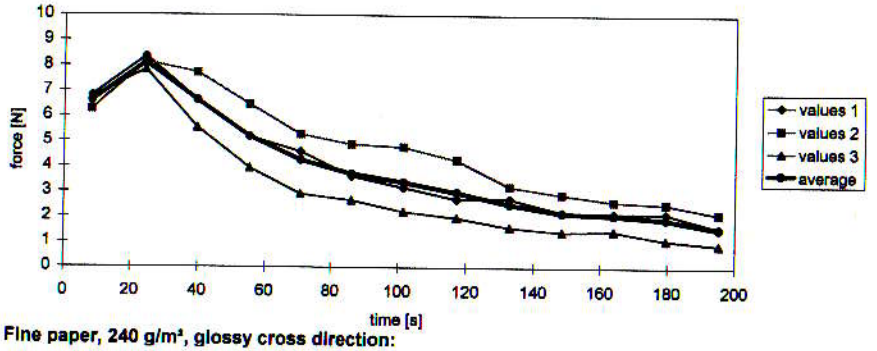

Fine paper, 240 g/m², glossy cross direction:

Data of average curve:

	time [s]	force [N]	Slope [N/s]
Max. forc	24.1	7.40	
beginning:		4.56	0.17774
average:			-0.0362
end:		1.20	

	curve 1	curve 2	curve 3	average
transf. ink [g]:	0.0074	0.0074	0.007	0.00727
transf. ink [g/m²]	1.37	1.37	1.30	1.35

		C.of Var.[%]:
aver. density of split film:	1.34	3.05
av. density of unspl. film:	1.71	3.17
av. coef. of var. of force values [%]:		7.82708

Fine paper, 240 g/m², glossy cross direction:

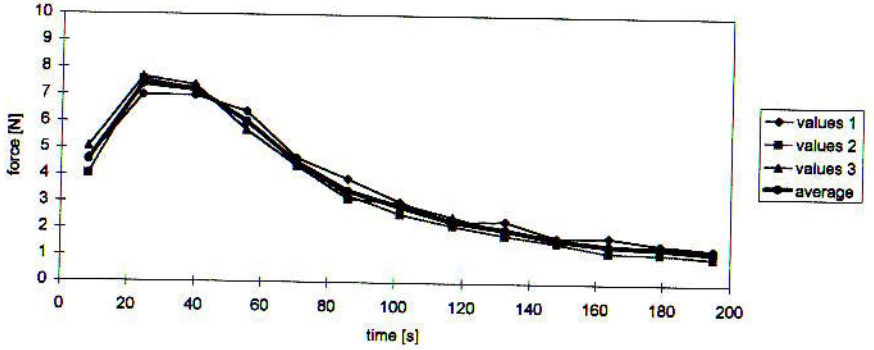

Substrate investigation of matt offset fine paper:

Fine paper 100 g/m², matt, cross direction:

Data of average curve:

	time [s]	force [N]	Slope [N/s]
Max.:	39.77	5.88	
beginning:		4.55	0.08516
average:			-0.0279
end:		1.11	

	curve 1	curve 2	curve 3	average
transf. ink [g]:	0.0076	0.0076	0.0077	0.00763
transf. ink [g/m²]	1.41	1.41	1.43	1.41

		C.of Var.[%]:
aver. density of split film:	1.31	5.24
av. density of unspl. film:	1.74	5.22
av. coef. of var. of force values [%]:		9.56978

Fine paper 100 g/m² matt, cross direction:

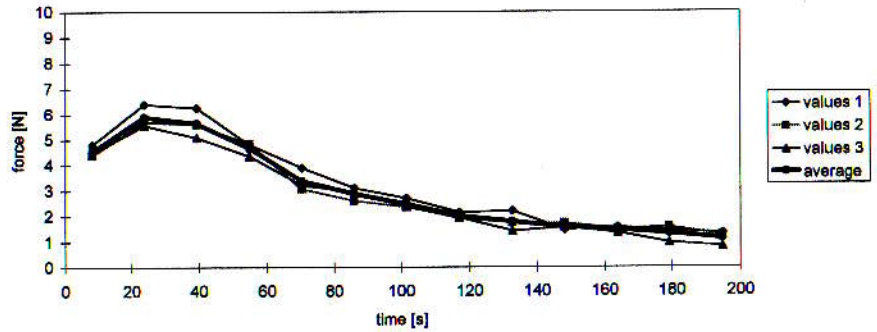

Fine paper 200 g/m², matt cross direction:

Data of average curve:

	time [s]	force [N]	Slope [N/s]
Max.:	39.6	7.48	
beginning:		3.54	0.15554
average:			-0.0188
end:		2.77	

	curve 1	curve 2	curve 3	average
transf. ink [g]:	0.0081	0.0067	0.008	0.0076
transf. ink [g/m²]	1.50	1.24	1.48	1.41

		C.of Var.[%]:
aver. density of split film:	1.30	1.87
av. density of unspl. film:	1.80	2.00
av. coef. of var. of force values [%]:		13.9441

Fine paper 200 g/m² matt cross direction:

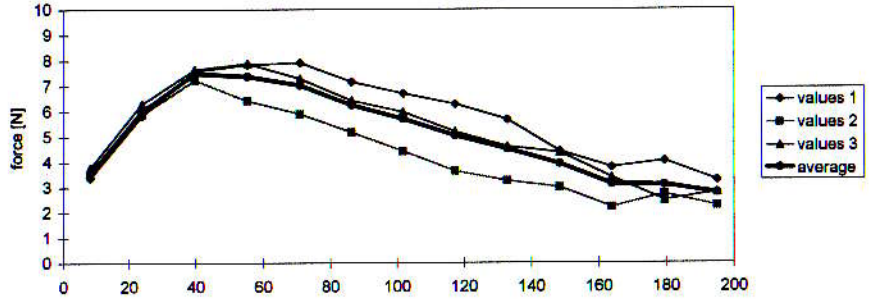

Fine paper 170 g/m², matt cross direction:

Data of average curve:

	time [s]	force [N]	Slope [N/s]
Max.:	23.8	5.93	
beginning:		4.66	0.08034
average:			-0.0274
end:		1.23	

	curve 1	curve 2	curve 3	average
transf. ink [g]:	0.0086	0.0075	0.009	0.00837
transf. ink [g/m²]	1.59	1.39	1.67	1.55

		C.of Var.[%]:
aver. density of split film:	1.24	3.18
av. density of unspl. film:	1.70	5.59
av. coef. of var. of force values [%]:		6.32765

Fine paper, 170 g/m² matt cross direction:

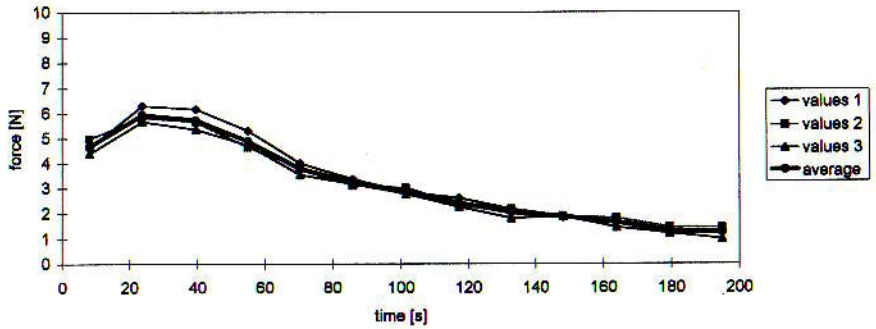

Fine paper 300 g/m², matt cross direction:

Data of average curve:

	time [s]	force [N]	Slope [N/s]
Max.:	55.2	6.92	
beginning:		3.37	0.1681
average:			-0.0214
end:		2.37	

	curve 1	curve 2	curve 3	average
transf. ink [g]:	0.007	0.0089	0.0076	0.00783
transf. ink [g/m²]	1.30	1.65	1.41	1.45

		C.of Var.[%]:
aver. density of split film:	1.36	3.34
av. density of unspl. film:	1.80	2.55
av. coef. of var. of force values [%]:		12.4878

Fine paper 300 g/m² matt, cross direction:

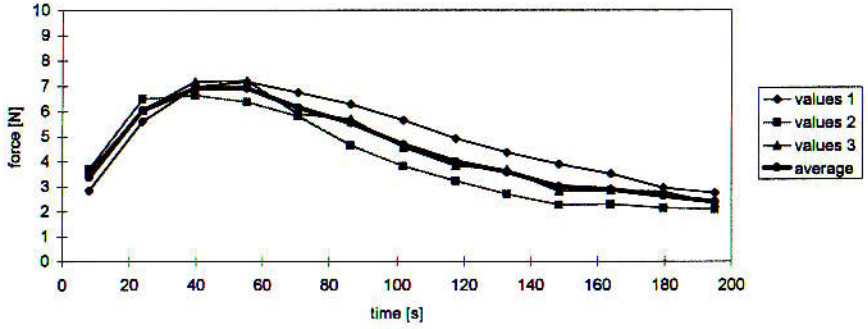

Substrate investigation of experimental boards

E 1, thin top coating with coarse $CaCO_3$, precoating: fine CaCO3

Data of average curve:

	time [s]	force [N]	Slope [N/s]
Max.:	54.9	5.16	0.094115
beginning:		2.50	-0.00425
average:			
end:		3.27	

	curve 1	curve 2	curve 3	average
transf. ink [g]:	0.0082	0.0074	0.0081	0.0079
transf. ink [g/m²]:	1.52	1.37	1.50	1.46

	C.of Var.[%]:	
aver. density of split film:	1.39	3.49
av. density of unspl. film:	1.60	7.67
av. coef. of var. of force values [%]:		11.18

E1

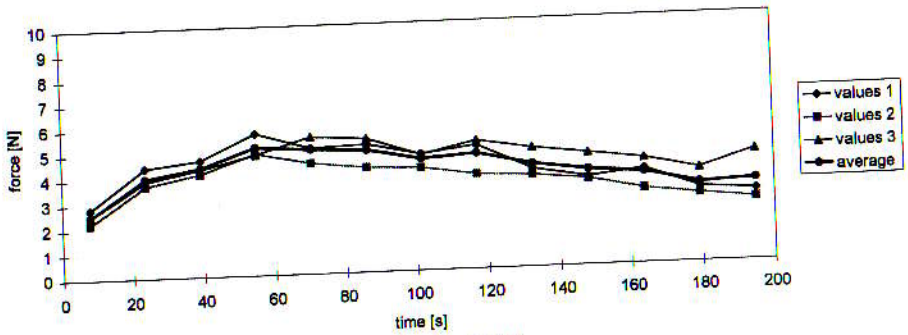

E 2, thicker top coating with coarse $CaCO_3$, precoating: fine CaCO3

Data of average curve:

	time [s]	force [N]	Slope [N/s]
Max.:	39.3	3.88	0.067723
beginning:		2.38	-0.010759
average:			
end:		1.60	

	curve 1	curve 2	curve 3	average
transf. ink [g]:	0.009	0.0078	0.001	0.00593
transf. ink [g/m²]:	1.67	1.44	0.19	1.10

	C.of Var.[%]:	
aver. density of split film:	1.41	2.58
av. density of unspl. film:	1.62	3.99
av. coef. of var. of force values [%]:		21.54

E 2

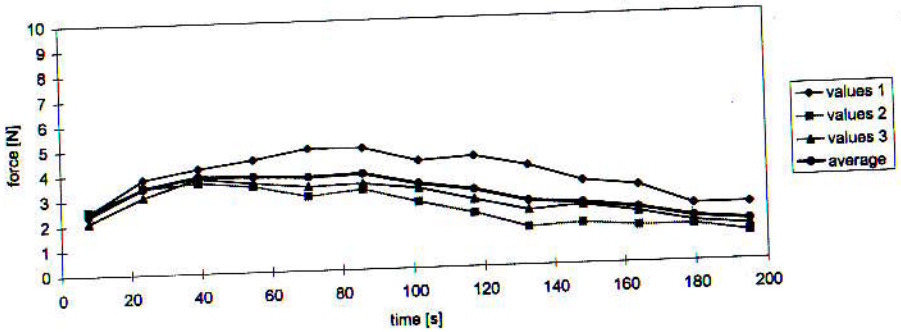

E 3, thickest top coating with coarse $CaCO_3$, precoating: fine CaCO3

Data of average curve:

	time [s]	force [N]	Slope [N/s]
Max.:	70.4	4.32	0.058362
beginning:		2.15	-0.005256
average:			
end:		2.16	

	curve 1	curve 2	curve 3	average
transf. ink [g]:	0.007	0.0087	0.0079	0.00787
transf. ink [g/m²]:	1.30	1.61	1.46	1.46

	C.of Var.[%]:	
aver. density of split film:	1.39	3.39
av. density of unspl. film:	1.62	2.86
av. coef. of var. of force values [%]:		22.39

E 3

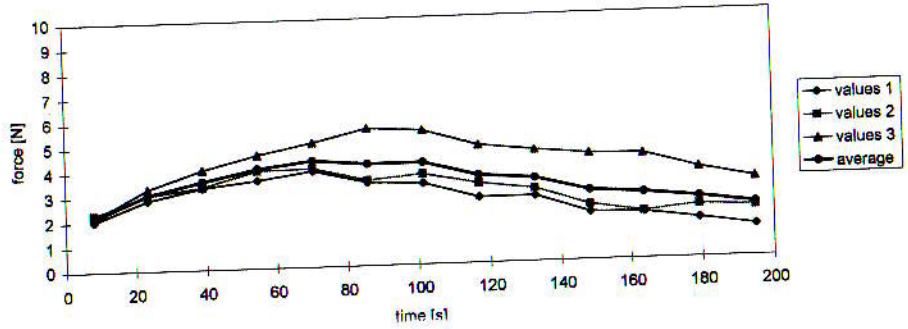

Substrate investigation of experimental boards

E 4, thin top coating with fine $CaCO_3$, precoating: coarse CaCO3

Data of average curve:

	time [s]	force [N]	Slope [N/s]
Max.:	23.8	6.29	
beginning:		5.95	0.021584
average:			-0.030728
end:		1.03	

	curve 1	curve 2	curve 3	average
transf. ink [g]:	0.0078	0.0078	0.0086	0.00807
transf. ink [g/m²]:	1.44	1.44	1.59	1.49

	C.of Var.[%]:	
aver. density of split film:	1.43	3.38
av. density of unspl. film:	1.75	3.41
av. coef. of var. of force values [%]:		16.12

E 4

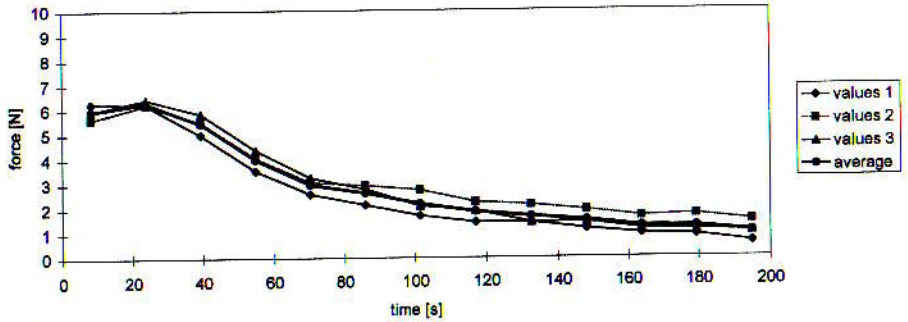

E 5, thicker top coating with fine $CaCO_3$, precoating: coarse CaCO3

Data of average curve:

	time [s]	force [N]	Slope [N/s]
Max.:	24	7.90	
beginning:		5.94	0.12314
average:			-0.039293
end:		1.19	

	curve 1	curve 2	curve 3	average
transf. ink [g]:	0.0071	0.0074	0.008	0.0075
transf. ink [g/m²]:	1.31	1.37	1.48	1.39

	C.of Var.[%]:	
aver. density of split film:	1.43	3.19
av. density of unspl. film:	1.80	3.45
av. coef. of var. of force values [%]:		14.68

E 5

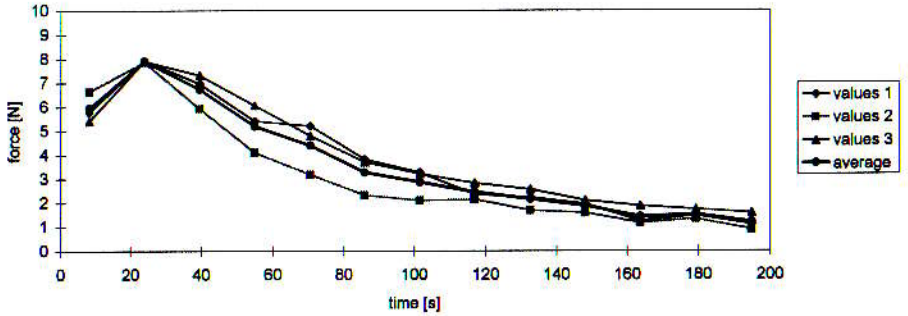

E 6, thickest top coatig with fine $CaCO_3$, precoating: coarse CaCO3

Data of average curve:

	time [s]	force [N]	Slope [N/s]
Max.:	24	7.34	
beginning:		6.47	0.055694
average:			-0.039507
end:		0.59	

	curve 1	curve 2	curve 3	average
transf. ink [g]:	0.007	0.0081	0.008	0.0077
transf. ink [g/m²]:	1.30	1.50	1.48	1.43

	C.of Var.[%]:	
aver. density of split film:	1.35	2.73
av. density of unspl. film:	1.67	6.15
av. coef. of var. of force values [%]:		7.59

E 6

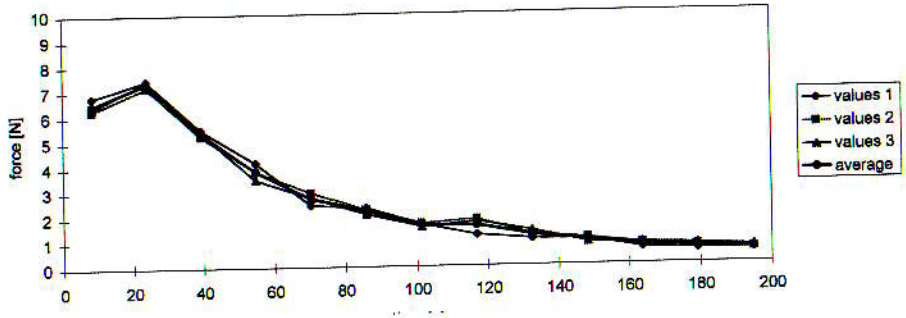

Substrate investigation of solid bleached boards:

SBB, ICCM, machine direction, 2 coating layers:

Data of average curve:

	time [s]	force [N]	Slope [N/s]
Max.:	39.8	8.29	
beginning:		5.94	0.1329
average:			-0.0251
end:		3.76	

	curve 1	curve 2	curve 3	average
transf. ink [g]:	0.0074	0.0071	0.007	0.00717
transf. ink [g/m²]	1.37	1.31	1.30	1.33

		C.of Var.[%]:
aver. density of split film:	1.30	2.63
av. density of unspl. film:	1.75	3.16
av. coef. of var. of force values [%]:		4.55

SBB, ICCM, machine direction

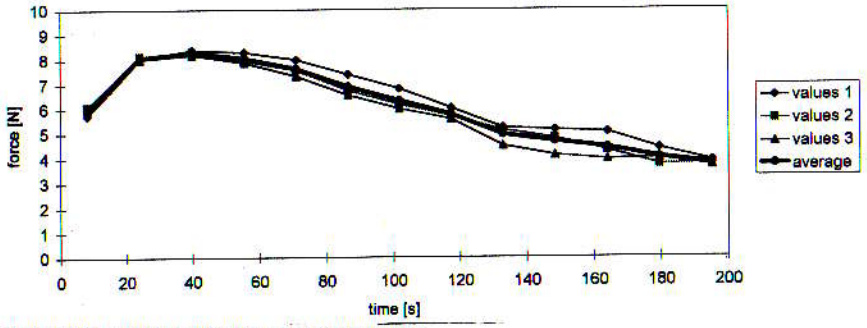

SBB, ICCG, machine direction , 2 coating layers:

Data of average curve:

	time [s]	force [N]	Slope [N/s]
Max.:	8.5	8.25	
beginning:		8.25	-0.0007
average:			-0.0368
end:		1.94	

	curve 1	curve 2	curve 3	average
transf. ink [g]:	0.0076	0.0081	0.0075	0.00773
transf. ink [g/m²]	1.41	1.50	1.39	1.43

		C.of Var.[%]:
aver. density of split film:	1.42	3.29
av. density of unspl. film:	1.82	3.45
av. coef. of var. of force values [%]:		6.03

SBB, ICCG, machine direction:

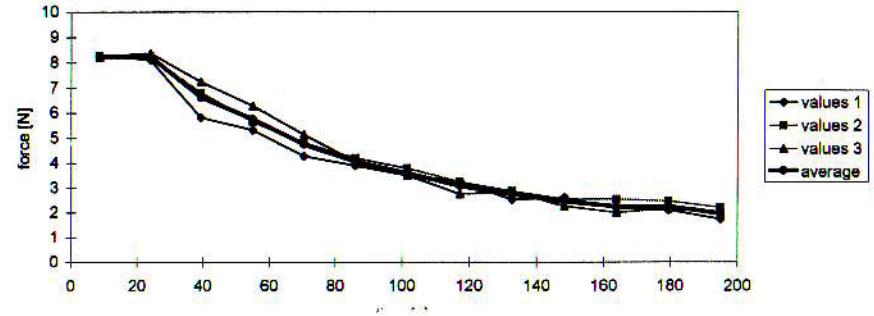

SBB, ICCM, cross direction, 2 coating layers:

Data of average curve:

	time [s]	force [N]	Slope [N/s]
Max.:	39.5	6.98	
beginning:		5.14	0.11379
average:			-0.0255
end:		2.58	

	curve 1	curve 2	curve 3	average
transf. ink [g]:	0.0069	0.0092	0.007	0.0077
transf. ink [g/m²]	1.28	1.70	1.30	1.43

		C.of Var.[%]:
aver. density of split film:	1.31	3.67
av. density of unspl. film:	1.71	3.82
av. coef. of var. of force values [%]:		6.40

SBB, ICCM, cross direction:

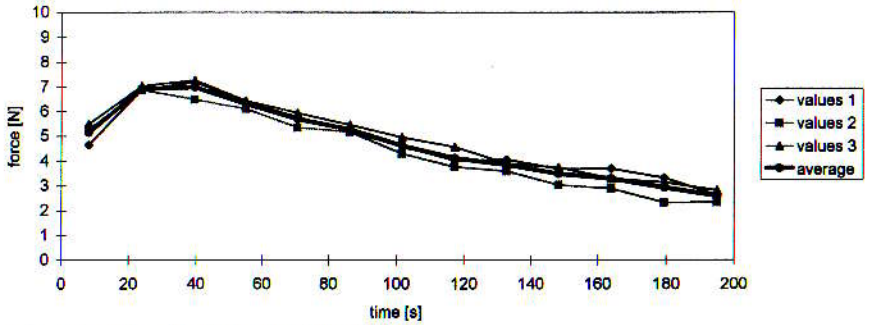

SBB, ICCG, cross direction, 2 coating layers:

Data of average curve:

	time [s]	force [N]	Slope [N/s]
Max.:	8.5	7.97	
beginning:		7.97	-0.0359
average:			-0.0357
end:		1.31	

	curve 1	curve 2	curve 3	average
transf. ink [g]:	0.0074	0.0075	0.0074	0.00743
transf. ink [g/m²]	1.37	1.39	1.37	1.38

		C.of Var.[%]:
aver. density of split film:	1.40	1.74
av. density of unspl. film:	1.76	2.12
av. coef. of var. of force values [%]:		14.24

SBB, ICCG, cross direction:

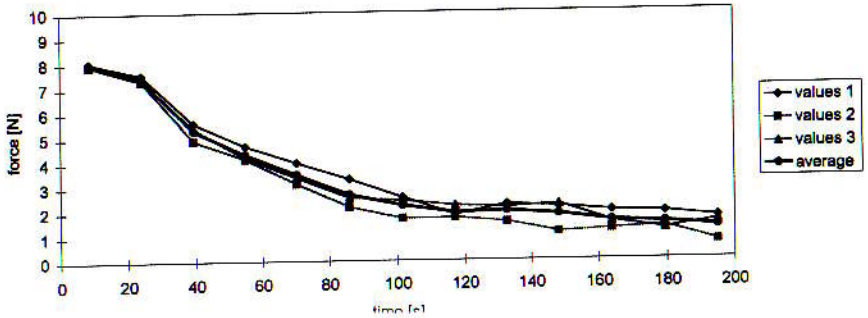

Substrate Investigation of solid bleached boards:

SBB, ICA, machine direction, 3 coating layers:

Data of average curve:

	time [s]	force [N]	Slope [N/s]
Max.:	39.77	8.05	
beginning:		5.89	0.12307
average:			-0.0217
end:		4.14	

	curve 1	curve 2	curve 3	average
transf. ink [g]:	0.0078	0.007	0.0066	0.00713
transf. ink [g/m²]	1.44	1.30	1.22	1.32

		C.of Var.[%]:
aver. density of split film:	1.23	6.10
av. density of unspl. film:	1.71	5.34
av. coef. of var. of force values [%]:		5.65

SBB, ICA, machine direction

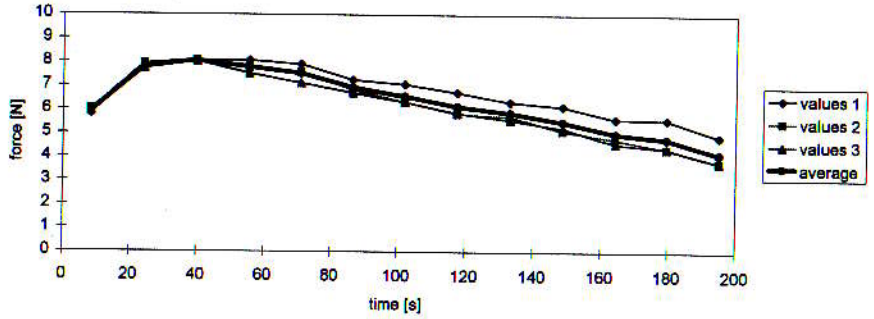

SBB, ICA, cross direction , 3 coating layers:

Data of average curve:

	time [s]	force [N]	Slope [N/s]
Max.:	39.6	7.39	
beginning:		5.51	0.11193
average:			-0.0226
end:		3.39	

	curve 1	curve 2	curve 3	average
transf. ink [g]:	0.0076	0.006	0.009	0.00753
transf. ink [g/m²]	1.41	1.11	1.67	1.40

		C.of Var.[%]:
aver. density of split film:	1.26	3.93
av. density of unspl. film:	1.70	3.46
av. coef. of var. of force values [%]:		7.37

SBB, ICA, cross direction

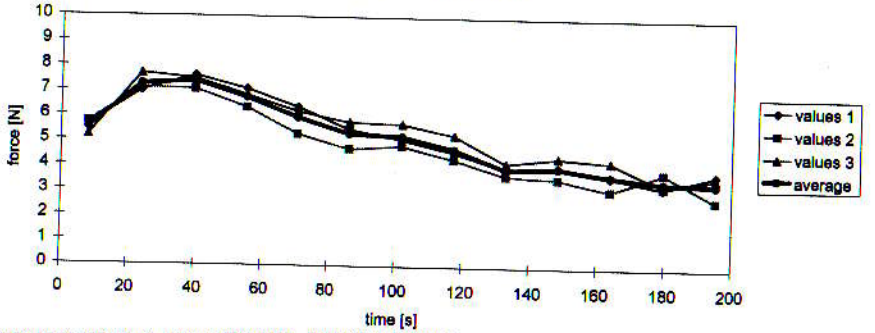

SBB, ICG 180 g/m², machine direction, 3 coating layers:

Data of average curve:

	time [s]	force [N]	Slope [N/s]
Max.:	39.6	7.77	
beginning:		5.46	0.120297
average:			-0.022402
end:		3.55	

	curve 1	curve 2	curve 3	average
transf. ink [g]:	0.0088	0.0064	0.0085	0.0079
transf. ink [g/m²]:	1.63	1.19	1.57	1.46

		C.of Var.[%]:
aver. density of split film:	1.24	3.18
av. density of unspl. film:	1.70	5.59
av. coef. of var. of force values [%]:		6.81435887

SBB, ICG 180 g/m² machine direction:

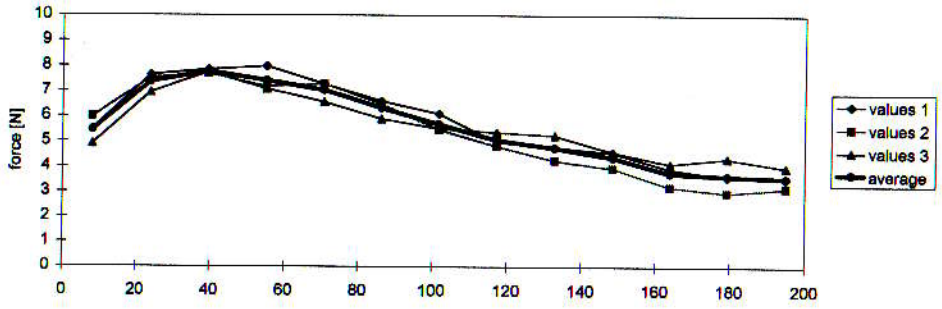

SBB, ICG 180 g/m², cross direction, 3 coating layers:

Data of average curve:

	time [s]	force [N]	Slope [N/s]
Max.:	39.77	7.86	
beginning:		4.98	0.15802
average:			-0.02291
end:		3.58	

	curve 1	curve 2	curve 3	average
transf. ink [g]:	0.0059	0.0069	0.0083	0.00703
transf. ink [g/m²]:	1.09	1.28	1.54	1.30

		C.of Var.[%]:
aver. density of split film:	1.31	5.24
av. density of unspl. film:	1.74	5.22
av. coef. of var. of force values [%]:		8.34445

SBB, ICG 180 g/m² cross direction

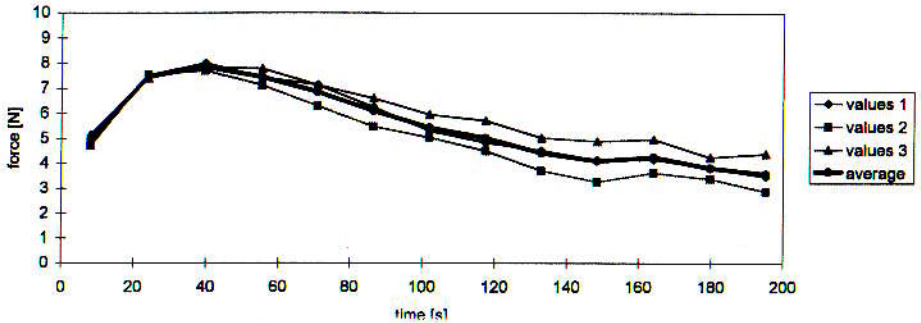

Substrate investigation of solid bleached boards:

SBB, OICG 180 g/m², machine direction, 2 coating layers:

Data of average curve:

	time [s]	force [N]	Slope [N/s]
Max.:	71.02	8.30	
beginning:		4.41	0.16372
average:			-0.0069
end:		5.83	

	curve 1	curve 2	curve 3	average
transf. ink [g]:	0.01	0.008	0.01	0.00933
transf. ink [g/m²]:	1.85	1.48	1.85	1.73

		C.of Var.[%]:
aver. density of split film:	1.30	1.87
av. density of unspl. film:	1.80	2.00
av. coef. of var. of force values [%]:		1.8348

SBB, OICG 180 g/m² machine direction:

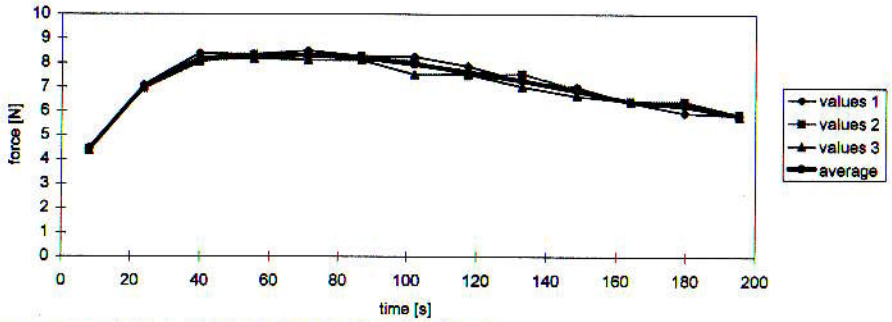

SBB, OICG 380 g/m², machine direction, 2 coating layers:

Data of average curve:

	time [s]	force [N]	Slope [N/s]
Max. force val.:	55.36	7.74	
beginning:		3.60	0.157
average:			-0.003
end:		5.52	

	curve 1	curve 2	curve 3	average
transf. ink [g]:	0.0069	0.0079	0.008	0.0074
transf. ink [g/m²]:	1.28	1.46	1.39	1.38

		C.of Var.[%]:
aver. density of split film:	1.39	2.38
av. density of unspl. film:	1.97	1.68
av. coef. of var. of force values [%]:		5.576

SBB, OICG 380 g/m² machine direction:

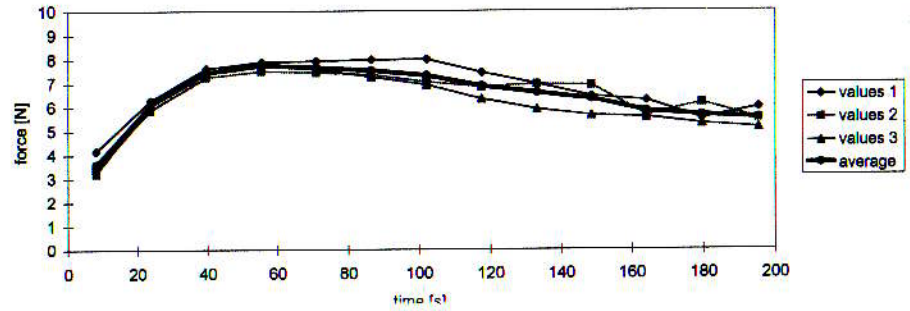

SBB, OICG 240 g/m², machine direction, 2 coating layers:

Data of average curve:

	time [s]	force [N]	Slope [N/s]
Max.:	55.2	7.34	
beginning:		3.77	0.13731788
average:			-0.0096642
end:		4.29	

	curve 1	curve 2	curve 3	average
transf. ink [g]:	0.0058	0.008	0.0082	0.0073
transf. ink [g/m²]:	1.07	1.48	1.52	1.36

		C.of Var.[%]:
aver. density of split film:	1.36	3.34
av. density of unspl. film:	1.80	2.55
av. coef. of var. of force values [%]:		6.83855

SBB, OICG G 240 g/m² machine direction:

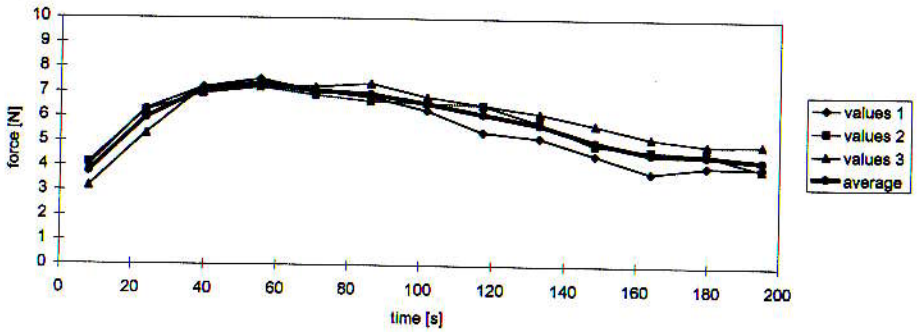

Substrate investigation of solid bleached boards:

SBB, ICG 260 g/m², machine direction, 3 coating layers:

Data of average curve:

	time [s]	force [N]	Slope [N/s]
Max.:	55.14	7.33	
beginning:		4.31	0.139
average:			-0.02
end:		3.01	

	curve 1	curve 2	curve 3	average
transf. ink [g]:	0.0079	0.0078	0.007	0.0076
transf. ink [g/m²]:	1.46	1.44	1.31	1.41

		C.of Var.[%]:
aver. density of split film:	1.34	3.73
av. density of unspl. film:	1.82	3.21
av. coef. of var. of force values [%]:		12.58

SBB, ICG 260 g/m² machine direction:

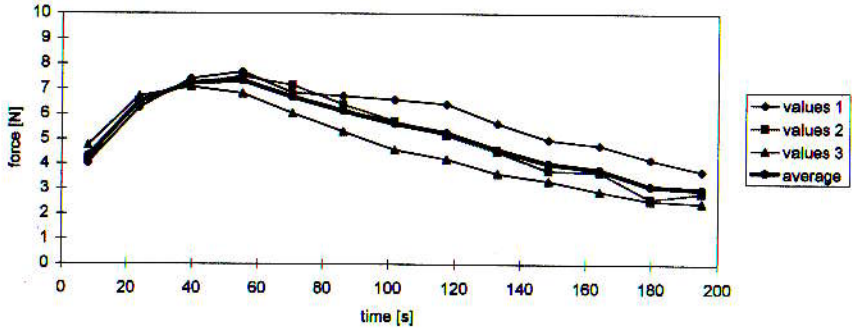

SBB, ICG 260 g/m², cross direction, 3 coating layers:

Data of average curve:

	time [s]	force [N]	Slope [N/s]
Max.:	55.36	7.99	
beginning:		4.50	0.144
average:			-0.014
end:		4.44	

	curve 1	curve 2	curve 3	average
transf. ink [g]:	0.008	0.0073	0.008	0.0079
transf. ink [g/m²]:	1.48	1.35	1.56	1.46

		C.of Var.[%]:
aver. density of split film:	1.30	1.83
av. density of unspl. film:	1.78	2.20
av. coef. of var. of force values [%]:		2.351

SBB, ICG 260 g/m² cross direction:

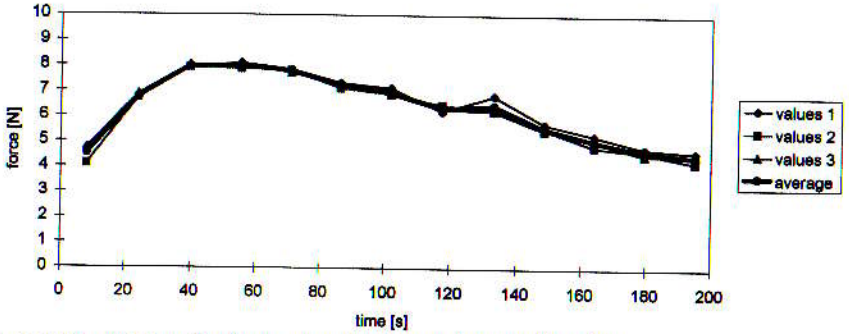

SBB, ICG 260 g/m², 3 coating layers, cross direction tested some weeks earlier:

Data of average curve:

	time [s]	force [N]	Slope [N/s]
Max.:	55.2	7.68	
beginning:		4.25	0.174894
average:			-0.01392
end:		4.63	

	curve 1	curve 2	curve 3	average
transf. ink [g]:	0.0074	0.0075	0.0076	0.0075
transf. ink [g/m²]:	1.37	1.39	1.41	1.39

		C.of Var.[%]:
aver. density of split film:	1.25	3.84
av. density of unspl. film:	1.70	3.33
av. coef. of var. of force values [%]:		4.96327

SBB, ICG 260 g/m² cross direction, tested some weeks earlier:

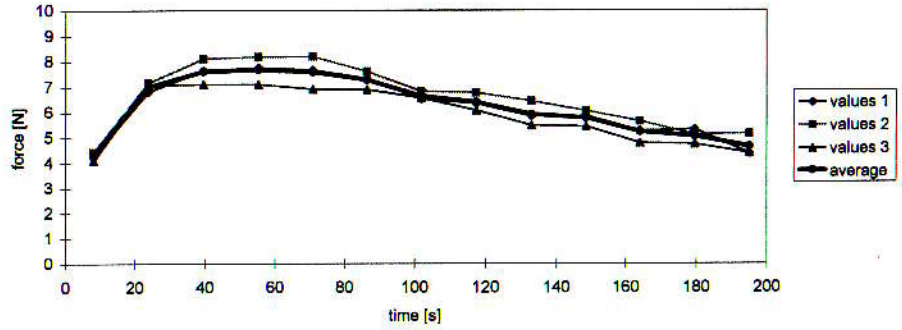

Substrate investigation of solid bleached boards

SBB, ICG 380 g/m², machine direction, 3 coating layers:

Data of average curve:

	time [s]	force [N]	Slope [N/s]
Max. force val.:	24.1	7.85	
beginning:		6.68	0.074
average:			-0.031
end:		2.57	

	curve 1	curve 2	curve 3	average
transf. ink [g]:	0.0087	0.0074	0.007	0.0078
transf. ink [g/m²]:	1.61	1.37	1.37	1.45

		C.of Var.[%]:
aver. density of split film:	1.31	2.81
av. density of unspl. film:	1.75	3.40
av. coef. of var. of force values [%]:		5.238

SBB, ICG 380 g/m² machine direction:

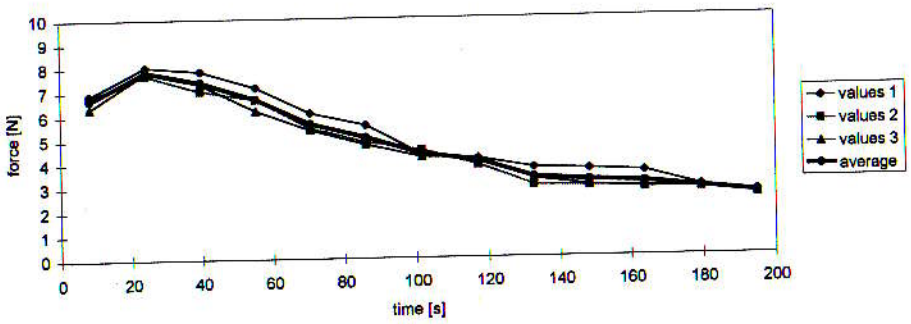

SBB, ICG 380 g/m², cross direction, 3 coating layers:

Data of average curve:

	time [s]	force [N]	Slope [N/s]
Max. force val.:	24.1	7.71	
beginning:		6.66	0.066785
average:			-0.03243
end:		2.17	

	curve 1	curve 2	curve 3	average
transf. ink [g]:	0.0074	0.0076	0.007	0.00743
transf. ink [g/m²]:	1.37	1.41	1.35	1.38

		C.of Var.[%]:
aver. density of split film:	1.34	3.05
av. density of unspl. film:	1.71	3.17
av. coef. of var. of force values [%]:		10.81

SBB, ICG 380 g/m² cross direction:

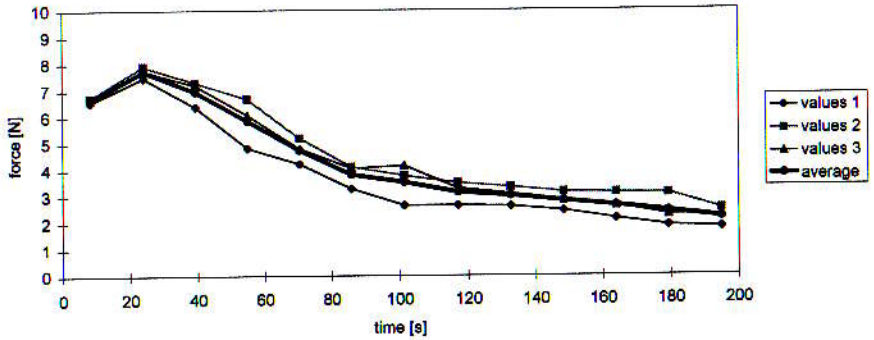

Substrate investigation of wood containing newsprint paper. (MWC paper):

MWC paper 1, wood containing

Data of average curve:

	time [s]	force [N]	Slope [N/s]
Max.:	132	6.18	
beginning:		2.75	0.0712
average:			0.01104
end:		5.76	

	curve 1	curve 2	curve 3	average
transf. ink [g]:	0.0069	0.0089	0.0068	0.00753
transf. ink [g/m²]	1.28	1.65	1.26	1.40

		C.of Var.[%]:
aver. density of split film:	1.20	3.95
av. density of unspl. film:	1.58	3.06
av. coef. of var. of force values [%]:		5.2084

MWC paper 1, 65g:

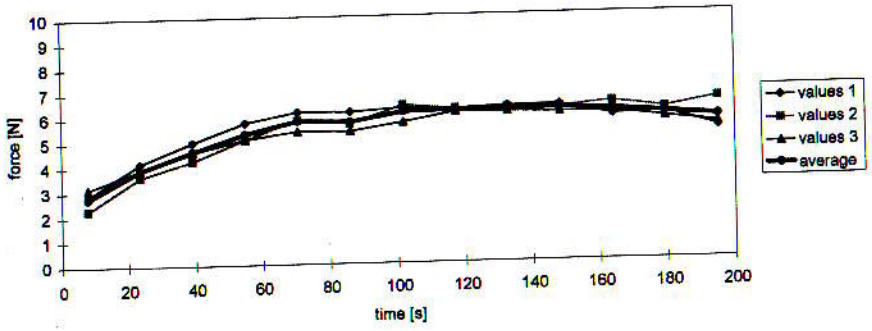

MWC paper 2, wood containing:

Data of average curve:

	time [s]	force [N]	Slope [N/s]
Max.:	102	7.53	
beginning:		3.10	0.11826
average:			0.00558
end:		5.91	

	curve 1	curve 2	curve 3	average
transf. ink [g]:	0.0073	0.0072	0.0064	0.00697
transf. ink [g/m²]	1.35	1.33	1.19	1.29

		C.of Var.[%]:
aver. density of split film:	1.27	6.99
av. density of unspl. film:	1.63	3.25
av. coef. of var. of force values [%]:		9.50206

MWC paper 2

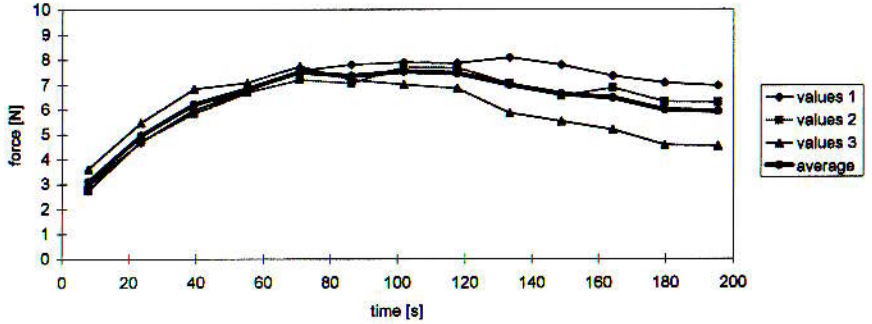

MWC paper 3, wood containing:

Data of average curve:

	time [s]	force [N]	Slope [N/s]
Max.:	86	6.35	
beginning:		3.10	0.07458
average:			0.00667
end:		5.41	

	curve 1	curve 2	curve 3	average
transf. ink [g]:	0.007	0.0062	0.0084	0.0072
transf. ink [g/m²]	1.30	1.15	1.56	1.33

		C.of Var.[%]:
aver. density of split film:	1.17	3.78
av. density of unspl. film:	1.52	6.34
av. coef. of var. of force values [%]:		5.21626

MWC 3:

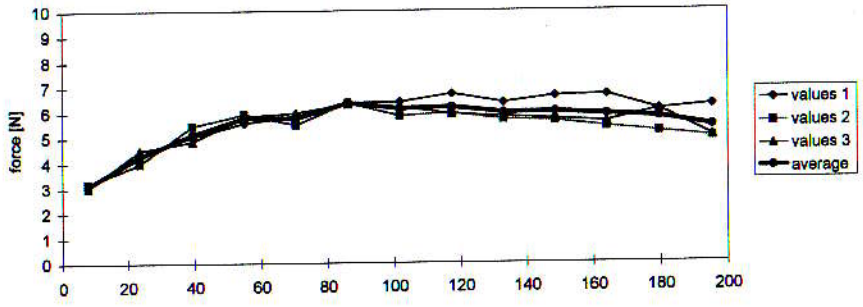

MWC paper 4, wood containing, sheet-fed:

Data of average curve:

	time [s]	force [N]	Slope [N/s]
Max.:	101	6.23	
beginning:		3.07	0.06719
average:			0.00813
end:		5.53	

	curve 1	curve 2	curve 3	average
transf. ink [g]:	0.0066	0.0072	0.0058	0.00653
transf. ink [g/m²]	1.22	1.33	1.07	1.21

		C.of Var.[%]:
aver. density of split film:	1.13	5.14
av. density of unspl. film:	1.53	8.65
av. coef. of var. of force values [%]:		7.80353

MWC paper 4, sheet-fed:

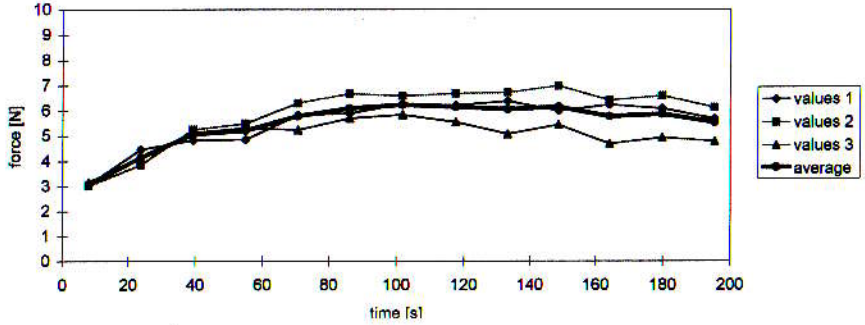

Substrate investigation of wood containing newsprint paper (MWC paper):

MWC paper 5, matt :

Data of average curve:

	time [s]	force [N]	Slope [N/s]
Max.:	117.2	4.29	
beginning:		1.79	0.04662
average:			0.00702
end:		3.72	

	curve 1	curve 2	curve 3	average
transf. ink [g]:	0.0075	0.0074	0.0069	0.00727
transf. ink [g/m²]	1.39	1.37	1.28	1.35

		C.of Var.[%]:
aver. density of split film:	1.23	4.12
av. density of unspl. film:	1.46	6.32
av. coef. of var. of force values [%]:		9.8095

MWC paper 5, matt:

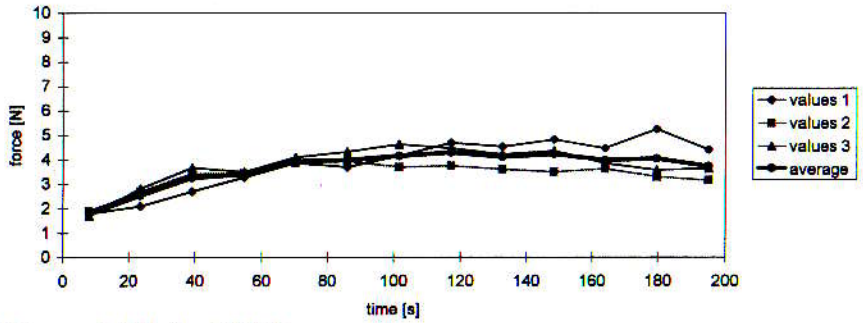

MWC paper 7, dubbelc., web-fed :

Data of average curve:

	time [s]	force [N]	Slope [N/s]
Max.:	55,2	6,64	
beginning:		2,99	0,1183
average:			-0,0076
end:		3,54	

	curve 1	curve 2	curve 3	average
transf. ink [g]:	0,0071	0,0065	0,0073	0,00697
transf. ink [g/m²]	1,31	1,20	1,35	1,29

		C.of Var.[%]:
aver. density of split film:	1,08	2,93
av. density of unspl. film:	1,50	3,23
av. coef. of var. of force values [%]:		6,956

MWC paper 7, doublecoated

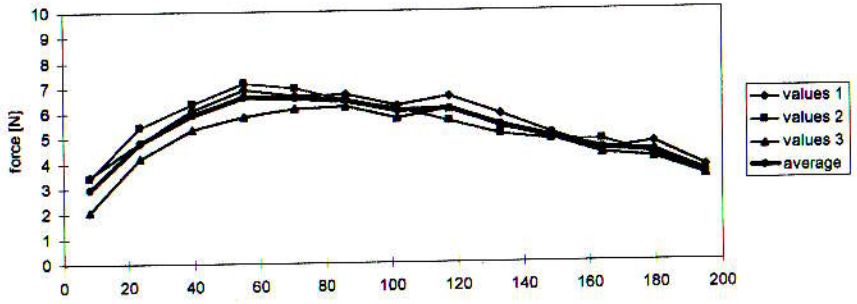

MWC paper 6, wood containing, web-fed:

Data of average curve:

	time [s]	force [N]	Slope [N/s]
Max.:	55.09	6.33	
beginning:		3.21	0.11268
average:			-0.0101
end:		3.26	

	curve 1	curve 2	curve 3	average
transf. ink [g]:	0.006	0.007	0.0068	0.0066
transf. ink [g/m²]	1.11	1.30	1.26	1.22

		C.of Var.[%]:
aver. density of split film:	1.17	7.37
av. density of unspl. film:	1.41	14.39
av. coef. of var. of force values [%]:		7.6369

MWC paper 6, wood containing, web-fed:

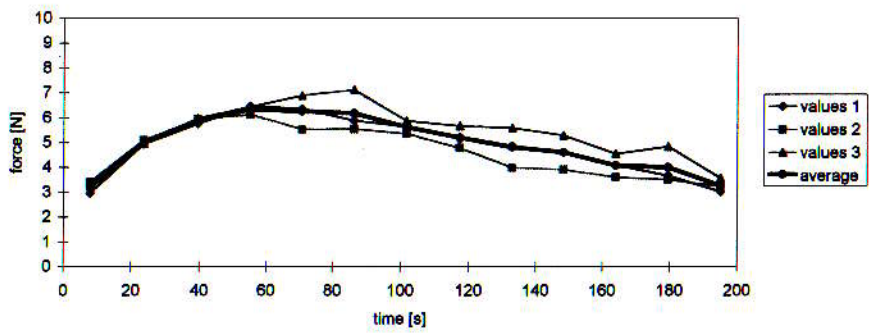

Substrate investigation of folding box board:

FBB1, 220 g/m², double coated, machine direction:

Data of average curve:

	time [s]	force [N]	Slope [N/s]
Max.:	39.77	6.79	
beginning:		4.10	0.14908
average:			-0.0261
end:		2.00	

	curve 1	curve 2	curve 3	average
transf. ink [g]:	0.0073	0.007	0.008	0.00743
transf. ink [g/m²]	1.35	1.30	1.48	1.38

		C.of Var.[%]:
aver. density of split film:	1.34	2.83
av. density of unspl. film:	1.75	4.00
av. coef. of var. of force values [%]:		12.1245

FBB1, 220 g/m², machine direction

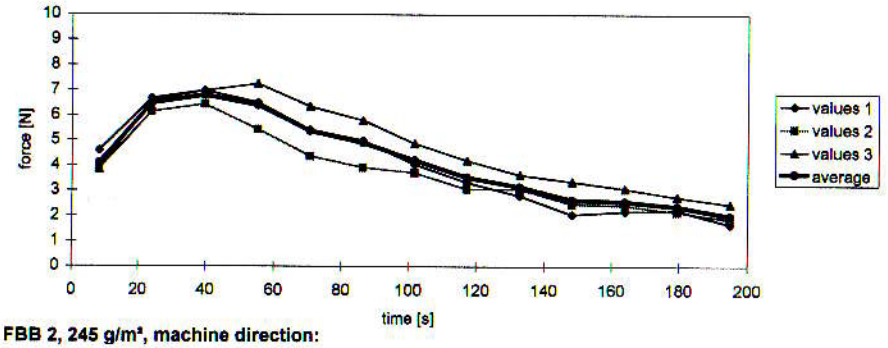

FBB 2, 245 g/m², machine direction:

Data of average curve:

	time [s]	force [N]	Slope [N/s]
Max.:	71.02	6.36	
beginning:		3.84	0.14179
average:			-0.0278
end:		1.32	

	curve 1	curve 2	curve 3	average
transf. ink [g]:	0.0074	0.0074	0.0074	0.0074
transf. ink [g/m²]	1.37	1.37	1.37	1.37

		C.of Var.[%]:
aver. density of split film:	1.25	4.95
av. density of unspl. film:	1.69	5.70
av. coef. of var. of force values [%]:		17.6227

FBB 2, 245g/m², machine direction:

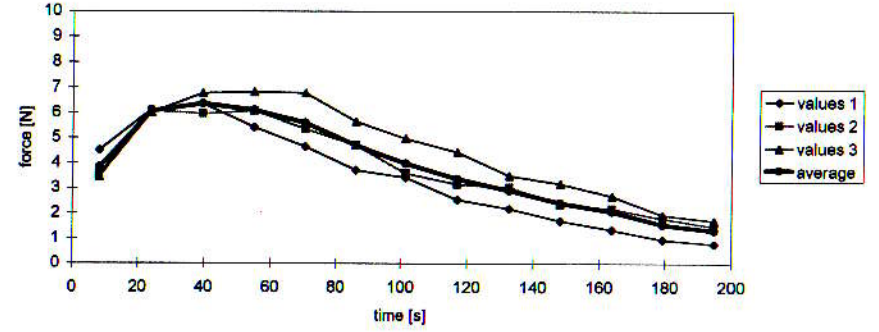

FBB 1, 220g/m², double coated, cross direction:

Data of average curve:

	time [s]	force [N]	Slope [N/s]
Max.:	39.6	6.79	
beginning:		3.52	0.16351
average:			-0.0197
end:		2.72	

	curve 1	curve 2	curve 3	average
transf. ink [g]:	0.0086	0.0077	0.0088	0.00837
transf. ink [g/m²]	1.59	1.43	1.63	1.55

		C.of Var.[%]:
aver. density of split film:	1.34	2.83
av. density of unspl. film:	1.75	4.00
av. coef. of var. of force values [%]:		8.48464

FBB1, 220 g/m², Cross direction:

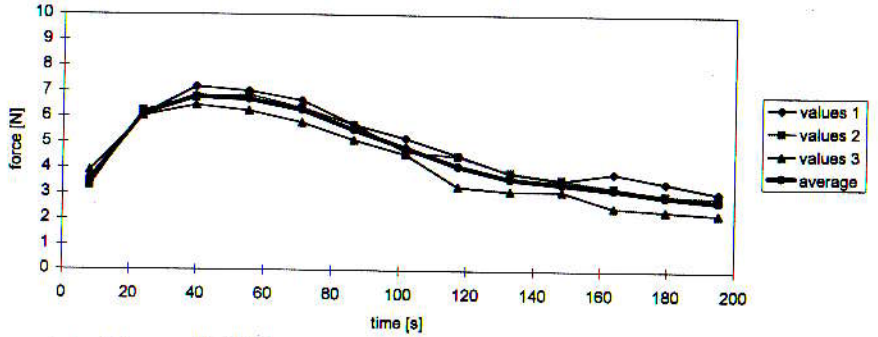

FBB 2, 245 g/m², cross direction:

Data of average curve:

	time [s]	force [N]	Slope [N/s]
Max. forc	55.36	7.15	
beginning:		3.83	0.13029
average:			-0.0224
end:		2.05	

	curve 1	curve 2	curve 3	average
transf. ink [g]:	0.0072	0.0069	0.0078	0.0073
transf. ink [g/m²]	1.33	1.28	1.44	1.35

		C.of Var.[%]:
aver. density of split film:	1.28	4.21
av. density of unspl. film:	1.77	3.82
av. coef. of var. of force values [%]:		8.76698

FBB 2, 245 g/m², cross direction:

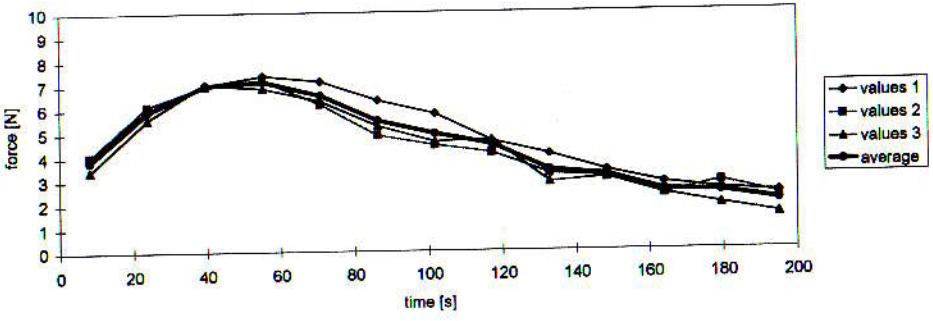

Substrate investigation of folding box board:

FBB 3, 328 g/m², double coated, machine direction:

Data of average curve:

	time [s]	force [N]	Slope [N/s]
Max.:	39.5	6.59	
beginning:		4.04	0.12061
average:			-0.0226
end:		2.08	

	curve 1	curve 2	curve 3	average
transf. ink [g]:	0.008	0.0078	0.0072	0.00767
transf. ink [g/m²]	1.48	1.44	1.33	1.42

		C.of Var.[%]:
aver. density of split film:	1.32	4.55
av. density of unspl. film:	1.74	5.80
av. coef. of var. of force values [%]:		16.268

FBB 3, 328 g/m², machine direction:

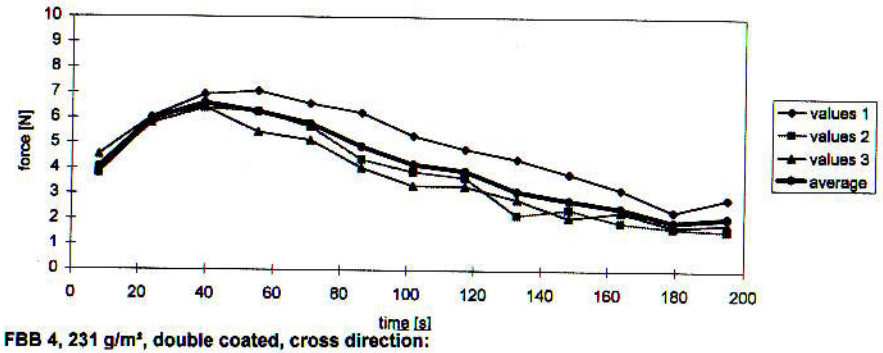

FBB 4, 231 g/m², double coated, cross direction:

Data of average curve:

	time [s]	force [N]	Slope [N/s]
Max.:	55.2	6.39	
beginning:		3.41	0.08703
average:			-0.0104
end:		2.99	

	curve 1	curve 2	curve 3	average
transf. ink [g]:	0.0066	0.008	0.007	0.0072
transf. ink [g/m²]	1.22	1.48	1.30	1.33

		C.of Var.[%]:
aver. density of split film:	1.27	4.61
av. density of unspl. film:	1.71	3.89
av. coef. of var. of force values [%]:		7.37531

FBB 4, 231 g/m², cross direction:

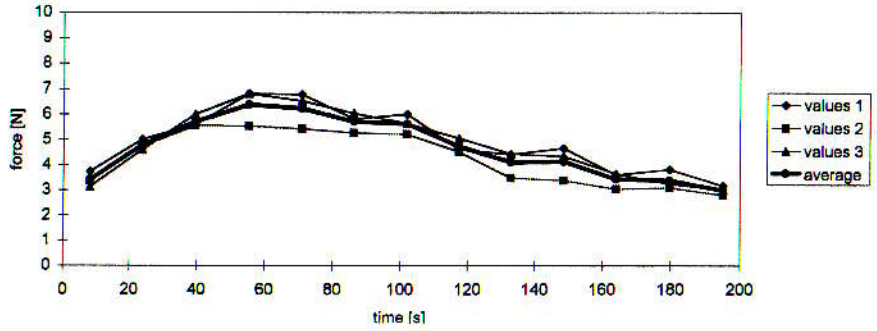

FBB 3, 328 g/m², double coated, cross direction:

Data of average curve:

	time [s]	force [N]	Slope [N/s]
Max.:	39.4	6.76	
beginning:		4.08	0.12468
average:			-0.0196
end:		2.69	

	curve 1	curve 2	curve 3	average
transf. ink [g]:	0.007	0.0076	0.008	0.00753
transf. ink [g/m²]	1.30	1.41	1.48	1.40

		C.of Var.[%]:
aver. density of split film:	1.41	3.85
av. density of unspl. film:	1.83	1.70
av. coef. of var. of force values [%]:		7.51275

FBB 3, 328 g/m², cross direction:

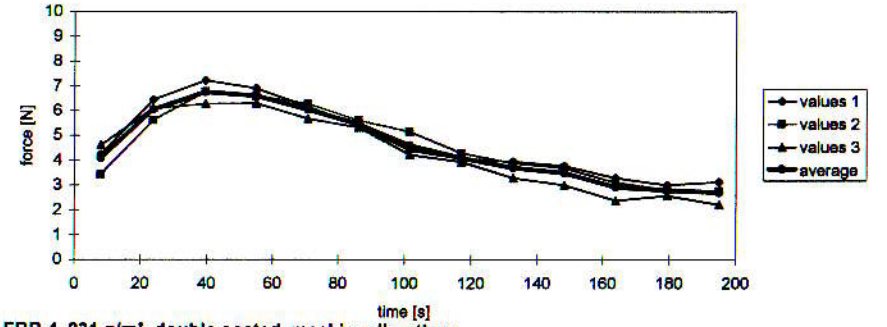

FBB 4, 231 g/m², double coated, machine direction:

Data of average curve:

	time [s]	force [N]	Slope [N/s]
Max.:	55.14	6.47	
beginning:		3.96	0.12227
average:			-0.0215
end:		2.22	

	curve 1	curve 2	curve 3	average
transf. ink [g]:	0.0087	0.0066	0.0069	0.0074
transf. ink [g/m²]	1.61	1.22	1.28	1.37

		C.of Var.[%]:
aver. density of split film:	1.34	5.32
av. density of unspl. film:	1.73	6.17
av. coef. of var. of force values [%]:		18.3937

FBB 4, 231 g/m², machine direction:

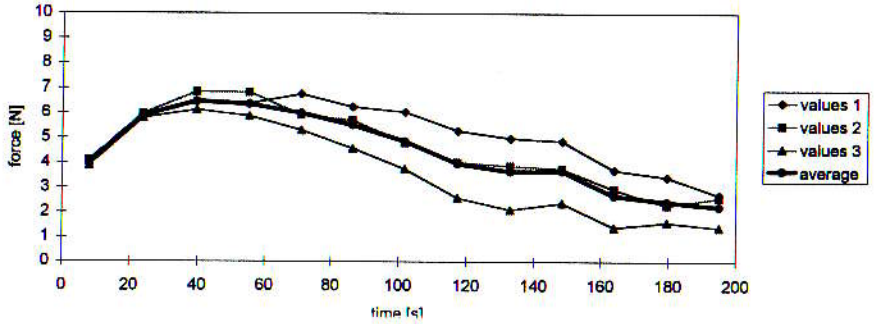

Substrate investigation of cast coated solid bleached board:

Cast coated, fully bleached board, machine direction:

Data of average curve:

	time [s]	force [N]	Slope [N/s]
Max.:	164.2	6.30	
beginning:		2.32	0.076
average:			0.015
end:		6.12	

	curve 1	curve 2	curve 3	average
transf. ink [g]:	0.0079	0.0055	0.009	0.0073
transf. ink [g/m²]:	1.46	1.02	1.59	1.36

		C.of Var.[%]:
aver. density of split film:	1.00	4.16
av. density of unspl. film:	1.47	3.97
av. coef. of var. of force values [%]:		4.901

Cast coated, machine direction

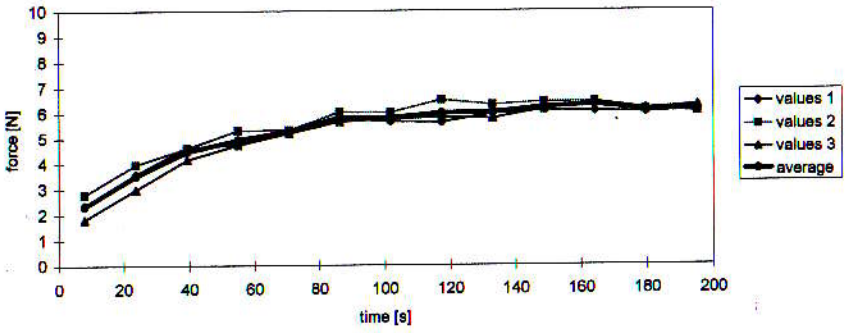

Substrate investigation, uncoated baseboards:

Exp Baseboard, 90 g/m², 115 µm,

Data of average curve:

	time [s]	force [N]	Slope [N/s]
Max.:	-	0.59	
beginning:		0.56	0.00167
average:			-0.0005
end:		0.51	

	curve 1	curve 2	curve 3	average
transf. ink [g]:	0.0072	-	-	0.0072
transf. ink [g/m²]	1.33	-	-	1.33

		C.of Var.[%]:
aver. density of split film:	1.14	-
av. density of unspl. film:	1.17	-
av. coef. of var. of force values [%]:		-

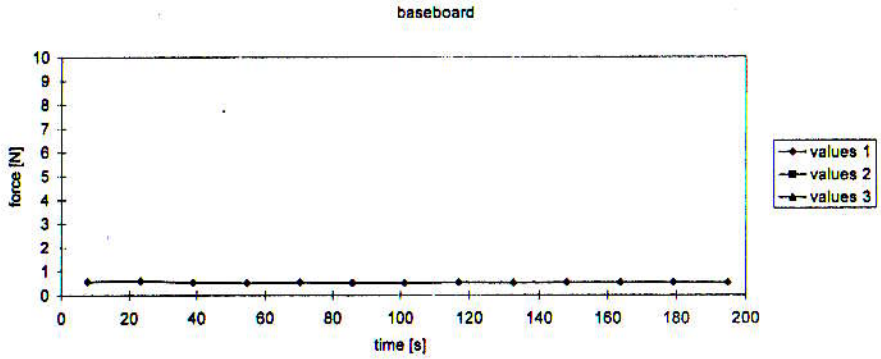

Substrate investigation: Cast coated fully bleached board:

Cast coated, fully bleached board, machine direction:

Data of average curve:

	time [s]	force [N]	Slope [N/s]
Max.:	164.2	6.30	
beginning:		2.32	0.076
average:			0.015
end:		6.12	

	curve 1	curve 2	curve 3	average
transf. ink [g]:	0.0079	0.0055	0.009	0.0073
transf. ink [g/m²]:	1.46	1.02	1.59	1.36

		C.of Var.[%]:
aver. density of split film:	1.00	4.16
av. density of unspl. film:	1.47	3.97
av. coef. of var. of force values [%]:		4.901

Cast coated, machine direction